المجلد ١ العدد ١ محرم ١٤٢٩هـ

المجلة العربية للكيميـاء

Arabian Journal of Chemistry ,Volume 1-Number 1 January 2008

Volume 1-Number 1- January 2008

ARABIAN JOURNAL OF CHEMISTRY

تصدر هذه المجلة بدعم من الجمعية الكيميائية السعودية

المجلة الرسمية لاتحاد الكيميائيين العرب

Published By Saudi Chemical Society

The Official Journal For the Arab Union of Chemists

ARABIAN JOURNAL OF CHEMISTRY

The international Journal of Pure and Applied Chemistry

Peer Review Policy for Arabian Journal of Chemistry

The practice of peer review is to ensure that good science is published. It is an objective process at the heart of good scholarly publishing and is carried out on all reputable scientific journals. Our referees therefore play a vital role in maintaining the high standards of Arabian Journal of Chemistry and all manuscripts are peer reviewed following the procedure outlined below.

Special issues are also subject to peer review and may involve the assistance of Guest Editors. Authors contributing to these projects will receive full details of the peer review process from the Editor in Charge . Arabian Journal of Chemistry applies the same criteria of acceptance of manuscripts to all types of submissions, irrespective of whether these are submitted for regular issue or special issues.

Initial manuscript evaluation

One of the Editors first evaluate the manuscript. Some manuscripts may be rejected at this stage if they are deemed insufficiently original, have serious scientific flaws, or are outside the aims and scope of the journal. Those manuscripts that meet these minimum criteria are passed on to experts for review.

Type of Peer Review

This journal employs double blind review, where the referees remain anonymous throughout the process.

How the reviewer is selected

Reviewers are matched to the paper by the Editor according to their expertise. Arabian Journal of Chemistry's reviewer database is constantly being updated. The Editors welcome suggestions for reviewers from the author though these recommendations may not be used, and these should not be close colleagues or collaborators, i.e., should be independent experts.

Reviewers reports

Reviewers are asked to evaluated whether the manuscripts:

- Is original and novel
- Is conceptually and scientifically sound
- Is methodologically sound
- Contributes significantly to advancement of the research area
- Follows appropriate ethical guidelines
- Has results which are clearly presented and support the conclusions
- Correctly references previous relevant work

Reviewers are not expected to correct or copyedit manuscripts.
Language correction is not part of the peer review process.

How long does the review process take?

Typically the manuscript will be reviewed within 2 months. Should the reviewers` reports contradict one another or a report is unnecessarily delayed a further expert opinion may be sought. Revised manuscripts may be returned to the initial referees. The Editors may request more than one revision of a manuscript.

Final Report

A final decision to accept or reject the manuscript will be sent to the author along with any recommendations made by the reviewers, and may include verbatim comments by the reviewers and Editor.

Editor's decision is final

Reviewers advise the Editor, who is responsible for the final decision to accept or reject the article.

Arabian Journal of Chemistry

EDITORIAL BOARD

INTERNATIONAL ADVISORY BOARD

INTERNATIONAL ADVISORY BOARD

Author Guidelines

Scope and Description

Arabian Journal of Chemistry (AJC) is an international quarterly peer-reviewed research journal issued by the Arab Union of Chemists, and published by the Saudi Chemical Society, Riyadh, Saudi Arabia. The Journal publishes new and original Research Articles, Short Communications, Technical Notes, Feature Articles and Review Articles encompassing all fields of chemistry, experimental and theoretical, written either in English or Arabic.

Introduction to Authors

Instructions to authors concerning manuscript organization and format apply to hardcopy submission by mail, and also to electronic online submission via the Journal homepage website (under construction).

Manuscript Submission

1- Hardcopy: The Original and three copies of the manuscript, together with a covering letter from the corresponding author, should submitted to the:

Editor-in-chief:
Prof. Abdulrahman. A. Alwarthan
Editor-in-Chief
Arabian Journal of Chemistry
Chemistry Department, Faculty of Science
King Saud University
P.O.Box: 2455, Riyadh-11451
Saudi Arabia
Tel: 00966 1 4676005
Fax: 00966 1 4675888
E-mail:awarthan@ksu.edu.sa

2- Online: follow the instructions at the journal homepage website.

Original Research Articles, Communications and Technical Notes are subject to critical review by at least two referees. Authors are encouraged to suggest names of competent reviewers. Feature Articles in active chemistry research fields, in which the author's own contribution and its relationship to other work in the field constitutes the main body of the article, appear as a result of an invitation from the Editorial Board, and will be so designated. The author of a Feature Article will be asked to provide a clear, concise and critical status report of the field as an introduction to the article. Review Articles on active and rapidly changing chemistry research fields will also be published. Authors of Review Articles are encouraged to submit two-page proposals to the Editor-in-Chief for approval. Manuscripts submitted in Arabic should also include an Abstract and Keywords in English.

Organization of the Manuscript

Manuscripts not exceeding 30 pages should be typed double-spaced on one side of high quality white A4 sheets (21.6×27.9 cm) with 3.71 cm margins, using Microsoft Word 2000 or a later version thereof. The sections should be arranged in the following order: Title Page, Abstract, Keywords, Introduction, Materials and Methods, Results, Discussion, Conclusion, Acknowledgments, Abbreviations (if any), References, Tables, a list of Figure Captions, and Figures. Only the first letters of words in the Title, Headings and Subheadings are capitalized. Headings should be in bold while Subheadings in italic fonts.

Title Page: Includes the title of the article, authors' names with full first names and middle initials, and affiliations. The affiliation should comprise the department, institution (university or company), city and state and should be typed as a footnote to the author's name. The name and complete mailing address, telephone and fax numbers, and e-mail address of the author responsible for correspondence (who is designated with an asterisk) should also be included for office purposes. The title should be carefully, concisely and clearly constructed to highlight the emphasis and content of the manuscript, which is very important for information retrieval.

Abstract: A one paragraph abstract not exceeding 200 words is required, which should be arranged to highlight the purpose, methods used, results and major findings, with the results comprising no less than 50% of the abstract.

Keywords: A list of 4-6 keywords, which express the precise content of the manuscript for indexing purposes, should follow the abstract.

Introduction: Should present the purpose of the studies to be reported and their relationship to earlier work in the field, but it should not be an extensive review of the literature (e.g., should not exceed 1 ½ typed pages).

Materials and Methods: Should be sufficiently informative to allow competent reproduction of the experimental procedures presented, yet concise enough not to be repetitive of earlier published procedures. Note that all unusual hazards in the chemicals, equipment or procedures used in the study must be clearly identified.

Results: Should present results in Tables and Figures plus some complimentary data in the Text without extensive discussion of results.

Discussion: Should be concise and focusing on the interpretation of the results without repetition of same results.

Conclusion: Should be a brief account of the major findings of the study not exceeding one typed page at the most.

Nomenclature: Registered trade names should be capitalized whenever they are used, while trade or trivial names should not be capitalized. The chemical name or composition should be given in parentheses at the first occurrence of that name. Nomenclature should be systematic conforming to those used by the Chemical Abstracts Service and recommended by IUPAC and IUBMB.

Abbreviations: Abbreviations are to be used sparingly, otherwise

provide a notation section indicating all nonstandard abbreviations on a separate page prior to the references section. The metric system should be used for all measurements, which must be indicated in lower case letters (e.g., g, kg, m, ml, s), while Standard International (SI) units are to be used conforming to IUPAC. Define all symbols used in equations and formulas. Include a list of all symbols in the notation section when extensively used.

Acknowledgments: Acknowledgments, including those for grant and financial support, should be typed in one paragraph directly preceding the References section.

References: References should be typed double-spaced and numbered sequentially in the order in which they are cited in the text. References should be cited in the text by the appropriate Arabic numerals, which are superscripted while enclosed in square brackets. Titles of journals are abbreviated according to the Chemical Abstracts Service Source Index (American Chemical Society). Authors are responsible for the accuracy of the references. The style and punctuation should conform to the following examples:

1. Journal Article:

For journals that are not paginated continuously throughout the year (e.g., page numbering does not continue from issue to the next), the volume number should be followed by the issue number in regular parentheses. In contrast, only the volume number is required for journals that are paginated continuously throughout the year. Examples:

a) Metallo, S. J.; Kane, R. S.; Holmlin, R. E.; Whitesides, G. M., J. Am. Chem. Soc. 2003, 125, 4534-4540.

b) Stevens, M. J., Langmuir 1999, 15, 2773-2778.

c) Walmsley, I.; Rabitz, H., Phys. Today 2003, 56(8), 43-49.

d) Freemantle, M., Chem. Eng. News 1988, 76(28), 15-16.

2. Books with authors, No Editors:

a) Calvert, J. G.; Pitts, J. N., Photochemistry; Wiley: New York, 1966, pp 156-186.

b) Zewail, A. H., Femtochemistry-Ultrafast Dynamics of the Chemical Bond; World Scientific: Singapore, 1994; Vol. I, pp 52-58.

3. Books with Authors and Editors:

a) The carbohydrates: Chemistry and Biochemistry; Pigman, W. W., Ed.; Academic Press: New York, 1970; pp 45-50.

b) Hilman, L. W., In Dye Laser Principles with Applications; Durate, F. J.; Hilman, L. W.; Eds.; Academic press: New York, 1990; Chapter 1.

c) Lochbrunner, S.; Stock, K.; De waele, V.; Riedle, E., Ultrafast Excited-State Proton Transfer: Reactive Dynamics by Multidimensional Wavepacket Motion. In Femtochemistry and Femtobiology: Ultrafast dynamics in Molecular Science; Douhal, A.; Santamaria, J., Eds.; World Scientific: Singapore, 2002; pp 202-212.

d) Femtochemistry and Femtobiology: Ultrafast Reaction Dynamics at Atomic Scale Resolution; Sundstrom, V., Ed.; World Scientific: Singapore, 1997; Chapter 2.

4.TechnicalReport: Schneider, A. B. Technical Report No. 1234-56, 1985; ABC Company, New York.

5.Patent: Kealy, T. J. US Patent 3 062 820, 1962; Chem. Abstr. 1963, 58, 9101.

6. Thesis:

Flink, S. Sensing Monolayers on Gold and Glass. Ph.D. Thesis, University of Twente, Enschede, the Netherlands, 2000.

7. Conference or Symposium Proceedings:

Huber, O.; Szejtli, J. Proceedings of the IV International Symposium on Cyclodextrins; Munchen; Kluwer Academic Publishers: Dordrecht, 1988.

8. Software Acquired from a Company:

Alchemy: A Molecular Modeling System for the IBMPC; Tripos Associates, Inc.: St. Louis, MO, 1988.

9. Software Accessed through the Internet:

CLOGP Program. Daylight Chemical Information systems, Inc. http://www.daylight.com/daycgi/clogp.

10. Internet Source:

Should include Author names (if any), Title, Internet website, URL, and (date of access).

11. Prepublication Online Articles (Already accepted for publication) :

Should include Author names (if any), Title of Digital Database, Database Website, URL, and (date of access).

Tables: Tables should be numbered with Arabic numerals and referred to by number in the Text (e.g., Table 1). Each Table should be typed on a separate page with the legend above the Table, while explanatory footnotes, which are indicated by superscript lowercase letters, should be typed below the Table.

Illustrations: Figures, drawings, diagrams, charts and photographs are to be numbered in a consecutive series of Arabic numerals in the order in which they are cited in the text. Computer-generated illustrations and good-quality digital photographic prints are accepted. They should be black and white originals (not photocopies) provided on separate pages and identified with their corresponding numbers. Actual size graphics should be provided, which need no further manipulation, with lettering (Arial or Helvetica) not smaller than 4.5 points, lines no thinner than 0.5 points, and each of uniform density. All color should be removed from graphics except for those graphics to be considered for publication in color. If graphics are to be submitted digitally, they should conform to the following minimum resolution requirements: 1200 dpi for black and white line art, 600 dpi for grayscale art, and 300 dpi for color art. All graphic files must be saved as TIFF images, and all illustrations must be submitted in the actual size at which they should appear in the journal. Note that good quality hardcopy original illustrations are required for both online and mail submissions of manuscripts.

Text Footnotes: The use of text footnotes is to be avoided. When their use is absolutely necessary, they should be typed at the bottom of the page to which they refer, and should be cited in the text by a superscript asterisk or multiples thereof. Place a line above the footnote, so that it is set off from the text.

Supplementary Material: Authors are encouraged to provide all supplementary materials that may facilitate the review process, including any detailed mathematical derivations that may not appear in whole in the manuscript, crystallographic information files (CIFs) and cited preprints. As to CIF files, the author must deposit the corresponding CIFs with the Cambridge Crystallograghic Data Centre (CCDC). The E-mail address of CCDC is: (deposit@ccdc.cam.ac.uk).

The deposited material is indicated in the manuscript by a footnote as follows:

Supplementary data: Crystallographic data for the structural

analysis reported in this paper have been deposited with the Cambridge Crystallographic Data Centre, CCDC, Number (...). Copies of the information may be obtained free of charge from Director, CCDC, 12 Union Road, Cambridge, CB2 1EZ, UK (Fax: +44-1223-336033; e-mail; deposit@ccdc.cam.ac.uk, home page: http//www.ccdc.cam.ac.uk).

Theoretical Calculations: Reporting the results of electronic structure calculations should follow the guidelines in J. E. Boggs (Pure and Appl. Chem. 1998, 70(4), 1015-1018). Reporting force field parameters and other energy surface data should follow the guidelines in D. J. Raber and W. C. Guida (Pure and Appl. Chem. 1998, 70(10), 2047-2049). Both sets of guidelines are available online at the IUPAC Website (http://www.iupac.org/reports/1998/index.html).

X-Ray Data: X-ray data presented in the text and/or tables should provide information on the empirical formula, unit cell dimensions (a, b, c in pm or Å; α, β, χ in degrees) with corresponding standard error estimates, number of formula units in the unit cell, density (measured or calculated), crystal system, space group symbol, diffractometer type, radiation, and monochromator used, temperature, data collection mode, the θ-range and reciprocal lattice segments, number of reflections measured, number of symmetry-independent reflections, cut-off criterion, linear absorption coefficient, absorption correction method, method of solution and refinement, positional and atomic displacement parameters, final R and Rw. A table of selected bond distances and bond angles may also be included.

Revised Manuscript and Computer Disks: Following the acceptance of a manuscript for publication and the incorporation of all required revisions, authors should submit an original and one more copy of the final manuscript typed double-spaced plus a 3½" disk containing the complete manuscript in Microsoft Word for Windows 2000 or a later version thereof. Original Figures should be submitted with the final, revised manuscript even if art is submitted electronically. All graphic files must be saved as TIFF images, and all illustrations must be submitted in the actual size at which they should appear in the journal. A list of the software programs used for text, art and file names on the disk should also be provided. Label the Disk with the author's last name, title of the manuscript, and date. Package the disk in a disk mailer or protective cardboard.

Reprints: Twenty (20) reprints are provided to the author responsible for correspondence free of charge. For orders of more reprints, a reprint order form and prices will be sent with article proofs, which should be returned directly to the Editor for processing.

Copyright

Submission is an admission by the authors that the manuscript has neither been previously published nor is being considered for publication elsewhere. A statement transferring copyright from the authors to Saudi Chemical Society is required before the manuscript can be accepted for publication. The necessary form for such transfer is supplied by the Editor-in-Chief with the article proofs. Reproduction of any part of the contents of a published work is forbidden without a written permission by the Editor-in-Chief.

Disclaimer

Articles, communication or editorials published by AJC represent the sole opinions of the authors. The publisher shoulders no responsibility or liability whatsoever for the use or misuse of the information published by AJC.

Indexing

AJC is currently applying for indexing and abstracting to all related International Services, including the Chemical Abstract Service and the Science Citation Index Service

Arabian Journal of Chemistry

Table of Contents

Arabian J. Chem. Vol. 1, No. 1, 1-8 (2008).

Colorimetric Determination in Pure Form and in Pharmaceutical Formulations

Hosny A. El-Moazen[a] and Alaa S. Amin[b]

[a]Department of Chemistry, Faculty of Applied Science, Umm Al-Qura University, Makkah Ulmokarramah Kingdom of Saudi Arabia, E-mail-asamin2002@hotmal.com

[b]Chemistry Department, Faculty of Science, Benha University, Benha, Egypt

Abstract

A simple, accurate, precise and sensitive colorimetric method for the determination of Paracetamol is described. This method is based on the formation of charge transfer complex with 4-chloro-7-nitro-2,1,3-benzoxadiazole (NBC-Cl) in acetone-aqueous medium [30% (v/v)]. The orange color product is measured at 475 nm for the formed complex. The optimization of various experimental conditions is described. Beer′s law is obeyed in the range 0.5-3.5 μg ml^{-1}, while that obtained applying Ringbom is 1.5-32.5 μg ml^{-1} . The molar absorptivity , sandell sensitivity, detection and quantification limits are calculated. The results obtained showed good recoveries of 100.3± 1.1, with relative standard deviation of 0.98% for the formed colored complex. Application of the proposed method to representative pharmaceutical formulations are successfully compared to the official method .

Keywords: Paracetamol determination ; 4-chloro-7-nitro2,1,3-benzoxadiazone; colorimetry; charge transfer complexes; pharmaceutical formulations.

1.Introduction

Paracetamol [CAS 103-90-2](acetaminophen or N-acetyl-4aminophenol) is widely used as an analgesic and antipyretic agent [1]. Analytical interest in Paracetamol has been discussed in review [2,3]. Overdoses of Paracetamol causes hepatic necrosis, probably owing to its metabolite, N-acetal-p-benzoquinone . Diagnosis must be quick and rapid method for the determination of Paracetamol are, therefore, needed. Several types of analytical procedure for Paracetamol determination have been proposed e.g. fluorometric [4], titrimetric [5,6], electroanalytical [7,8], colorimetric [9-13], UV-visible absorption [14-16],turbidimetric [17] and chromatographic[18-22].

Paracetamol and its dosage form are officially in the BP [23]and USP [24]. The BP describes the titrimetric assay for the bulk drug, whereas a spectrophotmetric method is used for the dosage forms. In the USP [24], Paracetamol is determined spectrophotometrically in the bulk drug but in the dosage forms it is determined using various techniques including colorimetry, spectrophotometry, high performance liquid chromatography (HPLC) and gas liquid chromatography (GLC) due to the presence of Paracetamol in combination with other analgesics, e.g. salicylamide, oxyphenbutazone, analgin, caffeine, and mefenamic acid . The aim of the present work is to investigate a new procedure for the determination of Paracetamol in pure and in dosage forms without interference of other analgesics, additives and exipients usually present in its dosage forms.

The molecular interaction between electron donors and acceptors are generally associated with the formation of

intensely coloured charge transfer complexes, which absorb radiation in the visible region [25]. The colorimetric methods based on these interactions are simple and convenient because of the rapid formation of the complexes. 4-Chloro-7-nitro-2,1,3-benzoxadiazole has been the subject of many investigations in analytical methods as a chromogenic reagent [26]. Yet, no work has been performed to use NBD-Cl as π- acceptor. The goal of the present work is to apply NBD-Cl to react with paracetamol yielding a colored CT complex and presenting a simple and rapid assay procedure for the studied drug in pure and in pharmaceutical formulations. This work describes a colorimetric method that can be used in laboratories where modern and expensive apparatus such as that required for GLC or HPLC is not available.

2. Experimental

Materials

Reference standard of salicylamide, oxyphenbutazone, analgin, caffeine, mefenamic acid and paracetamol were obtained from Egyptian International Pharmaceutical Industries Company (EIPICO). A 10^{-3} M of paracetamol was prepared by dissolving 0.0378 g in least amount of water in a 250 ml measuring flask and completed to the mark with water. Working solutions of lower concentration were freshly prepared by appropriate dilution of the standard one. Either standard or working solution was protected from the light during this investigation.

Reagents :

Analytical reagent grade chemicals were used whenever possible, unless otherwise stated.

Stock solution 1.5 x 10^{-2} M of NBD-Cl (Aldrich product) was prepared by dissolving 0.2994 g of pure reagent in 10 ml acetone in a 100 ml measuring flask and completed to the mark with the same solvent.

Apparatus :

A Perkin-Elmer Lambda 3B and Shimadzu 260 spectrophotometers with matched 10 mm quartz cells were used for all absorbance measurements during the development of the procedure.

General Procedure :

Aliquot containing 5.0 - 350 µg of the standard drug solution was transferred into a l0 ml calibrated flask. 1.0 ml of 1.5 x 10^{-2} M solution of NBD-Cl was added and heated on a water bath at 70 °C for 5.0 min. After cooling, the mixture was diluted with acetone and water to achieve 30% (v/v). The absorbance was measured at 475 nm for the formed CT complex, against a reagent blank prepared in the same manner.

Stoichiometric ratio

The molar ratio and continuous variation methods were applied to study the stoichiometric ratio of the charge transfer formed. A 5 x 10^{-3} M standard solution of paracetamol and reagent were used. In the former method a constant volume of 5 x 10^{-3} M paracetamol solution was employed and the reagent concentration was changed to obtain different ratios for the CT complex, while in the latter method, a series of solutions was kept at 2.0 ml. The reagent was mixed in various proportions and heated in a water bath of 70 °C for 5.0 min, cooled and then diluted to volume in a 10 ml calibrated flask with acetone and water to achieve 30% (v/v) solvent ratio as mentioned in the general procedure.

Procedure for pharmaceutical formulations

A known number of tablets are weighed and ground into a fine powder. A portion of the powder containing about 100 mg paracetamol is weighed accurately, mixed with about 50 ml of water and stirred for 10 min. The insoluble mass is filtered off on a Whatman No.41 filter paper, washed

with water and the filtrate plus washings are diluted to 500 ml with water in a measuring flask.

Known volumes of syrup are directly diluted with water. Granules of paracetamol for making the suspension produce viscous slurry owing to the presence of gelatinous material that is difficult to filter. Such samples, and those, which also contain analgin, are finely ground and paracetamol is extracted with three successive 20 ml portions of acetone. The combined extracts are warmed in a boiling water-bath to evaporate acetone and remaining residue is dissolved in water. Aliquot of this solution was transferred and follows the general procedure to determine paracetamol contents in its dosage forms.

3. Results and discussion

Paracetamol, which does not have a chromophore that absorbs above 330 nm, can be determined colorimetrically by the formation of acetone-aqueous soluble complex with NBD-Cl. The formation of orange color species of charge transfer complex is based on π-π^* interaction between benzene ring present in the donating drug to that present in the NBD-Cl moiety and produces a bathochromic shift of 105 nm for the formed complex, since NBD-Cl absorbed at 370 nm. The absorbance of the complex is then measured at its maximum wavelength (475 nm). Investigations were carried out to establish the most favourable conditions for the charge transfer formation. The influence of some variables on the reaction has been tested as follow.

Effect of reagent concentration

The amount of NBD-Cl necessary to obtain a linear graph for a drug concentration was studied. When various concentrations of the reagent were added to 15 µg ml^{-1} of paracetamol, 1.0 ml of 1.5 x 10^{-2} M NBD-Cl solution was found to be sufficient for the production of maximum and reproducible color intensity. Higher concentrations of NBD-Cl did not affect the color intensity [Fig. 1].

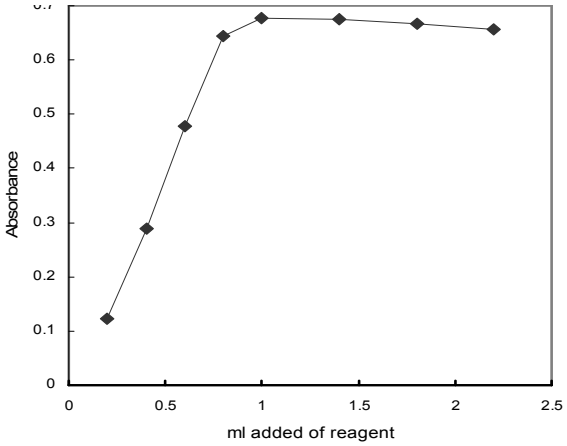

Figure 1. Effect of 1.5× 10^{-2} M reagent on 15 µg ml^{-1} of paracetamol.

Effect of time and temperature

The optimum reaction time was determined by following the color development at ambient temperature (25 ± 2 °C). Complete color development was attained after 1.0 hr. Whereas this time was reduced to 5.0 min on raising the temperature to 70 °C on a water bath to obtain complete color development. The color remained stable for 15 hrs for paracetamol charge transfer complex, [Fig. 2].

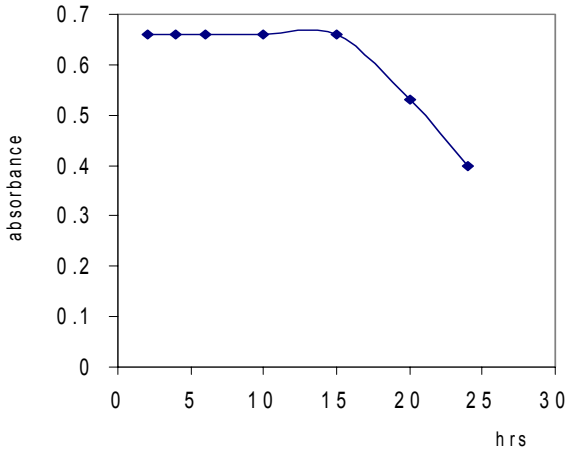

Figure 2. Effect of time on the stability of 15 µg ml^{-1} of paracetamol complex.

Effect of pH

When using acidic, neutral or basic buffer media, the reagent forms an orange yellow color which is absorbed at λ_{max} 373 and 450 nm. This will decrease the absorbance of the sample solution when it used as, blank, so the sensitivity of the procedure decrease in addition to an increase in the detection and quantification limits.

Effect of solvent

Several organic solvents, i.e methanol, ethanol, propanol, acetone, dioxane, acetonitrile and dimethylformamide (DMF), were investigated. Acetone was found to be the best solvent for the charge transfer complex formation, because it has a high relative permittivity which ensures the maximum yield of CT complexes. Moreover, the percentage of solvent was also investigated and it was found that 30% (v/v) gave the highest absorbance (Fig. 3).

On the other hand, ethanol and acetonitrile are possible substitutes, but it takes more time to achieve the same sensitivity using the former, whereas using the later a yellow orange reagent blank is formed which decreases the sensitivity of the procedure.

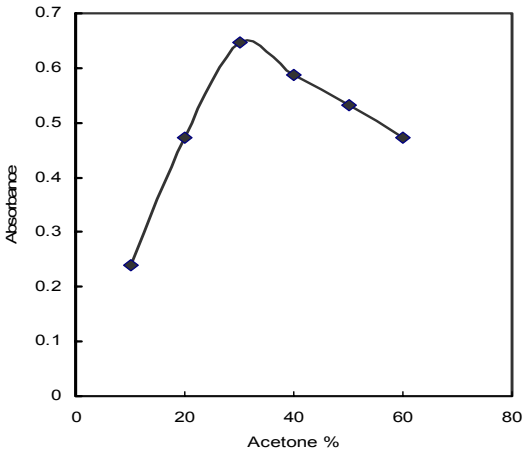

Figure 3. Effect of acetone ratio on 15 µg ml^{-1} paracetamol complex.

Stiochiometric ratio

The stoichiometric ratio of paracetamol to NBD-Cl in the colored complex was determined using the molar ratio and continuous variation methods. It is apparent from the data that charge transfer complex with paracetamol to NBD-Cl ratio 1:1 are formed. The logarithmic stability constants of the formed complex are calculated from the Harvey and Manning method [27] using the data of the molar ratio and continuous variation method [Table 1].

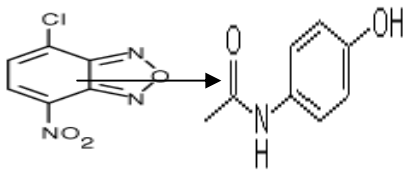

Charge transfer complex

Quantification

A linear correlation was obtained between absorbance and concentration in the range given in Table 1. For more accurate analysis, the Ringbom optimum concentration range was obtained by plotting the percentage of transmittance *vs* the logarithmic value of concentration in µg ml^{-1} (Fig. 4). Regression plots showed that there was a linear dependence of absorbance on concentration over the Beer's law ranges. The molar absorptivity, Sandell sensitivity, slope, intercept and correlation coefficients obtained by the linear least squares treatment of the results are also given in Table 1.

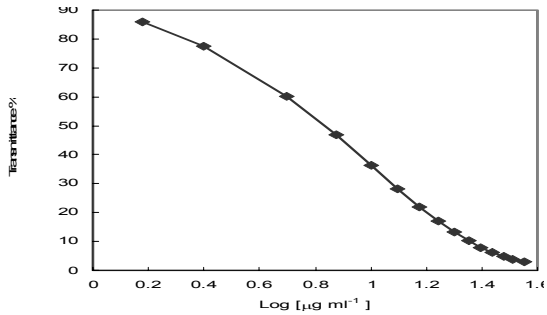

Figure 4. Ringbom optimum concentration range for paracetamol

The precision of the proposed method was tested by analyzing eight replicate samples of paracetamol (15 μg ml^{-1}). The relative standard deviation and range of recovery obtained are given in Table 1. The standard deviation of the absorbance measurements was obtained from a series of 13 blank solutions. The limits of detection (K=3) and of quantification (K=10) of the methods were established according to IUPAC definition, (C_1= KS_o/s where C_1 is the limit of detection, S_o is the standard deviation of the blank determination, s is the slope of the standard curve and K is the constant related to the confidence interval [28]). The values were calculated and recorded in Table 1.

The performance of the proposed method was assessed by comparison with the official method [23] (depending on titration with 0.1 M ammonium cerium(IV) sulphate using 0.1 ml ferroin). Mean values were obtained in a Student's t- and F- tests at 95% confidence limits for five degrees of freedom [29], and the results recorded in Table 1 showed that the calculated t- and F- values did not exceed the theoretical values.

Comparison of the recovery obtained with the proposed method with the purity of paracetamol as determined according to the official methods [23] showed a high accuracy of the present method. The proposed method is simpler, less time consuming and more sensitive than the official method. Moreover, the proposed method could be used for the routine determination of paracetamol in pure form or in pharmaceutical formulations.

Comparison of the results obtained by the proposed method with those obtained by HPLC methods [18-22] showed that the recommended procedure is more economical as regards reagent consumption and time required for the analysis without any loss of accuracy or precision in addition to a wider range of determination.

Interferences

The diluents and additives such as calcium lactate, lactic acid, zinc stearate, magnesium stearate, lactose, starch, carboxymethyl cellulose did not interfere with the analysis of the drugs in the proposed method, even when present in high concentration. Also there is no interference from either the synthesis respective byproducts or from the degraded products resulting from thermal and hydrolytic treatment as phenol, acetylamine and p-aminophenol. The obtained results indicate a high selectivity of the method examined in the determination of the studied drugs.

Analytical applications

The proposed colorimetric method was applied to the determination of paracetamol in dosage forms (commercial products randomly collected from Makkah El- Mokarama). Table 2 lists the results obtained by the proposed colorimetric and official methods [23] (based on titration with 0.1 M ammonium cerium(IV) sulphate using 0.1 ml ferroin). The results indicate good agreement with the official method. The proposed method has the advantage of being virtually free from interferences by excipients such as glucose, lactose and starch or from common degradation product as p-aminophenol. The proposed colorimetric procedure can be recommended for routine analysis in the majority of drug quality control laboratories. Another favourable characteristic of the proposed method is that the absorbance of the CT complex is stable for at least 15 hrs.

The performance of the proposed colorimetric method was assessed by calculation of the t- and F- values compared with our previously work [12,16,17] for the same drug. Mean values were obtained in a Student's t- and F- tests and 95% confidence limits for five degrees of freedom [29] and the results showed that the calculated t- and F- values did not exceed the theoretical values. On comparing The results obtained by the proposed colorimetric

procedure with those of the BP [23] method using the t- test for the accuracy and F- test for the precision assessment [29], the calculated values did not exceed the corresponding theoretical values, indicating insignificant differences between results. The relative standard deviation of the proposed method was 0.98, for the forme CT complex, whereas for the pharmacopoeial method it was 1.88 (six determinations). The proposed colorimetric method is simple, sensitive and accurate with high recoveries amounting to 100.3 ± 1.1% compared with 100.5 ± 2.2 % using the official method.

4. Conclusion

The proposed method is simple, sensitive, rapid, precise, selective and accurate compared with the official method [23]. Although the color development of the charge transfer complex formed at room temperature (25 ± 2°C) requires one hr for complexation, this can be shortened to 5.0 min by raising the temperature to 70 °C on a water bath. The proposed method is suitable for the determination of paracetamol in pharmaceutical formulations and biological fluids without interferences of excipients or degradation products, suggesting applications in bulk analysis.

Although the high performance liquid chromatographic methods have a higher selectivity, they require complicated sample pretreatment and using expensive apparatus. The proposed method has the advantages of sensitivity, selectivity, ease of performance, economy, wider range of determinations, less time consumption, high accuracy and precision compared to the official methods [23].

Table 1. Analytical characteristics of the proposed procedure, precision and accuracy

Parameter	Paracetamol complex	Parameter	Paracetamol complex
λ_{max} (nm)	475	Regression equation*	
Acetone –Aqueous ratio, %	30	Slope	0.044
Beer's law limits, µg ml^{-1}	0.5 – 35.0	Intercept	-0.007
Ringbom optimum conc., µg ml^{-1}	1.5 -32.5	Correlation coefficient (r)	0.9998
Molar absorptivity, L mol^{-1} cm^{-1}	$6.64x10^3$	RSD % of slope	4.34×10^{-4}
Sandell sensitivity, µg cm^{-2}	0.0227	RSD % of intercept	1.92×10^{-4}
Detection limits, ng ml^{-1}	45	Range of error, %	± 0.9
Quantification limits, µg ml^{-1}	0.15	Standard deviation, %	0.58
Stoichiometric ratio	1 : 1	RSD, %	0.98
Stability constant	6.56	Student t-value (2.57)**	1.24
Stability / hr	15	Variance ratio F-test (5.05)**	2.59

* A= a + bC, where C is the concentration in µg ml^{-1}.

** Theoretical values for five degree of freedom and 95% confidence limits.

Table 2: Assay of paracetamol in bulk dosage forms by the proposed colorimetric and official procedures

Tablets Sample	Company	Taken μg ml^{-1}	Proposed method Found* μg ml^{-1}	Proposed method Recovery ± SD (%)	Official method [23] Found* μg ml^{-1}	Official method [23] Recovery ± SD (%)
Panadol[a]	Australia	10.0	9.88	98.80 ± 0.80	9.80	98.00 ± 1.70
		20.0	20.25	101.25 ± 1.00	20.36	101.8 0 ± 2.00
Panadol [b]	Indonesia	8.0	8.04	100.50 ± 0.50	8.10	101.25 ± 1.30
		16.0	16.15	100.94 ± 0.70	15.75	98.44 ± 1.50
Panadol [c]	Saudi Arabia	7.0	7.05	100.71 ± 0.60	6.85	97.86 ± 2.20
		14.0	14.25	101.79 ± 0.90	13.70	97.86 ± 1.80
Panadol [d]	Ireland	5.0	4.93	98.60 ± 0.90	4.90	98.00 ± 2.30
		15.0	15.15	101.00 ± 0.50	14.75	98.33 ± 2.00
Panadol [e]	Pakistan	14.0	14.15	101.07 ± 0.70	13.75	98.21 ± 1.60
		28.0	27.75	99.11 ± 0.60	28.50	101.79 ± 2.10
Panadol [f]	India	11.0	10.80	98.18 ± 1.20	11.25	102.27 ± 1.90
		22.0	22.30	101.36 ± 0.90	22.40	101.82 ± 2.00
Panadol [g]	Kuwait	15.0	15.20	101.33 ± 0.90	14.75	98.33 ± 2.00
		30.0	29.65	98.83 ± 1.10	30.50	101.67 ± 1.80
Panadol [h]	Bangladesh	6.0	5.96	99.33 ± 0.80	5.90	98.33 ± 2.00
		12.0	11.93	99.41 ± 1.20	12.10	100.83 ± 1.70
Panadrex[i]	Qatar	13.0	13.08	100.62 ± 1.10	12.85	98.58 ± 1.30
		26.0	25.80	99.23 ± 0.90	26.30	101.15 ± 1.10
Panadrex[j]	El Bahrain	9.0	8.96	99.56 ± 0.60	8.85	98.33 ± 1.80
		18.0	18.05	100.28 ± 0.40	17.65	98.06 ± 1.90
Panadol [k]	United Arab Emaret	7.0	6.46	99.43 ± 0.70	7.10	101.43 ± 1.60
		14.0	14.10	100.71 ± 0.50	13.73	98.21 ± 1.50

***** Mean of six determinations.

[a]: Sinus Smithkline Beecham, Australia.

[b]: Cold &Flu, Glaxo Smithkline (500 mg paracetamol, 30 mg pseudoephedrine HCl and 2 mg chlorpheniramine maleate).

[c]: Spimaco, El-Dwaiia, Kingdom of Saudi Arabia.

[d]: Glaxo Smithkline, Dungarvan Ltd., Ireland.

[e]: Sinus Smithkline Beecham, Australia.

[f]: Smithkline Beecham (Dungarvan), Dungarvan Ireland.

[g]: Sinus Smithkline Beecham, Australia.

[h]; Smithkline Beecham (Dungarvan), Dungarvan Ireland.

[i]: El-Dwaiia, Kingdom of Saudi Arab

[j]: El-Dwaiia, Kingdom Saudi Arabia.

[k]: Smithkline Beecham (Dungarvan), Dungarvan Ireland.

References

[1] Rent, B.G.; Wittcoff, H.A., Pharmaceutical Chemicals in Perspective, Wiley New York, 1989, P. 308.

[2] Fairbrother, J. E., Analytical Profiles of Drug Substance, Academic, Orlando, 1972, P.2.

[3] El-Obeid, A.; Al-Bard, A., Analytical Profiles of Drug Substance, Academic, Orlando, 1985, P.551.

[4] Moreira, A.B.; Oliveira, H.P.M.; Atvars, T.D.Z.; Dias, I.L.T.; Neto, G.O.; Zagatto, E.A.G.; Kubota, L.T., Anal. Chim. Acta 2005, 539, 257.

[5] Walash., M. I.; Agrawal, S. P.; Martin, M. I., Can. J. Pharm. Sci. 1972, 7, 123.

[6] Verma, K. K.; Jain, A., Anal. Chem. 1986, 58, 821.

[7] Bezuglyi, V.D.; Zhukova, T.V.; Shapovalov, V.A.; Slyusar, S.N., Farmatsiya 1982, 31, 42.

[8] Nicolic, K.I.; Velasevic, K.R., Acta Pol. Pharm. 1985, 42, 209.

[9] Verma, K.K.; Gulati, A.K.; Palod, S.; Tyagi, P., Analyst 1984, 109, 735.

[10] Mohamed, F.A.; Abd-Allah, M.A.; Shamoa, S.M., Talanta 1997, 44, 61.

[11] El-Dien, F.A.N.; Zayed, M.A.; Mohamed, G.G., Fenxi Ceshi Xue Bao 1999, 18, 31.

[12] Amin A.S., Quim. Anal. 2000, 19, 135.

[13] Issopoulos, P.B., Anal. Lett. 1990, 23, 1057.

[14] Dogan, H.N., IL. Farmaco 1996, 51, 145.

[15] Filik, H.; Hayvali,M.; Kilic, E., Anal. Chim. Acta 2005, 535, 177.

[16] Amin, A.S., Sci. Pharm. 2001, 69, 179.

[17] Amin, A.S.; El-Maamly, M.Y., Qum. Anal. 2002, 19, 275.

[18] EL-Shanawany, A.; EL-Sadek, M.; Khier, A.A.; Rucker, G., Indian J. Pharm. Sci. 1991, 53, 209.

[19] Markovic, S.; Kusec, Z., Pharmazie 1990, 45, 935.

[20] Cockaerts, P.; Roets, E.; Hoogmartens, J., J. Pharm. Biomed. Anal. 1986, 4, 367.

[21] Bohnenstengel, F.; Kroemer, H.K.; Sperker, B., Chromatogr. B.; Biomed. Appl. 1999, 721, 295.

[22] Patil, S.T.; Sundaresan, M.; Bhoir, I.C.; Bhagwat, A.M., Talanta 1998, 47, 3.

[23] British Pharmacopoeia, H.M. Stationary Office, London, 1993, 483-484.

[24] USP Pharmacopoeia XXIV, US Parmacopoeia Convention, Inc., Mack. Publishing Company, Easton, 2000.

[25] Faster,R., Ed "Organic Charge Transfer Complexes", Academic Press, London, p. 387, 1969.

[26] Saleh, H.; Schnekenburger, J., Analyst 1992, 117, 87.

[27] Harvey, A.E.; Manning, D.L., J. Am. Chem. Soc. 1950, 72, 4488.

[28] IUPAC Compendium of Analytical Nomenclature, Definitive Rules, In: Irving, H.M.N.H.; Freiser, H.; West, T.S., (Eds.) Pergamen Press, Oxford, 1981.

[29] J.C. Miller, J.N. Miller, “Statistics in Analytical Chemistry”, 3rd Edn., Ellis Horwood, Chichester, 1993.

Arabian J. Chem. Vol. 1, No.1, 9-24 (2008)

Spectroscopic Studies of Charge Transfer Complexes of Meso-tetratolylporphyrin With π-electron Acceptors in Different Organic Solvents

Mohamed E. El-Zaria, Ahmed O. Alnajjar* and Afaf R. Genady

Department of Chemistry, College of Science, King Faisal University, P.O. box 380, 31982-Hofuf, Saudi Arabia

Abstract

The charge-transfer complex (CTC) formation of 5,10,15,20-tetra(4-tolyl)porphyrin (TTP) and Zn-5,10,15,20-tetra(4-tolyl)porphyrin (Zn-TTP) with some aromatic nitro acceptors such as picric acid (PIC), 3,5-dinitro-salicylic acid (DNS), 3,5-dinitro-benzoic acid (DNB), and 2,4-dinitro-phenol (DNP) has been studied spectrophotometrically in dichloromethane, chloroform and carbon tetrachloride solutions at different temperatures. The spectrophotometric titration, Job's and straight line methods indicate the formation of 1:1 charge-transfer complexes. The values of the equilibrium constant (K_{CT}) and molar absorbitivity (ε_{CT}) were calculated for each complex. The ionization potential of the donors and the dissociation energy of the charge transfer excited state for the CTC in different solvents also determined and was found to be constant. The spectroscopic and thermodynamic properties were observed to be sensitive to the electron affinity of the acceptors and the nature of the solvent. No CT band was observed between Zn-TTP as donor and DNP or DNB as acceptors in various organic solvents at different temperatures. Bimolecular reactions between singlet excited TTP (^{1}TTP*) and the acceptors were investigated in solvents with various polarity. A New emission band was observed. The fluorescence intensity of the donor band decreases with increasing the concentration of the acceptor accompanied by increasing in the intensity of the new emission. The new emission of the CTCs can be interpreted as a CT excited complex (exciple).

Keywords: Charge Transfer Complexes; Porphyrin; Stoichiometry; Donor-acceptor; Fluorescence.

*To whom correspondence should be addressed. Phone:+966-(0)3-5800000- Ex. 1564, Fax: +966-(03) 5886437, E-mail: anajjar@kfu.edu.sa

1. Introduction

Porphyrins and metalloporphyrins have received much attention since their discovery. Porphyrins are very important compounds because of its wide use for photosensitizer in the model system of photosynthesis [1]. Furthermore, it has been found to be a suitable candidate for use in the photodynamic and boron neutron capture therapies of cancer of internal organs [2–5]. Thus its optical properties and photophysical behaviors continue to attract much interest.

The composition, the interchromophore separation/angular relationship, the overall dynamic and stimulus-induced reorganization, and the electronic coupling are crucial factors in the development of charge transfer reaction centers. EDA complexes are materials of current interest since they can be utilized as organic semiconductors [6], photocatalyst [7] and drug analysis [8,9] Such complexes have also found application in studying redox processes [10], microemulsion [11], non-linear optical properties [12], and electrical conductivities [13]. Formation energy of charge-transfer complexes depends on the ionization potential of the donor and the electron affinity of the acceptor. Absorption spectrum of the formed molecular complex shows a characteristics absorption band either in the visible or in the UV region [14]. Such band does not appear in the absorption spectra of both the donor and acceptor and can be used for identification of the charge transfer complex (CTC), particularly when the complex could not be isolated [15]. Recently there has been a considerable interest in the study of charge-transfer complexes (CTCs) between porphyrins and a variety of acceptor molecules [16-18].

In connection with our previous studies carried out on the charge-transfer complexes of porphyrins with TCNE acceptor [17], here we report on the results of UV-vis studies, equilibrium constant, extinction coefficient, stoichiometry, thermodynamic parameters, ionization potential, and fluorescence quenching data concerning the interaction of 5,10,15,20-tetra(4-tolyl)porphyrin (TTP) and Zn-5,10,15,20-tetra(4-tolyl)porphyrin (Zn-TTP) with aromatic nitro acceptors such as picric acid (PIC), 3,5-dinitro-salicylic acid (DNS), 3,5-dinitro-benzoic acid (DNB), and 2,4-dinitro-phenol (DNP) in different organic solvents.

2. Experimental

The acceptors (PIC, DNS, DNB, and DNP) were commercially available from Aldrich Co. and were used without any further purification. TTP and Zn-TTP of the highest purity was prepared according to the literature method [19]. BDH solvents such as dichloromethane (CH_2Cl_2), chloroform ($CHCl_3$), and carbon tetrachloride (CCl_4) were redistilled before using. All UV–vis spectra were recorded on a Shimadzu 1601 PC spectrophotometer within the wavelength range 200–800 nm using the same solvent in the examined solution as a blank. Absorbance measurements as a function of time, at fixed wavelengths,

were made with the same instrument. For thermodynamic studies, the apparatus was equipped with a temperature controlled cell holder. Both sample and blank compartment were kept at constant temperature by a Shimadzu TCC-240A thermostat which allowed the temperature to be maintained constant to ±0.1 ^{o}C. The fluorescence (excitation and emission) spectra were determined with Shimadzu RF-5301 PC spectrophotometer: excitation slit width = 5 nm, emission slit width = 5 nm. Fresh solutions of porphyrins and acceptors were prepared before each series of measurements by dissolving precisely weighed amounts of the component in the appropriate volume of solvent. All solutions were kept in the dark except during sampling. Acceptor and donor solutions were added by a Finn pipette.

Photometric titrations at 670 and 665 nm were performed for the reactions of TTP with the acceptors (PIC, DNS, DNP, and DNB) and Zn-TTP with PIC and DNS, respectively. The donor was dissolved in dichloromethane at room temperature and the titration was monitored using a Shimadzu 1601 PC spectrophotometer. The procedure was as follows: X mL of (1.5 $\times 10^{-4}$ M acceptors = PIC, DNS and 0.2 M, acceptors = DNP, DNB) (where X = 0.25, 0.50, 0.75, 1.00, 1.50, 2.00, 2.50 and 3.00 mL) was added to 0.5 mL of 7.0 $\times 10^{-5}$ M TTP and Zn-TTP. The concentration of TTP and Zn-TTP in the reaction mixture was kept fixed at 7.0 $\times$ 10^{-6} M while the concentration of acceptors was varied. These concentrations produced donor:acceptor ratio from 1:0.5. The stoichiometry of the molecular CT-complexes under investigation were determined by the application of the conventional spectrophotometric molar ratio according to the known methods [20].

3. Results and Discussion

Absorption spectra

The electronic absorption spectra of the CTC of the TTP/PIC, TTP/DNS, TTP/DNP, and TTP/DNB systems were recorded using constant donor concentration 7 $\times 10^{-6}$ mol l^{-1} (in a given solvent) while the concentrations of the acceptors were varied within the range from 8 $\times 10^{-5}$ to 0.06 mol l^{-1} depending on the donor. The absorption spectra of mixed donor–acceptor solutions are characterized by the appearance of two new absorption bands at 455 nm and 670 nm which are stable under the studied conditions. The representative CT-spectra formed between TTP and DNP in CH_2Cl_2 at 25 ^{o}C is shown in Figure 1.

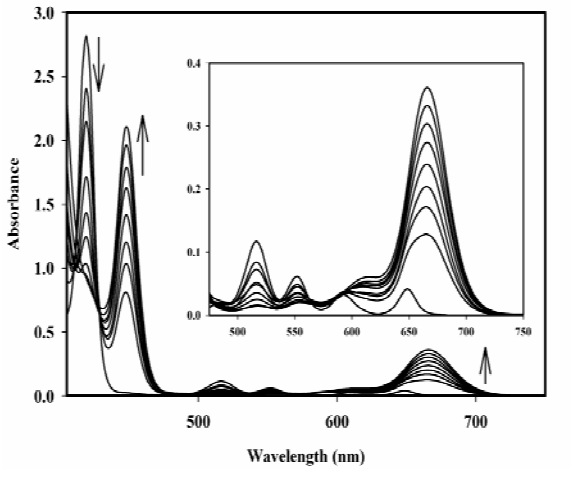

Figure 1. Electronic absorption spectra of the CTC solutions of TTP/DNP in CH_2Cl_2 at 25 ^{o}C. The concentration of TTP is 7 x 10^{-6} mol l^{-1}

Furthermore, the absorption intensities of these two new bands increases as the concentration of the acceptor is increased (Figure 1). Moreover, the absorbance increases as the temperature is decreased as shown in Figure 2.

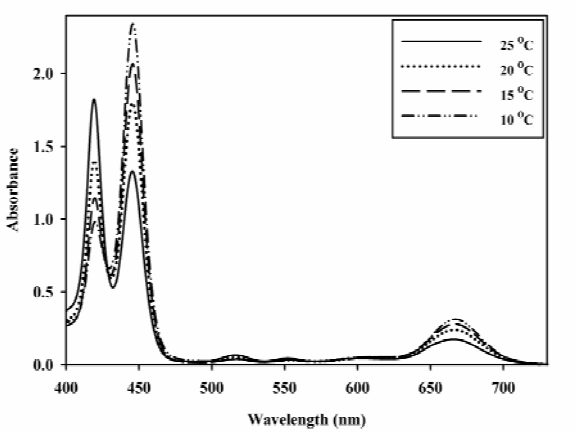

Figure 2. Variation of absorbance spectra of TTP/PIC system with temperature in $CHCl_3$. [TTP] = 7 x 10^{-6} mol l^{-1}, [PIC] = 2 x 10^{-5} mol l^{-1}.

These new absorption bands, which are attributed to the formation of CTCs, are stable at constant temperature.The new and broad absorptions bands indicates the formation of EDA complexes. The porphyrin is relatively electron rich and PIC, DNS, DNP, and DNB are relatively electron poor compounds. Consequently when a solution containing both an electron rich and electron poor compounds, they tend to associate with one another in a loose interaction known as EDA complexes. The new, low energy absorptions observed in solutions containing both a donor and an acceptor have been described by Mulliken [21] as charge transfer transitions involving the excitation of an electron on the donor to an empty orbital on the acceptor. The interaction between the TTP and acceptors gave the reaction by the formation of radical ion pairs as shown in Scheme 1. This phenomena was also supported by the decrease of absorption intensity on Q-bands at 525 nm, 560 nm, and 585 nm as well as slightly red shifting as the concentration of the acceptor increases. Two isoesbestic points are observed at 475 nm and 595 nm, indicating a single equilibrium (Figure 1). The interaction between TTP and π-acceptors gave π-π* transitions.

Although no reaction was found to occur between Zn-TTP/DNB or Zn-TTP/DNP systems under the same reaction conditions. A green color was obtained the on interaction of the Zn-TTP with PIC and DNS acceptors. The reaction is time dependent. The optimum reaction time is determined by following the color development spectrophotometrically at temperature of 293 ^{o}K for PIC and DNS reagents. It is found that, complete color development is attained after 30 min for PIC and DNS reagents, respectively as shown in Figure 3.

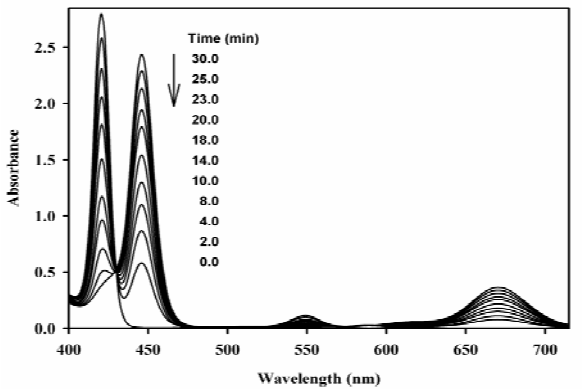

Figure 3. Effect of time on the absorbance of Zn-TTP/DNS system in CH_2Cl_2 at 20 ^{o}C. [TTP] = 7 x10^{-6} mol l^{-1}, [DNS] = 2.5 x 10^{-2} mol l^{-1}.

An interpretation of the small red shift phenomena of the CT band on going from CCl_4 to CH_2Cl_2 for such stronger complexes (K_{CT} = 75643-2.3668 l mol^{-1} at 298 ^oK), can be explained by taking into account that the contribution of the dative structure relative to the ground state becomes larger. One can expect that the red shift of the CT band caused by polarity change is smaller in stronger complexes than in weak ones since the solvent stabilization energy difference at ground and CT excited would be smaller for a strong complex than for a weak complex. A similar effect has been observed for the relatively strong complex between diethyl sulfide and iodine [22].

Determination of the stoichiometry .

Photometric titration measurements on the characteristic absorption bands of the CTCs prove that the complex formation occurs in 1:1 donor:acceptor ratio. These measurements were based on the detected bands at 670 nm for TTP/PIC and TTP-DNS; and at 665 nm for TTP/DNP, TTP/DNB, Zn-TTP/PIC, and Zn-TTP/DNS. In these measurements, concentration of TTP and Zn-TTP was kept fixed, while the concentration of the acceptors were varied as illustrated in the experimental section. Photometric titration curves based on these measurements are shown in Figure 4.

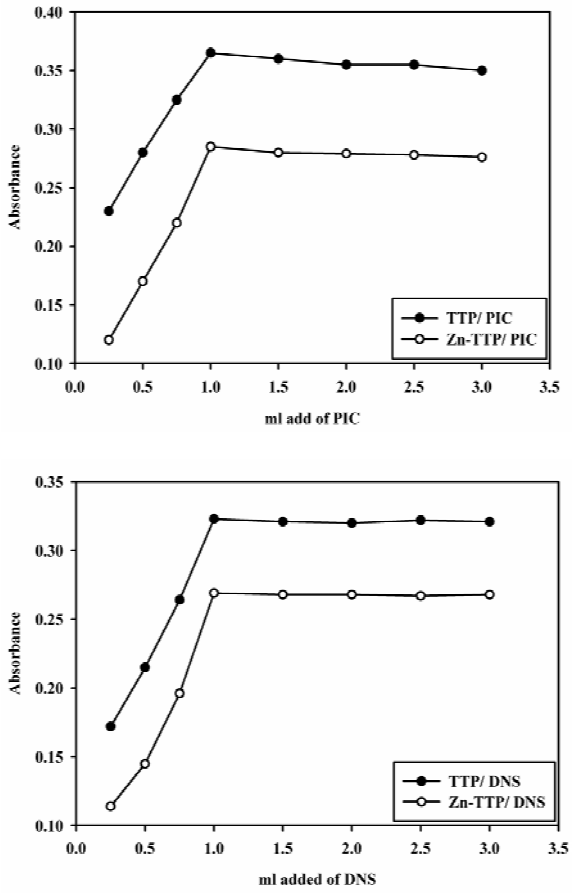

Figure 4. Photometric titration curves for the TTP/PIC, Zn-TTP/PIC, TTP/DNS, ZnTTP/DNS reactions in $CHCl_3$ at 670 nm.

The base acceptors equivalence points indicate that the ratio in all cases is 1:1 and this result agrees quite well with Job's continuous variation method as shown in Figure 5 [23, 24]. Further support has been observed in the straight line method which can be used as a qualitative mean for the determination of the stoichiometry ratio of the donor and acceptor in the complex [25]. In this case the logarithmic . Plot of absorbance (logA) versus volume (logV) gave straight lines with slopes varying from 0.95 to 1.0 which also proves the formation of the 1:1 CTC.

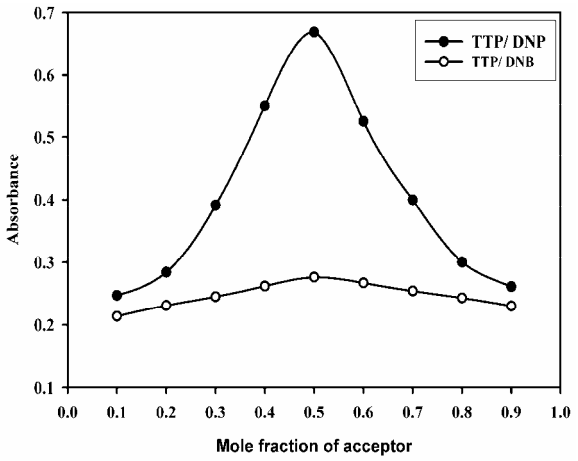

Figure 5. The plot of Job's method for TTP/DNP and TTP/DNB systems at 665 nm.

Formation constant and molar extinction coefficients of the CTC

Estimation of the formation constant (K_{CT}) and the molar absorption coefficients (ε_{CT}) of the CTCs are calculated using the known equation 1 [26].

$$\frac{[D_o]}{A-A_o} = \frac{1}{\varepsilon_{CT}-\varepsilon_D} + \frac{1}{(\varepsilon_{CT}-\varepsilon_D)K_{CT}[A_o]} \qquad (1)$$

Where A_o and A are the absorbance of the free donor solution and with acceptor complex at given wavelength, ε_D and ε_{CT}, are the molar extinction coefficients of the donor and the complex respectively, and $[D_o]$ is the initial concentration of the donor. For this purpose, the absorption spectra of solutions containing constant donor concentration and variable acceptor concentrations were recorded at four different temperatures within the range of 10–25 °C. The values of K_{CT} and ε_{CT} obtained at different temperature in all the solvents studied are listed in Table 1 and shown in Figure 6.

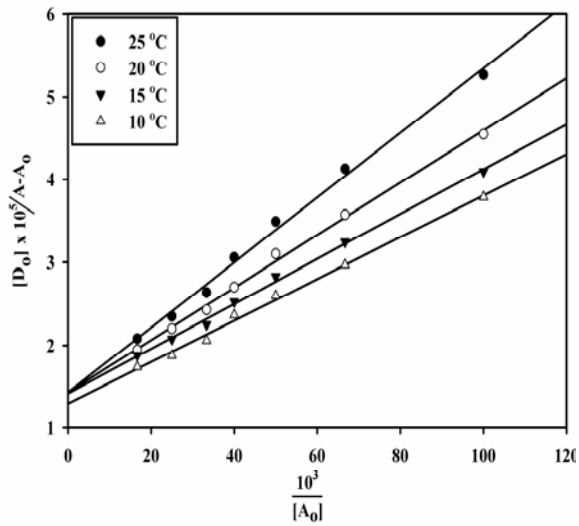

Figure 6. Relation between [Do]/A-Ao and 1/[Ao] for CTC of TTP/TCNE system in CH_2Cl_2 at different temperature.

The observed decrease in formation constant values with rise in temperature indicates the exothermic nature of the interaction between the studied acceptor and donor molecules. However, the increase in K_{CT} value with decreasing solvent polarity can be attributed to the stability of the dative structure D^+-A^- in a more polar solvent (Scheme 1).

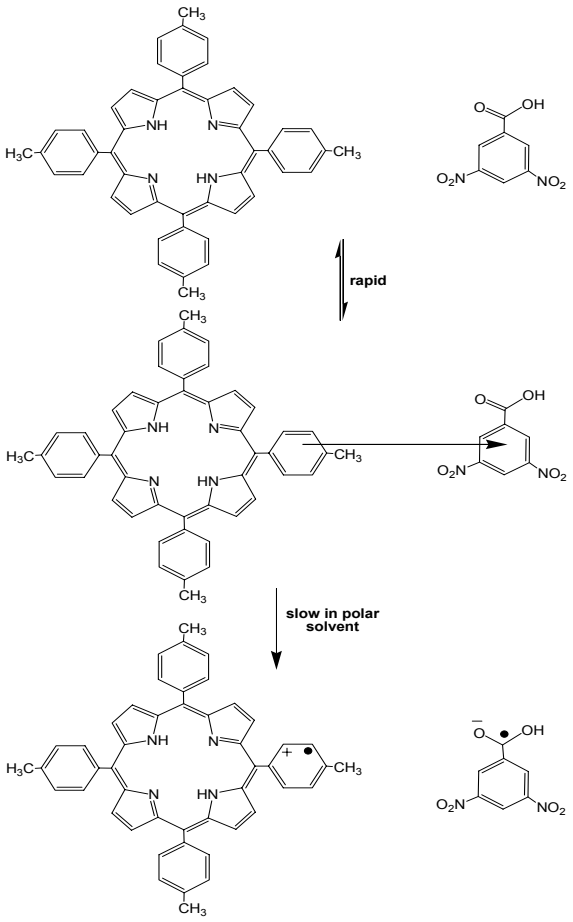

Scheme 1. The molecular structure of the compound and charge transfer transition between donor and acceptor.

To obtain information about the effect of the insertion of Zn into the porphyrin core on the K_{CT} values of TTP, it can be found that K_{CT} increases on going from TTP to Zn-TTP donors. The presence of Zn into the porphyrin core decreases the aromaticity and the ability of TTP as donor resulted in decreasing the values of K_{CT} (Table 2). As could be observed from the reported ε_{CT} values, there is a slight decrease with rising temperature in most cases. The decrease in ε_{CT} values with rising temperature is in agreement with Mulliken's theory [14] and can be attributed to the broadening of the CT band with increasing the temperature. The variation of ε_{CT} for the CTCs almost obeys the following sequence: TTP >Zn-TTP.

Thermodynamic parameters .

The thermodynamic parameters viz. Gibb's free energy, enthalpy and entropy changes were evaluated from the temperature dependence of the formation constant using the Van't Hoff plots and a representative plot is shown in Figure 7. As we can seen, there is no evidence of deviation from the linearity over the investigated temperature range indicating that a 1:1 complex formed over all investigated temperatures for all systems. The parameters thus obtained are represented in Table 3, and these values show that complexation is thermodynamically favored. The enthalpy change of the complexation also reveals that the CTC formation between the used donors and the acceptors is of exothermic in nature. The values of ΔH^o and ΔS^o generally become more negative as the stability constant values for molecular complexes increase.

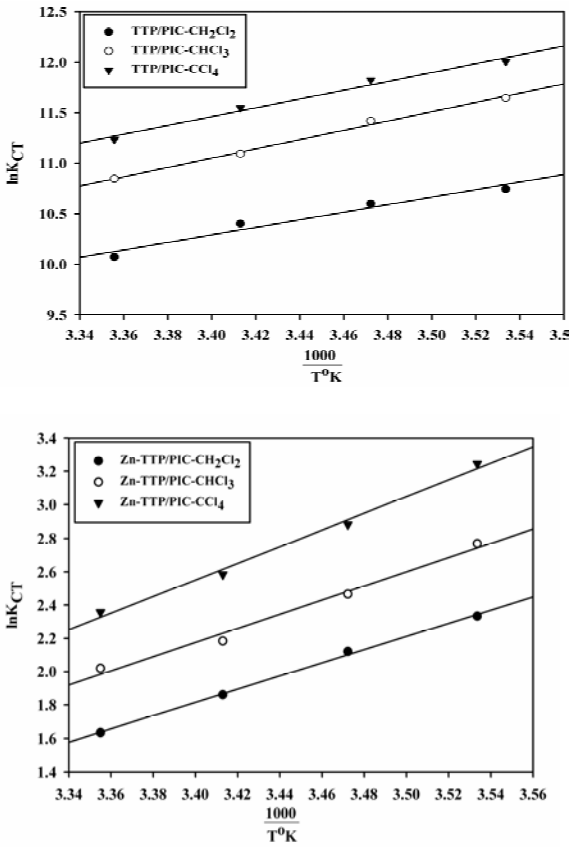

Figure 7. Relation between $\ln K_{CT}$ and 1000/TK for CTC of TTP/PIC and Zn-TTP/PIC systems in CH_2Cl_2, $CHCl_3$, and CCl_4.

As the bond between the components becomes stronger and thus the components are subjected to more physical strain or loss of freedom, the values of ΔH^o and ΔS^o should be more negative. Finally, the enthalpy of formation ΔH^o for both TTP and Zn-TTP complexes increases with increasing electron affinity of the acceptors, accompanied by parallel increases in ΔG^o and ΔS^o.

Spectral properties of the CTC

The experimental oscillator strength (f) and the transition dipole moment (μ) were calculated using the following approximate formula [27]:

$$f = 4.32 \times 10^{-8} [\varepsilon_{max} \Delta \nu 1/2] \quad (2)$$

$$\mu = 0.0958 \left[\frac{\varepsilon_{max} \Delta \nu 1/2}{\nu_{max}} \right] \quad (3)$$

where $\Delta\nu_{1/2}$ is the band width at half intensity, ε_{max} and ν_{max} the molar extinction coefficient and wavenumber at the absorption maximum of the complex, respectively. The $\Delta\nu_{1/2}$, f and μ values are reported in Table 4. The values of the calculated oscillator strength are rather relatively large indicating a strong interaction between the donor–acceptor pair with relative high probabilities of CT transitions.

Ionization potential of the donor

The ionization potential (I_p) of the free donor of the highest filled molecular orbital on the donor was determined by using the relation:

$$I_p = a + b(h\nu_{max}) \quad (4)$$

where $h\nu_{max}$ is the lowest transition energy in electron volts; a and b are 5.11 and 0.701 [28]; 4.39 and 0.857 [29] or 5.156 and 0.778 [30], respectively. The average value of calculated I_p of donors by this method is 6.5 eV.

The values of I_p determined are given in Table 5. It has been reported that the ionization potential of the electron donor may be correlated with the charge transfer

transition energy of the complex [31]. Comparison of the transition energies of the CT-complex in different solvents with the I_p values of the electron donors in the corresponding solvents forming the complex reveals a regular relationship, which is in accord with the results obtained by McConnel et al. [32].

Further evidence for the nature of CT-interaction in the present systems is the calculation of the dissociation energy (W) of the charge transfer excited state of the complex in different solvents. Hence the dissociation energies of the complex were calculated from their CT-energy ($h\nu_{CT}$), I_p, and electron affinity (E^A) of the acceptor using the empirical relation [32] given in Eq. (5).

$$h\nu_{CT} = I_p - E^A - W \quad (5)$$

The calculated values of W are include in Table 5. The plot of W versus I_p shown in Figure 8. is linear as was expected. Thus, the acquired values of W of charge transfer excited states of the complex in different solvents are constant, which suggests that the investigated complex is reasonably strong and stable under the studied conditions with higher resonance stabilization energy [33].

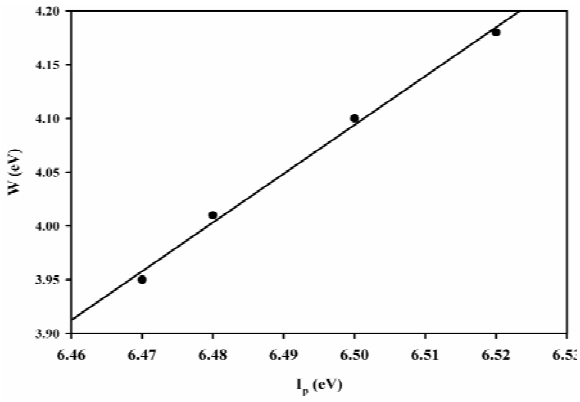

Figure 8. The plot of dissociation energy (W) versus the ionization potential of (I_p) of TTP/PIC system in CH_2Cl_2, $CHCl_3$, and CCl_4.

Fluorescence spectra

The fluorescence quenching of TTP by PIC, DNS, DNP, and DNB was studied by steady-state emission measurements in dichloromethane, chloroform, and carbon tetrachloride (Figure 9, Table 6). The second order Stern Volmer (SV) quenching constants ($K_{SV} = K_q\tau_o$) of the fluorescence quenching were determined from the SV plots using the method of linear regression according to the following relation [34].

$$I_0/I = 1 + K_q\tau_0[Q] \quad (6)$$

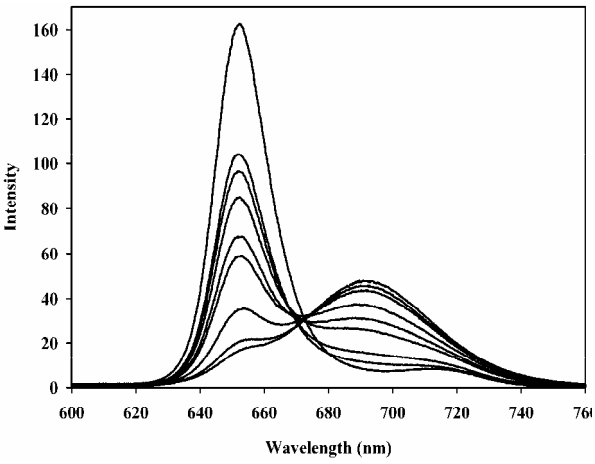

Figure 9. The emission spectra of free TTP (7x 10^{-6} mol l^{-1}) and TTP/DNP solution at different DNP (1.0, 1.5, 2.0, 2.5, 3.0, 4.0, 5.0 and 6.0 x 10^{-2} mol l^{-1}) in CH_2Cl_2 at room temperature.

Where I_o and I are the relative fluorescence intensities in the absence and presence of the quencher of concentration [Q], K_q and τ_o are the quenching rate constant of the fluorescence quenching and the fluorescence lifetime of the

fluorophore in the absence of the quencher, respectively. Typical SV plots are linear in the investigated concentration range as shown in Figure 10. At relatively high quencher concentrations, SV plots show positive deviations, especially with stronger quenchers, indicating the formation of ground state complexes. Hence, all studies were performed at low [Q]. It is readily seen that the quenching efficiency (magnitude of K_{SV}) increases with increasing E^A of the quencher. There is a good linear dependency of ln K_{SV} on E^A of the quencher as shown in Figure 11.

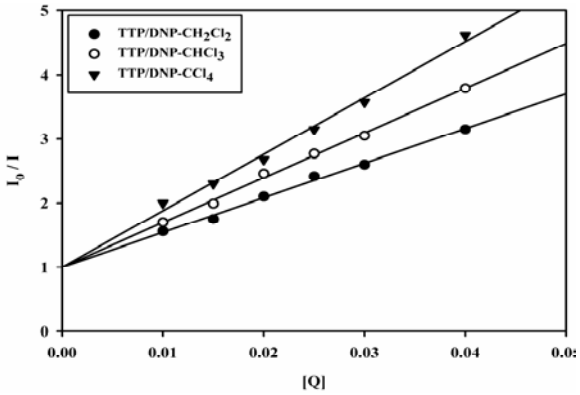

Figure 10. Stern-Volmer plots for the TTP/DNP system in in CH_2Cl_2, $CHCl_3$, and CCl_4.

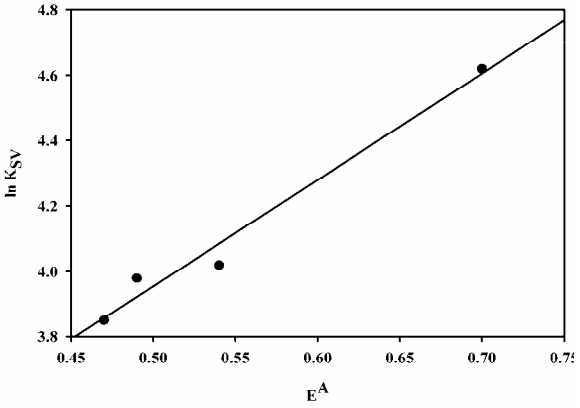

Figure 11. Relation between lnK_{SV} against E^A at 25 °C.

It indicates the probable involvement of charge transfer type quenching. Table 6 shows that the K_{SV} values decreased with increasing solvent polarity. It was observed that all systems exhibit a new emission fluorescence band in all solvent under investigation (Figure 9). This band is not due to either of the individual components or impurities.

The new emission of the CTCs is characteristic of a CT excited state. The resulting new band is red shifted on increasing the solvent polarity. The emitting excited state was obtained via an exciplex formed between singlet-excited TTP (^{1}TTP*) and the acceptors in its ground state. It can also obtained by absorption of a photon by the ground state of the complex. Also, there is no spectral overlap between the emission of the TTP and the absorption of the nitro aromatic acceptor, and hence electronic energy transfer from ^{1}TTP* to the acceptor can be ruled out. According to these considerations, it is possible to say that charge transfer is the major pathway for quenching of ^{1}TTP*. The quenching efficiency decreases as the temperature is increased from 10 to 25 °C.

4. Conclusions

It may be concluded that the TTP donors form strong CTC of 1:1 stoichiometry with the nitro aromatic acceptors in all the solvents studied. However, Zn-TTP do not display any detectable CT band with DNP and DNB even at higher donor and acceptor concentrations at different temperatures in various organic solvents. Strong CTC was only formed from the reaction of Zn-TTP with acceptors of highly EA

such as PIC and DNS. The equilibrium constant (K_{CT}) values decreased with increasing temperature and solvent polarity. The spectroscopic and thermodynamic parameters of the complex were found to be highly solvent dependent. From the trends in the CT-absorption bands, the ionization potential of the donor molecules has been estimated. The oscillator strength and transition dipole moment of the CTCs have also been determined. The studied complexes are stable and exothermic in nature. A Detectable emission band was formed between TTP and all studied acceptors in non polar and moderately polar solvents. The fluorescence emission observed is not due to either of the individual components. The fluorescence quenching increase with increasing electron affinity of acceptors.

Acknowledgments

This work was supported by a grant from King Abdulaziz City for Science and Technology, Saudi Arabia, award # MT-1-2. The financial contribution is gratefully acknowledged. The author also thanks the Department of Chemistry, College of Science, King Faisal University for allowing them to conduct this research in their laboratories.

Table 1. Spectral data of CTC of TTP with various acceptors at different temperatures.

System	T/K	K_{CT} (l mol^{-1})	ε_{CT}(l mol^{-1} cm^{-1})	λ_{CT} (nm)	*r*
TTP/PIC-CH_2Cl_2	298	2.3668 x 10^4	4.89611 x 10^5	665	0.996
	293	3.2973 x 10^4	4.91926 x 10^5		0.972
	288	4.1814 x 10^4	4.92337 x 10^5		0.975
	283	4.6350 x 10^4	4.97582 x 10^5		0.979
TTP/DNS-CH_2Cl_2	298	1.8772 x 10^4	5.67928 x 10^5	670	0.951
	293	2.1918 x 10^4	5.75583 x 10^5		0.936
	288	2.4986 x 10^4	5.90143 x 10^5		0.973
	283	2.7818 x 10^4	6.01992 x 10^5		0.959
TTP/DNB-CH_2Cl_2	298	7.6075	5.05888 x 10^5	667	0.965
	293	9.0321	5.43817 x 10^5		0.949
	288	15.9360	5.64030 x 10^5		0.962
	283	29.8689	5.85015 x 10^5		0.954
TTP/DNP-CH_2Cl_2	298	24.3546	4.56744 x 10^5	665	0.991
	293	33.5666	4.79859 x 10^5		0.983
	288	43.7048	4.80982 x 10^5		0.995
	283	56.7645	4.85391 x 10^5		0.976
TTP/PIC-$CHCl_3$	298	5.1345 x 10^4	5.56783 x 10^5	662	0.966
	293	6.5684 x 10^4	5.63624 x 10^5		0.993
	288	9.0985 x 10^4	5.73245 x 10^5		0.989
	283	11.4327 x 10^4	5.74567 x 10^5		0.972
TTP/DNS-$CHCl_3$	298	3.6285 x 10^4	4.71114 x 10^5	668	0.999
	293	4.5473 x 10^4	4.71241 x 10^5		0.999
	288	4.9636 x 10^4	4.713585 x 10^5		0.999
	283	5.1516 x 10^4	4.788878 x 10^5		0.989
TTP/DNB-$CHCl_3$	298	12.5689	5.124678 x 10^5	665	0.96
	293	19.7653	5.23467 x 10^5		0.949
	288	45.1297	5.25689 x 10^5		0.962
	283	65.7865	5.43342 x 10^5		0.954
TTP/DNP-$CHCl_3$	298	33.1572	5.65451 x 10^5	665	0.991
	293	43.5117	5.56744 x 10^5		0.983
	288	58.8758	5.87658 x 10^5		0.995
	283	73.7847	5.99456 x 10^5		0.976
TTP/PIC-CCl_4	298	7.5643 x 10^4	4.97582 x 10^5	661	0.996
	293	8.4578 x 10^4	4.92337 x 10^5		0.999
	288	13.6543 x 10^4	4.89611 x 10^5		0.978
	283	16.345 x 10^4	4.91926 x 10^5		0.992
TTP/DNS-CCl_4	298	5.7865 x 10^4	6.76383 x 10^5	667	0.951
	293	7.7893 x 10^4	6.79425 x 10^5		0.936
	288	9.9654 x 10^4	7.11433 x 10^5		0.973
	283	13.6732 x 10^4	7.21455 x 10^5		0.959
TTP/DNB-CCl_4	298	16.1654	5.18530 x 10^5	665	0.96
	293	23.1267	5.19435 x 10^5		0.949
	288	49.6543	5.87894 x 10^5		0.962
	283	71.321	5.95553 x 10^5		0.954
TTP/DNP-CCl_4	298	39.1790	5.04391 x 10^5	665	0.991
	293	48.4532	5.36678 x 10^5		0.983
	288	67.8758	5.46743 x 10^5		0.995
	283	82.7847	5.87855 x 10^5		0.976

Table 2. Spectral data of CTC of Zn-TTP/PIC and Zn-TTP/DNS at different temperatures.

System	T/K	K_{CT} (l mol^{-1})	ε_{CT}(l mol^{-1} cm^{-1})	λ_{CT} (nm)	*r*
Zn-TTP/PIC-CH_2Cl_2	298	5.12	4.23167 x 10^5	667	0.99
	293	6.43	4.54876 x 10^5		0.99
	288	8.34	4.78432 x 10^5		0.98
	283	10.32	4.975823 x 10^5		0.99
Zn-TTP/DNS-CH_2Cl_2	298	3.94	3.897654 x 10^5	668	0.97
	293	4.86	3.956732 x 10^5		0.98
	288	6.56	4.125674 x 10^5		0.99
	283	8.78	4.23561 x 10^5		0.97
Zn-TTP/PIC-$CHCl_3$	298	7.54	5.234567 x 10^5	665	0.99
	293	8.03	5.45327 x 10^5		0.99
	288	11.78	5.87654 x 10^5		0.99
	283	15.95	5.976543 x 10^5		0.98
Zn-TTP/DNS-$CHCl_3$	298	5.67	4.77443 x 10^5	665	0.99
	293	5.98	4.79867 x 10^5		0.98
	288	7.56	4.87432 x 10^5		0.99
	283	9.65	4.98765 x 10^5		0.99
Zn-TTP/PIC-CCl_4	298	10.56	6.12365 x 10^5	665	0.96
	293	12.87	6.436243 x 10^5		0.99
	288	17.87	6.732456 x 10^5		0.98
	283	25.67	6.755688 x 10^5		0.97
Zn-TTP/DNS-CCl_4	298	8.86	5.743218 x 10^5	665	0.99
	293	9.89	5.876543 x 10^5		0.99
	288	14.56	5.987654 x 10^5		0.99
	283	18.45	6.125679 x 10^5		0.98

Table 3. Thermodynamic standard reaction quantities of TPP/PIC and Zn-TTP/PIC complexes in different organic solvents.

System	$-\Delta H^o$/KJ mol^{-1}	$-\Delta S^o$/J mol^{-1} K^{-1}	$-\Delta G^o$(298 K)/KJ mol^{-1}	*r*
TTP/PIC-CH_2Cl_2	448.28 ± 0.55	14.20 ± 1.9	24.95 ± 0.24	0.99
TTP/PIC-$CHCl_3$	551.35 ± 0.23	16.66 ± 0.8	26.87 ± 0.34	0.96
TTP/PIC-CCl_4	524.53 ± 0.41	17.60 ± 1.4	27.83 ± 0.15	0.98
Zn-TTP/PIC-CH_2Cl_2	478.59 ± 0. 12	15.92 ± 0.42	4.04 ± 0.12	0.99
Zn-TTP/PIC-$CHCl_3$	512.62 ± 0.31	17.03 ± 1.22	5.00 ± 0.21	0.97
Zn-TTP/PIC-CCl_4	599.109 ± 0.32	19.90 ± 1.07	5.83 ± 0.11	0.98

Table 4. Bandwidth $\bar{\nu}_{max}$, half bandwidth $\Delta\bar{\nu}$ ½, oscillator strength *f*, and transition dipole moment μ of TPP/DNS, and Zn-TTP/DNS complexes at various temperatures.

System	$\Delta\bar{\nu}$ ½ (cm^{-1})	*f*	μ (debyes)	*r*
TPP/DNS-CH_2Cl_2	$\bar{\nu}_{max}$ = 14925.37			
298	1462.31	3.63	22.59	0.99
293	1475.27	3.66	22.85	0.99
288	1497.25	3.81	23.30	0.99
283	1512.47	3.93	23.66	0.99
TTP/DNS-$CHCl_3$	$\bar{\nu}_{max}$ = 14970.05			
298	1484.21	3.08	20.70	0.99
293	1524.41	3.1	20.98	0.98
288	1556.59	3.16	21.2	0.97
283	1587.12	3.28	21.58	0.99
TPP/DNS-CCl_4	$\bar{\nu}_{max}$ = 14992.5			
298	1595.64	4.64	25.65	0.99
293	1614.23	4.71	25.85	0.99
288	1645.47	5.05	26.76	0.99
283	1678.51	5.23	27.66	0.99
Zn-TTP/DNS-CH_2Cl_2	$\bar{\nu}_{max}$ = 14970.05			
298	1510.14	2.54	18.99	0.99
293	1552.16	2.65	27.15	0.98
288	1573.25	2.80	19.94	0.99
283	1595.34	2.91	20.35	0.98
Zn-TTP/DNS-$CHCl_3$	$\bar{\nu}_{max}$ = 15037.59			
298	1615.42	3.33	21.69	0.99
293	1658.1	3.43	22.03	0.97
288	1672.25	3.52	22.3	0.98
283	1686.25	3.63	22.65	0.99
Zn-TTP/DNS-CCl_4	$\bar{\nu}_{max}$ = 15037.59			
298	1635.74	4.05	23.94	0.97
293	1675.68	4.25	24.51	0.96
288	1692.36	4.37	24.86	0.99
298	1716.92	4.54	26.32	0.99

Table 5. Charge transfer energy, ionization potential, and dissociation energy of CTCs of TTP and Zn-TTP with different acceptors.

Acceptor	E_{CT} (eV)	TTP- I_p (eV)	Zn-TTP-I_p (eV)	W (eV)
PIC	1.86	6.47	6.46	3.95
DNS	1.86	6.48	6.48	4.01
DNP	1.87	6.50	6.50	4.11
DNB	1.87	6.52	6.51	4.18

Table 6. Fluorescence quenching data of TTP (7×10^{-6} mol l^{-1}) with PIC, DNS ($1\text{-}3 \times 10^{-5}$ mol l^{-1}), DNP ($1\text{-}4 \times 10^{-2}$ mol l^{-1}), and DNB ($1\text{-}8 \times 10^{-2}$ mol l^{-1}) in different organic solvents with λ_{max} excitation = 420 nm and λ_{max} emission = 650 nm at room temperature.

	K_{SV} (min^{-1})				
Solvents	PIC	DNS	DNP	DNB	r
CH_2Cl_2	101.49 ± 0.05	55.70 ± 0.11	53.93 ± 0.03	46.99 ± 0.21	0.999
$CHCl_3$	127.03 ± 0.02	82.32 ± 0.08	69.71 ± 0.07	51.03 ± 0.32	0.999
CCl_4	143.12 ± 0.08	132 ± 0.06	87.91 ± 0.04	63.12 ± 0.15	0.999

References

[1] P. Neta, M. C. Richoux, A. Harriman, L.R. Milgrom, *J. Chem. Soc. Faraday Trans.,* **282**, 209 (1986).

[2] Y. Ferrand, L. Bourre, G. Simonneaux, S. Thibaut, F. Odobel, Y. Lajat, T. Patrice, *Bioorgan. Med. Chem. Lett.*, **13**, 833 (2003).

[3] J. Zhang, X. Wu, X. Gao, F. Yang, J. Wang, X. Zhou, X. Zhang, *Bioorgan. Med. Chem. Lett.*, **13**, 1097 (2003).

[4] W. M. Sharman, J. E. Van Lier, C. M. Allen, *Adv. Drug Deliv. Rev.,* **56**, 53 (2004).

[5] A. R. Genady, *Org. Bio mol. Chem.*, **3**, 2102 (2005).

[6] A. Eychmuller, A. L. Rogach, *Pure Appl. Chem.,* **72**, 179 (2000).

[7] R. Dabestani, K. J. Reszka, M. E. Sigman, *J. Photochem. Photobiol. A*, **117**, 223 (1998) .

[8] P.Y. Khashaba, S.R. El-Shabouri, K.M. Emara, A.M. Mohamed, *J. Pharm. Biomed. Anal.*, **22**, 363 (2002).

[9] F. A. N. El-Dien, G. G. Mohamed, E. Y. Z. A. Farag, *Spectrochimica Acta* Part A*,* **64**, 210 (2006).

[10] K. Brueggermann, R.S. Czernuszewicz, J.K. Kochi, *J. Phys. Chem.*, **96**, (1992) 4405.

[11] S. M. Andrade, S. M. B. Costa, R. Pansu, *J. Colloid Interf. Sci.*, **226**, 260 (2000).

[12] F. Yakuphanoglu, M. Arslan, S.Z. Yıldız, *Opt. Mater.*, **27**, 1153 (2005).

[13] F. Yakuphanoglu, M. Arslan, M. Küçükislamoğlu, M. Zengin, *Solar Energy*, **79**, 96 (2005).

[14] R. S. Mulliken, *J. Phys. Chem.*, **56**, 801 (1952).

[15] A. A. Salem, Y.M. Issa, M.S. Bahbouh, *Anal. Lett.*, **30**, 1153 (1997).

[16] M. A. El-Kemary, S. A. Azim, M. E. El-Khouly, E. M. Ebeid, *J. Chem. Soc., Farady Trans.,* **93**, 63 (1997).

[17] M. E. El-Zaria, *Spectrochim. Acta* Part A, In the press (2007).

[18] H. Guo, J. Jiang, Y. Shi, Y. Wang, S. Dong, *Spectrochimica Acta* Part A, In the press (2007).

[19] J. S. Lindsey, I. C. Schreiman, H. C. Hsu, P. C. Kearney, *J. Org. Chem.*, **52**, 827 (1987).

[20] D. A. Skoog, Principle of Instrumental Analysis, 3rd., Saunder College Publishing, New York, 1985 (Chapter 7).

[21] R. S. Mulliken, *J. Chim. Phys.*, **61**, 20 (1964).

[22] M. Tamres, J. M. Goodenew, *J. Phys. Chem.*, **71**, 1982 (1967).

[23] P. Job, *Ann. Chim.*, **10**, 113 (1928).

[24] M. Stalko, J. F. Yanus, J. M. Pearson, *Macromolecules*, **9**, 715 (1976).

[25] Z. Asmus, *Anal. Chem.*, **178** (1960) 104.

[26] Y. Sato, M. Morimoto, H. Segawa, T. Shimidzu, *J. Phys. Chem.*, **99**, 35 (1995).

[27] G. Aloisi, S. Pignataro, *J. Chem. Soc. Farady Trans. I*, **69**, 534 (1972).

[28] D. C. Wheat, Handbook of Chemistry and Physics, 50th ed., 1969–1970.

29. A. F. Mosten, *J. Chem. Phys.*, **24**, 602 (1956).

[30] S. R. Becker, F. W. Worth, *J. Am. Chem. Soc.*, **84**,4263 (1962); S. R. Becker, F. W. Worth, *J. Am.Chem. Soc.*, **85**, 2210 (1963).

[31] A. E. Mourad, *Spectrochim. Acta* part A, **41**, 347 (1985).

[32] H. H. McConnel, J. S. Ham, J. R. Platt, *J. Chem. Phys.*, **21**, 66 (1964).

[33] G. M. Neelgund, M. L. Budni, *Monats. für Chemie*, **135**, 1395 (2004).

[34] S. Radzki, P. Krausz, *Monatsh. Chem.*, **126**, 51 (1985).

Arabian J. Chem. Vol. 1, No. 1, 25-35 (2008)

The Effects of Organic Additives on Photochromism: Part II. The Photochromic Properties of (E)-dicyclopropylmethylene-(2,5-dimethyl-3-furylethylidene)-succinic Anhydride with Styryl Dye Doped in PMMA Polymer Film

Gameel A. Baghaffar[a] **, and Abdullah M. Asiri**[b]

[a] *Chemistry Department, Faculty of Science, Hadhramout University of Science & Technology, P.O. Box 50512, Mukalla, Republic of Yemen.*
[b] *Chemistry Department, Faculty of Science, King Abdul Aziz University, Jeddah- 21413, P.O. Box 80203 , Saudi Arabia.*

Abstract

Four films of fulgide **1-E** with styryl dye **2** compound doped in a film of polymethylmethacrylate (PMMA) and spread over glass plates. Three of them were heated for three hours at 40° C, 62° C, and 80° C, respectively. The four films were irradiated with UV light (365 nm) and were turned red– pink (closed form **1-C**). The later color was switched back to the original color (opened form **1-E**) when the films were irradiated with a white light. The kinetics of photocoloration and photobleaching processes were followed spectrophotometrically by monitoring the absorbance of the fulgide **1** at its λ_{max} (515 nm). The first-order plots of photocoloration reaction shows two distinct linear lines. The slopes of which corresponding to the first-order rate constants k_1 and k_2, where k_1 is the rate constant at initial times of reaction and k_2 is that at late reaction times. These results suggest the probable presence of two conformers of the ring opened form **1-E** which reacts in sequence. On the other hand, photobleaching reaction shows a simple first-order reaction rate. It was found that for photocoloration reaction, the rate constants at initial stages are slower than those at late reaction stages. Similarly, the rate constants of photocoloration reaction are slower than those of photobleaching reaction. The rate constant of photocoloration reaction increases with increasing annealing temperatures, but for photobleaching reaction, almost the rate constants are similar with increasing temperatures. The photochromic properties of fulgide **1-E** with styryl dye **2** compound were improved significantly upon annealing at 80° C with better fatigue resistance.

Keywords: Fulgides; Photochromic; Polymer film; Photocoloration; Photobleaching; Fatigue resistance; Styryl dyes**.**

1. Introduction

The development of a reversible optical information storage medium based on photochromic organic compounds had become a potential commercial reality [1-3]. This is because of the discovery of the first thermally stable fatigue resistance photochromic fulgides which undergo almost quantitative conversion into their highly colored cyclized form upon ultraviolet light exposure [4,5]. Besides that this color change due to the above transformation, other properties could be equally controlled. Some of them include the dichroism and birefringence properties [6], control of cholesteric liquid crystalline properties and control of the stereochemistry of the ring-closure [7]. Heller and co-workers have

shown that fulgides containing heterocyclic structure such as furyl, thienyl and pyrrolyl were excellent candidates for data storage media because of their efficient thermal stability [8]. Yokoyama and co-workers have studied indolylfulgides, which have interesting photochromic properties [9,10]. Organic photochromes such as fulgides have found potential applications in fields of optical storage memories [11], holographic recording [12], and multi-level recording [13].

The application of photochromic compounds in optical data storage or any other application will certainly be provided as films. This necessitates studying the photochromic performance of fulgides doped in or bounded to polymer matrices. In a previous paper, photochromic properties of fulgide **1-E** doped in PMMA polymer film were reported [14a, b]. Now, we report the photochromic properties of the same fulgide doped in the same polymer but with additive styryl dye **2.**

2. Experimental

Fulgide **1-E** was prepared according to a general procedure previously reported [15]. Styryl dye **2** was prepared and characterized in our lab and their preparations and studies will be published soon. Three solutions were prepared in chloroform (1×10^{-4} molar): one of the fulgide **1**, the second of is PMMA (Aldrich Chemicals), and the third of is styryl dye **2** compound. A mixture from the three solutions was prepared (3% Fulgide, 2% Dye and 10% PMMA)[in weight by weight (w/w)]. From the mixture, four films were prepared by taking about 0.5 ml of the mixture (for one film), and spread over a glass plate. These plates were covered and left overnight in the dark. One of these films was used without heating (at room temperature, 20° C). The other three films were heated in the oven for three hours: one at 40° C, the second at 62° C, and the third at 80° C. Ultraviolet and visible spectra were measured by using Perkin-Elmer lambda EZ210 spectrophotometer. Photocoloration (365 nm) was carried out using Blak-Ray lamp model UVL-56 and photobleaching was obtained by using a tungsten filament lamp. The fatigue resistance of fulgide **1-E** with styryl dye **2** was carried out by photocoloring and photobleaching **1-E** with styryl dye **2,** consecutively for eleven cycles.

3. Results and discussion

Effect of annealing

The absorption spectrum of fulgide **1-E** with additive styryl dye **2** doped in PMMA polymer film was firstly recorded before UV irradiation. It was found that with increasing annealing temperature, absorption increases at λ_{max} (390 nm). (Fig.1). This was attributed to the thermal isomerization of **E**-form to **Z**-form of the additive compound. At λ_{max} =390 nm, an absorption band for additive compound was observed.

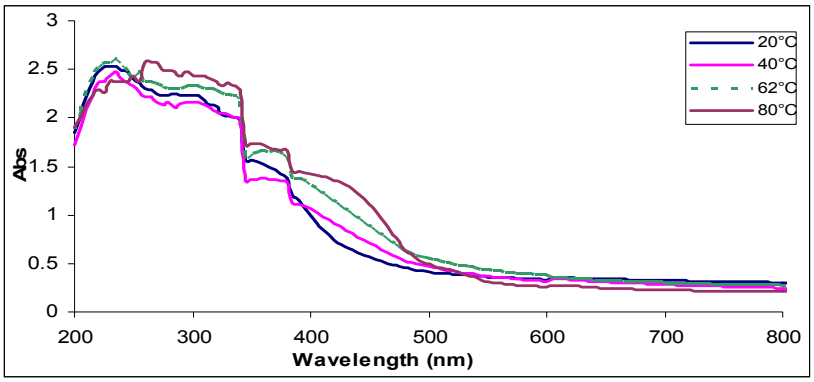

Fig.1. The effect of annealing for 3 hours on PMMA films of fulgide 1 with additive styryl dye 2

Photocoloration

Fulgide **1** is a mixture of two geometrical isomers, the cis and trans **(1-Z, 1-E**), the trans is the major one. Both isomers absorb UV light and only the **E**-form undergoes a conrotatory photocyclization upon irradiation with UV light (365 nm) to give 7, 7a-dihydro-7, 7-dicyclopropyl-2,4,7a-trimethylbenzo[b]furan-5,6-dicarboxylic anhydride **1-C** as a yellow color with absorption maximum at λ_{max} (515 nm). On the other hand, only the cyclized product **1-C** absorbs the visible light upon irradiation with white light and converted to open form **1-E** (Scheme 1).

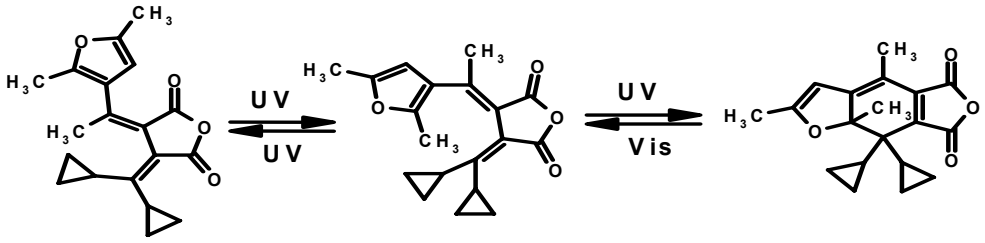

Scheme 1: Photochemical reactions of fulgide 1

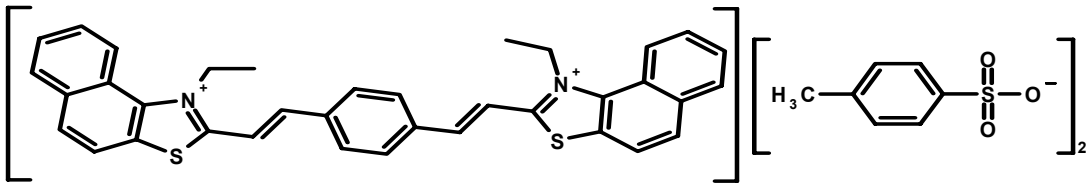

Styryl 2

Since upon UV irradiation all the three isomers absorb, a photostationary state will soon be reached. The rate of each step depends on its quantum yield and the intensity of absorbed light [16]. Fig. 2 is a representative sample showing the spectrum of the photocholoration of the annealed film of fulgide **1** with additive styryl dye **2** at

62° C. Increasing the exposure time, increases the amount of the cyclized form **1-C,** which has a maximum absorption at λ_{max} (515 nm). It is well documented that the polymer free volume controls and influences the rate and/or the course of a photochromic dye reaction [17,18]. It is difficult to evaluate the polymer free volume, because it depends on the thermal and mechanical history of the sample [17]. Kinetics of fulgides show in general first-order rate dependence, but in polymer matrices deviation from simple first-order reaction was observed [17]. Such non-linearity of the first-order plots was attributed to several factors . One of them is the possible existence of two or more conformers of the reactant trapped in the solid matrix. These conformers might undergo a parallel first-order reaction and thus giving rise to composite first-order rate kinetics or reacts in sequence to give two distinct first-order slopes [17,18].

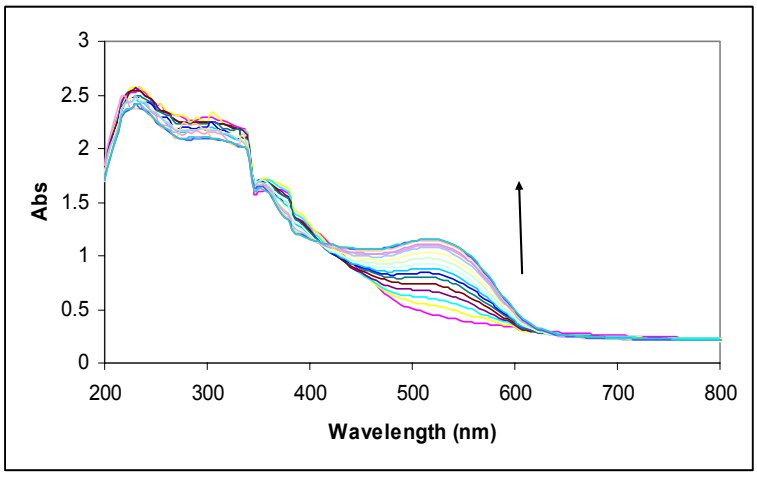

Fig.2. Photocholoration reaction of fulgide 1-E with additive styryl dye 2 polymer film annealed at 62° C for 3 hours. The arrow direction indicates the increase of absorbance with increasing exposure time.

The integrated form of the first-order rate law for the photocoloration process is

$$\ln\left(\frac{A_\infty - A_0}{A_\infty - A_t}\right) = kt$$

Where k is the rate constant, A_∞ is the absorbance of the cyclized product **1-C** at infinite time, A_0 is its absorbance at zero time, and A_t is its absorbance at time t. Plot of [ln (A_∞ - A_0) / (A_∞ - A_t)] against time, gives a straight line with slope equal to k. We found that two straight lines could be extracted from this plot, one corresponding to the apparent rate constant (k_1) at initial stages (Fig. 3) and the other apparent rate constant (k_2) corresponding to late stages of reaction times (Fig. 4). Table 1 shows the apparent rate constants (k_1, k_2) and half-lives for the photocoloration of fulgide **1-E** with and without additive styryl dye **2** doped in PMMA polymer film at various annealing temperatures. From table 1, it is clear that the rate constants at late stages of reaction times (k_2) are higher than those at initial reaction stages (k_1). On the other hand, the rate constants for photocoloration of fulgide **1-E** doped in PMMA [14a] are higher than those of fulgide **1-E** with additive styryl dye **2**, it may be explained, that styryl dye **2** firstly absorbs energy then some of this energy transfers to fulgide **1-E.**

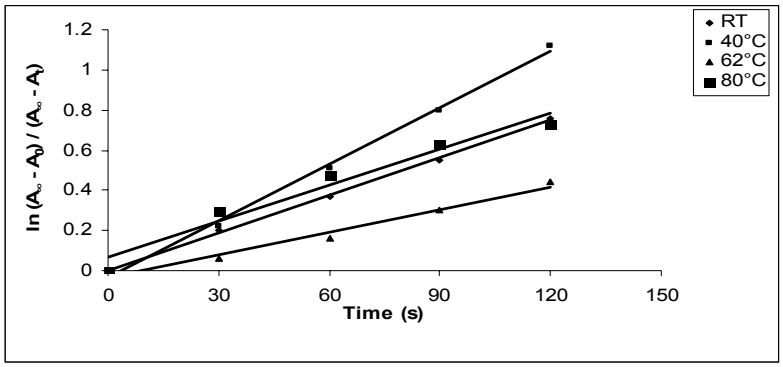

Fig. 3. First-order of photocoloration reaction of fulgide 1 with additive styryl dye 2 at initial stages at different temperatures for 3 hours.

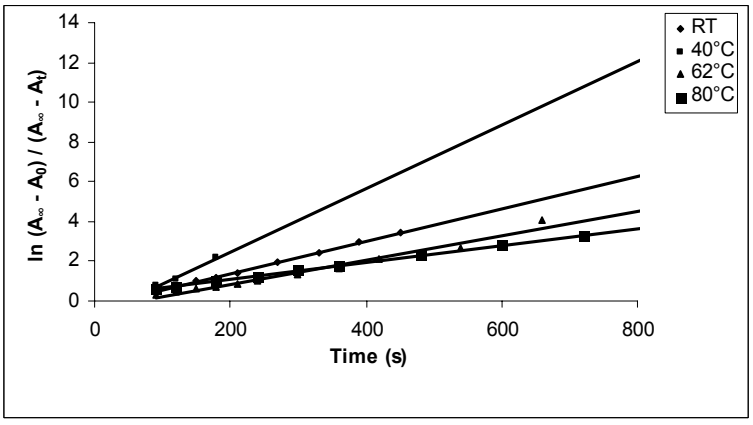

Fig.4. First-order of photocoloration reaction of fulgide 1 with additive styryl dye 2 at late stages at different temperatures for 3 hours.

Table 1. Comparison for half-lives of forward and backward first-order reactions of fulgide 1-E alone and with additive styryl dye 2.

	Fulgide Only		Fulgide with STYRYL DYE 2			
Reaction	$k(s^{-1})$	$t_{1/2}$(min)	$k_1(s^{-1})$	$t_{1/2}$(min)	$k_2(s^{-1})$	$t_{1/2}$(min)
Photocoloration RT	1.49×10^{-2}	0.78	6.2×10^{-3}	1.86	8.1×10^{-3}	1.43
Photocoloration 40°C	-------	------	9.4×10^{-3}	1.23	1.6×10^{-2}	0.72
Photocoloration 62°C	1.26×10^{-2}	0.91	3.7×10^{-3}	3.12	6.1×10^{-3}	1.89
Photocoloration 80° C	2.25×10^{-2}	0.51	6.0×10^{-3}	1.92	4.2×10^{-3}	2.75
Photobleacing RT	5.75×10^{-2}	0.20	7.2×10^{-2}	0.16	-----	-----
Photobleacing 46° C	--------	------	3.9×10^{-2}	0.30	-----	-----
Photobleaching 62° C	5.30×10^{-2}	0.22	4.6×10^{-2}	0.25	-----	-----
Photobleach 80°C	5.18×10^{-2}	0.22	4.3×10^{-2}	0.27	----	----

It was found [17] that the kinetics of the photocoloration of Aberchrome 540 in various polymer matrices shows two distinct slopes in accordance to what we observe. These results were explained on the bases that there are two major conformers of the **E**-form which cyclizes in sequence. The first conformer reacts at the initial

stages of the reaction time (reaction 1, scheme 2) and the other begins to react towards the late stages (reaction 2, scheme 2). These observations are in accordance with our results.

$$E' \xrightarrow{K_1} C \qquad (1)$$

$$E'' \xrightarrow{K_2} C \qquad (2)$$

Scheme 2. Sequence reactions of the two conformers.

The existence of two or more conformers for fulgide **1-E** in solutions or solid matrices is expected, since it is known, from X-ray crystal structure of several fulgides [19], that these molecules are not planar. The slower apparent rates (k_1 and k_2) of fulgide **1-E** trapped in the solid matrix compared to those in solution ($k_1 = 0.6x10^{-2}$ s^{-1} and $k_2 = 1.69\times10^{-2}$ s^{-1}) (see table 1), might be due to the polymer free volume which might restricts the molecular motion of fulgide **1-E**. This effect of polymer free volume is most clear in the case of fulgide **1-E** with additive styryl dye **2**.

Effect of Additives on photocoloration of fulgide 1

It is important to investigate the effect that might happen upon irradiation on the photochromic performance and properties such as rate of the reaction and the half-live of the photocoloration. The result obtained in table 1 indicates that the rates of photocoloration of fulgide **1-E** in the presence of additive styryl dye **2** decrease, for example, about two and half fold compared to the rate in the absence of additive styryl dye **2** at room temperature. Similarly, at 62°C and 82°C, it decreases more than three and half and more than three, respectively. This effect may be due to the free volume of the polymer matrix, which decreases due to the crosslinking by heating [26], and therefore, restricts the collisions between the molecules of fulgide **1-E** and those of additive styryl dye **2** causing, a decreases in the energy transfer from the additive styryl dye **2** to the fulgide **1-E** (Scheme 3).

Styryl dye2 $\longrightarrow$ **Styryl dye2***

Styryl dye2* **+ 1-E** $\longrightarrow$ **Styryl dye2 + 1-C**

Scheme 3. Mechanism of some energy transfer from Styryl dye 2 to 1-E upon irradiation.

Photobleaching

Rappon and co-workers reported that photobleaching reaction of Aberchrome 540 doped in solid matrix at low temperature range (83-283 °K) was characterized by two first-order slopes [20]. The first one at initial irradiation stages begins with a very slow induction period followed by the second slope which is much steeper toward the end of reaction times. This behavior was attributed to the cooperative molecular motion of the dye and the polymer [20]. On the other hand, at temperatures around and above room temperature, the photobleaching of the closed ring form **1-C** to the opened form **1-E** follows simple first-order rate equation [14a, 21].

When the closed ring form **1-C** was irradiated with white light, it converted to the pure opened ring form **1-E**. Thus the yellow color disappeared gradually with time. Fig. 5 shows the absorption spectrum of the photobleaching reaction of fulgide **1-C** with additive styryl dye **2** doped in PMMA polymer film annealed at 62° C.

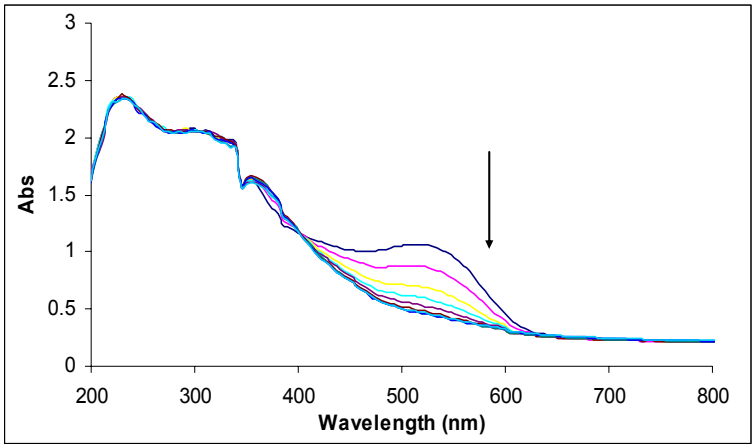

Fig. 5. Photobleaching reaction of closed form 1-C with additive styryl dye 2 polymer film annealed at 62° C for 3 hours. The arrow direction indicates the decrease of absorbance with increasing exposure time.

the integrated form of the first-order rate law for the photobleaching process is:

$$\ln\left(\frac{A_t}{A_0}\right) = -kt$$

Where k is the rate constant, A_t is the absorbance of the cyclized product **1-C** at time t, A_0 is its absorbance at zero time. Plot [ln (A_t / A_0)] against time, gives a straight line with a slope equals k. Fig. 6 shows the simple first-order plots of the photobleaching reaction of fulgide **1-C** with additive styryl dye **2** doped in PMMA film at different annealing temperatures and table 1 summarizes their apparent rate constants and half-lives. From table 1 it is obvious that the reaction rates for the photobleaching reaction are faster than those of the photocoloration reaction. In comparison with the values of fulgide **1-E** without additive [14a], we can say, that the rate constants of them are somewhat higher than those of fulgide with additive styryl dye **2**

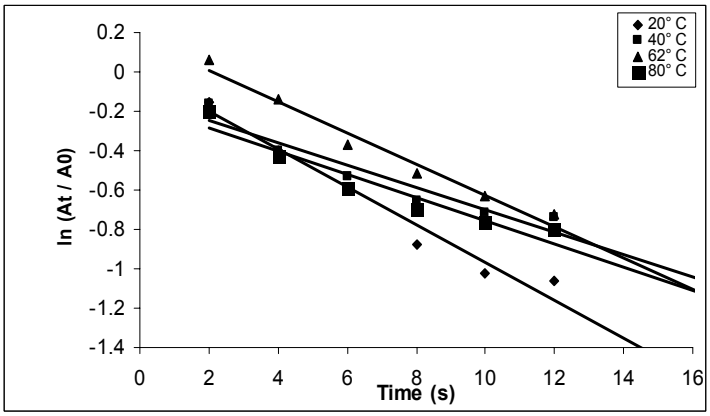

Fig. 6. First-order of photobleaching reaction of fulgide 1 with additive styryl dye 2 at different temperatures for 3 hours.

Effect of Additives on Photobleaching of fulgide 1

The effect of addition of styryl dye **2** on the bleaching of colored form **1-C** is shown in table 1 and can be summarized as follows: the presence of the additive increases the rate of photobleaching at room temperature. On heating at 62°C and 82°C the rate of photobleaching decreases at the two temperatures. This decrease may be due to crosslinking by heating [26], which decreases the polymer free volume, therefore, decreases the collision between molecules of fulgide and additive styryl dye **2**, and decreases the transfer of energy. This may be useful in some applications such as sunglasses.

Arrhenius plots of the photochemical reactions of fulgide 1 with additive styryl dye 2

The variation of the rate constants with the annealing temperatures for both the photocoloration at initial reaction times and for the photobleaching is plotted as the Arrhenius plot (i.e. ln(k) versus 1/T) as shown in Fig. 7.

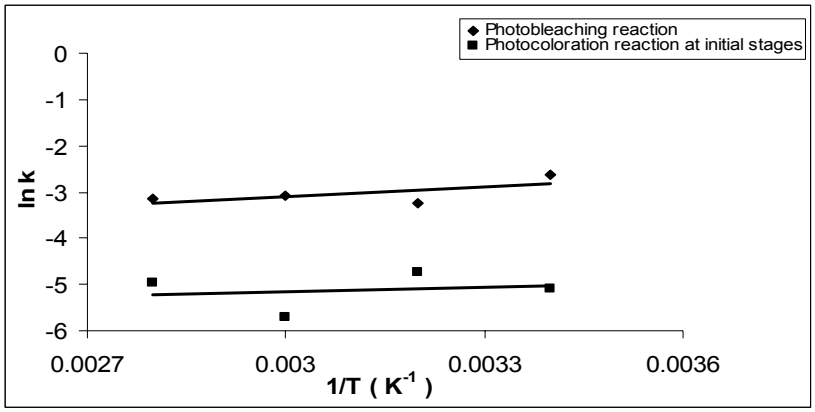

Fig.7. Arrhenius plot for photochemical reactions of fulgide 1 with additive styryl dye 2.

The apparent activation energies (E_a) and the pre-exponential factor (A) for the two reactions of fulgide **1** with additive styryl dye **2** in PMMA film were estimated from the slope and the intercept of the Arrhenius plot and are collected in table 2. The energy of activation for photobleaching reaction is less than that for photocoloration reaction. These small values of (E_a) are common for similar systems [17]. The pre-exponential factor (A) for the unimolecular reaction in the condensed phase could be related to the entropy of activation (ΔS^*) through the following equation [22]:

$$A = (ek_BT / h)e^{\Delta S^*/R}$$

Where k_B is the Boltzmann's constant and h is the Planck's constant. The estimated values of (ΔS^*) at room temperature (20° C) for the photocoloration and photobleaching reactions are (-303.9 $J.K^{-1}.mol^{-1}$) and (-296.2 $J.K^{-1}.mol^{-1}$), respectively (table 2). As expected, the entropy of activation for the photobleaching process is higher than that for photocoloration process. This is because photobleaching process is a ring opening reaction and the activated complex acquires higher degree of freedom. These results are in accordance to those for fulgide **1** without additive [14a].

Table 2. Thermodynamic parameters of the photochemical reactions of fulgide 1-E with additive styryl dye 2.

Parameter	Photocoloration reaction	Photobleaching reaction
E_a (kJ .mol^{-1})	2.59	5.74
A (s^{-1})	2.26x10^{-3}	5.71x10^{-3}
ΔS^{*}(J .K^{-1}. mol^{-1})	-303.9	-296.2

Photochemical fatigue resistance of fulgide 1 with additive styryl dye 2 in PMMA film

High resistance to photochemical degradation is an important property, which a photochrome should fulfill to be used as a data-storage medium. The fatigue resistance of fulgide **1** with additive styryl dye **2** doped in PMMA film is reported as the changes in absorbance with UV/visible irradiation for 11 repetitive cycles. In a previous paper [23], It was found that fulgide **1** doped in epoxy resin matrix possesses an excellent fatigue resistance. Similar results were found with other fulgides [24, 25]. This was attributed to the decrease of available polymer free volume due to increasing cross-linkage in the epoxy resin and thus preventing the photoisomerization of the **1-E** isomer to the uncyclizable **1-Z** form [24,25]. It was found a moderate decrease in fatigue resistance of the same fulgide doped in PMMA polymer film [14a]. Fig. 8 shows the fatigue resistance of fulgide **1** with additive styryl dye 2 doped in PMMA at 80° C, the fatigue resistance improved significantly with increasing the annealing temperature (70, 92, 80.6 and 80.9% for RT, 40, 62 and 80°C). The small decrease in absorbance of photocoloration reaction (fig.8) may be attributed to partial decomposition of fulgide **1-E** or its isomerization to **1-Z**. It is clear that the photochromic performance of annealed polymer film at 40° C is the best one. Thus, it might be recommended to apply photochromic fulgides as annealed polymer films.

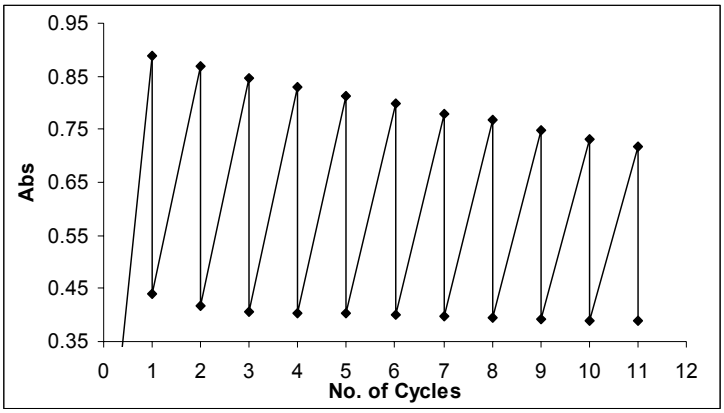

Fig. 8. Fatigue resistance of fulgide 1 with additive styryl dye 2 at 80 °C for 3 hours.

4. Conclusion

The photochromic properties of fulgide **1** with additive styryl dye **2** doped in PMMA polymer film at various annealing temperatures are studied. Kinetics of photocoloration and photobleaching reactions was followed spectrophotometrically. From the first-order plots of the photocoloration reaction for each run, two distinct linear lines were obtained with k_1 at initial stages and k_2 at late reaction stages.

These results were explained by the existence of two conformers of the trans isomer **1-E** which react in sequence. In contrast, kinetics of the photobleaching reaction followed a simple first-order reaction rate. Moreover, photocoloration reaction is slower than the photobleaching at a given annealing temperature. Also Rate constants of photocoloration for fulgide **1** without additive in PMMA [14a] are higher than those for fulgide **1** with additive styryl dye 2 in PMMA.

On the other hand, the rate constants of photobleaching for the two cases (with and without additive), are almost unchanged regardless of annealing temperature. Some thermodynamic parameters were calculated for the unannealed film (20° C). The photochemical fatigue resistance of fulgide **1** with additive styryl dye 2 in PMMA is improved with increasing annealing temperatures, especially at 40° C.

References

[1] Heller, H.G.; IEE Proc. Part **I** (1983) 130, 209.

[2] Whittal, J., in: H. Durr, B. Bouas-Laurent (Eds.), Photochromism Molecules and Systems, Elsevier, New York, (1990) p. 314.

[3] Yokoyama, Y., Chem. Rev. (2000)100, 1717.

[4] Heller, H. G., Fine Chemicals for Electronic Industry 1986, 60, 120.

[5] Alfimovy, M.V.; Fedorova, O. A.; Gromov, S. P., J. Photochem. Photobiol. A: Chem. (2003) 158, 183.

[6] Atassy, Y.; Chauvin, J.; Delaire, J. A.; Delaire, J. F.; Maltey, X.I.; Nakatani, K., Pure & Appl. Chem. (1998) 70, 2157.

[7] Yokoyama, Y.; Kose, M., J. Photochem. Photobiol. A: Chem. (2004)166, 9.

[8] Heller, H. G.; Langan, J. R., J. Chem. Soc. Perkin Trans. II (1981) 341.

[9] Yokoyama, Y.; Takahashi, K., Chem. Lett. (1996) 1037.

[10] Wolak, M. A.; Gillespie, N. B.; Thomas, C. J.; Birge, R. R.; Lees, W. J., J. Photochem. Photobiol. A: Chem. (2002) 147, 39.

[11] Chen, Y.; Xiao, J. P.; Fan, M. G.; Yao, B. Proc. SPIE (2005) 5643, 73.

[12] Chen, Y.; Wang, C.; Fan, M. G.; Yao, B., Opt. Mater. (2004) 26, 75.

[13] Chen, Y.; Li, T.; Fan, M.; Mai, X.; Zhao, H.; Xu, D., Mater. Sc. Eng. B (2005) 123, 53.

[14] (a) Bahajaj, A. A.; Asiri, A. M., Opt. Mater. (2006) 28, 1064.

(b) Baghaffar, G. A.; Asiri, A. M., Submitted, Pigment & Resin Techn, (2007)

[15] Asiri, A. M., J. Chem. Res. (S) (1997) 302.

[16] Francini, F.; Ottavi, G.; Sansoni, P.; Tribilli, B., Opt. Commun. (1996) 130, 235.

[17] Rappon, M.; Ghazalli, K. M., Eur. Polym. J. (1995) 31, 233.

[18] Rappon, M.; Ghazalli, K. M., Eur. Polym. J. (1995) 31, 1185.

[19] Yoshioka, Y.; Tanaka, T.; Sawada, M.; Irie, M. M., Chem. Lett. (1989) 18 (1), 19.

[20] Rappon, M.; Ghazalli, K. M.; Rochanakij, S., Eur. Polym. J. (1997) 33, 1689.

[21] Rappon, M.; Syvitski, R. T.; Chuenarm, A., Eur. Polym. J. (1992) 28, 399.

[22] Laidler, K. J. Ed., Chemical Kinetics, Haper & rows, New York, 3rd Ed., (1987) 114.

[23] Bahajaj, A. A.; Asiri, A. M., Pigment & Resin Techn. (2005) 34, 275.

[24] Lafond, C.; Bolte, M.; Lessard, R. A., Proc. SPIE 4833 (2002) 584.

[25] Lessard, R. A.; Lafond, C.; Dererian, G.; Gardette, J.L.; Rivaton, A.; Bolte, M., Proc. SPIE 5216 (2003) 139.

[26] Mleziva, J., Polymery: Struktura, Vlastnosti a Pouziti, Sobotales, Prague, 1st Ed., Czech Republic (1993) 512.

Arabian J. Chem. Vol. 1, No. 1,37-46 (2008)

Electroanalytical Determination of the Hypertensive Drug Propranolol by Anodic Stripping Voltammetric Technique

Ahmad H. Alghamdi[1*], Ali F. Alghamdi[1] and Mohammed A. Alomar[2]

[1]Department of Chemistry, College of Science, King Saud University
P.O Box 2455, Riyadh- 11451, Saudi Arabia
Tel.: +966-14676001, Fax: +966-14675992.

Abstract

A simple and sensitive electrochemical procedure for the analysis of propranolol drug in pharmaceutical formulation and biological samples was described. The technique involves adsorptive accumulation of the drug on the gold electrode followed by square wave voltammetric determination of the preconcentrated analyte. In acidic media, an anodic electrochemical process involving two protons elimination occurs and the mechanism for the oxidation process was suggested. The optimal experimental parameters for the assay of this drug include: Britton-Robinson supporting electrolyte (pH 2), accumulation time (180 s), accumulation potential (+0.8 V), scan rate (1000 mV s^{-1}), pulse amplitude (10 mV), frequency (100 Hz) and convection rate (3000 rpm). The calibration graph for the determination of propranolol was linear over the concentrations range 5×10^{-8}- 1×10^{-6} mol l^{-1} (r = 0.999) with a detection limit of 1.36×10^{-9} mol l^{-1} (0.35 ppb). The precision of the proposed procedure was estimated by 10 successive voltammetric measurements of 5×10^{-7} mol l^{-1} propranolol and the calculated relative standard deviation was 3.8%. The percent recovery indicating the accuracy of the analytical method has been found as 99.75%. Possible interferences by several substances usually present in the pharmaceutical formulations have been also evaluated. The developed electroanalytical method was successfully applied to assay propranolol in pharmaceutical dosage form and biological fluids such as urine and plasma.

Keywords: Propranolol, Square wave, Anodic stripping voltammetry, Au solid electrode.

* Correspondence Author: E-mail: ahalgamdy@hotmail.com

1. Introduction

Anodic stripping voltammetric (ASV)as a method of analysis over the last two decades have fulfilled an important role in the accomplishments of analytical chemistry for the determination of trace concentrations of many heavy metals, drugs and chemical molecules of biological significance. In fact, there have been many reviews devoted to emphasize and illustrate the wide spectrum and scope of ASV applications and potentialities in the analysis of toxic elements [1], pharmaceutical drugs [2] and forensic science [3]. In addition, various research workers have investigated the anodic voltammetric behavior and properties of several chemical drugs such as cefixime[4], domperidone [5], lansoprazole [6], methotrexate [7], pantoprazole [8], resveratrol [9] and metoclopramide [10].

Propranolol hydrochloride {1-(isopropylamino)-3-(1-naphthyloxy)propan-2-ol} is an β-blocker, used primarily to regulize the heart-beat and to treat and prevent angina pectoris (heart pain) and hypertension[11]. It may additionally be used to relieve the symptoms of excess throid hormones in the bloodstream. β-adrenergic blocking agents are competitive inhibitors of the effect of catecholamines at beta-adrenergic sites. Beta blocking agents drive their name from their ability to inhibit or block the adrenergic response of the heart, thereby decreasing the heart rate and heart contraction vigor and allowing the damaged heart muscle to work more easily[12].

There is a substantial need for analytical methods capable of monitoring propranolol drug at low concentration levels, hence, a wide variety of analytical techniques were introduced to determine trace concentrations of many drugs such as propranolol in pharmaceutical products and biological fluids. Instrumental methods of analysis successively used for determining propranolol include Spectrophotometry [13,14], Flow Injection technique [12,15], liquid chromatographic methods [16-19] and electrochemical methods such as differential pulse polarography, normal pulse voltammetry and differential pulse voltammetry [12,20-22].

Aim of the study: Due to the low content of this medicine compound in some pharmaceutical product, a powerful electrochemical procedure capable of ensuring far enhanced sensitivity is needed. In fact, no devoted research study for the analysis of this drug using especially square-wave anodic stripping voltammetric method (SW-ASV) have been reported in the literature. Accordingly, this work was devoted to a detailed study of the SW-ASV behavior of this medicine compound in order to develop an effective electroanalytical method for the determination of propranolol in pharmaceutical preparation and biological fluids such as serum and urine.

2. Experimental.

Apparatus

All adsorptive stripping measurements were carried out with 797 AV computrace (Metrohm, Switzerland) in connection with Dell computer and controlled by (VA computrace 2.0) control software. Stripping voltammograms were printed via an hp deskjet 5150 printer. A conventional three electrode system was used with gold electrode as the working electrode. Chromatographic determinations of the investigated drug were obtained by an HPLC instrumental model LC-20AT (Shimadzu, Japan) in connection with Dell computer. HPLC chromatograms were printed via an hp LaserJet 1020 printer. pH values were measured with Metrohm 632 pH meter. Biohit adjustable micropipette (USA) and Brand adjustable micropipette (Germany), were used to measure microliter volumes of the standard solutions.

Reagents

All chemicals used were of analytical reagent grade and were used without further purification. Propranolol (Winlab-UK) stock solution of 1×10^{-2} mol l^{-1} was prepared by dissolving an appropriate amount of propranolol in distilled water acidified by few drops of concentrated sulfuric acid in 25 ml volumetric flask. This stock solution was stored in the dark. Standard solutions with lower concentrations were prepared daily by diluting the stock solution with distilled water. Britton-Robinson supporting buffer (pH ≈ 2), 0.04 mol l^{-1} in each constituent was prepared by dissolving 2.47 g of boric acid (Winlab, UK) in 500 ml distilled water containing 2.3 ml of glacial acetic acid (BDH, UK) and then adding 2.7 ml of ortho-phosphoric acid (Riedal-deHaen, Germany) and diluting to liter with distilled water. The carbonate buffer was 0.1 mol l^{-1} in both sodium hydrogen carbonate (Winlab, UK) and disodium carbonate (BDH, UK), while phosphate buffer was prepared from 0.1 mol l^{-1} in both phosphoric acid (Riedal-deHaen, Germany) and sodium dihydrogen phosphate (Winlab, UK). The acetate buffer was prepared from 0.02 M in both sodium acetate (Winlab, UK) and acetic acid (BDH, UK). While, ammonia buffer was prepared by dissolving 4.5 g of ammonium chloride (BDH, UK) in 20 ml distilled water and then adding 35 ml of concentration ammonia (Winlab, UK) and diluting to a liter with distilled water.

Procedure

The general procedure adopted for obtaining adsorptive stripping voltammograms was as follows: A 10 ml aliquot of Britton-Robinson supporting buffer (unless otherwise stated) at desired pH was pipetted in to a clean and dry voltammetric cell and the required standard solutions of propranolol were added. The test solutions were purged with nitrogen for 5 minutes initially, while the solution was stirred. The accumulation potential of +0.8 V vs. Ag/AgCl was applied to a gold electrode while the solution was stirred for 180 seconds. Following the preconcentration period, the stripping was stopped and after 20 seconds had elapsed, anodic scans were carried out over the range 0.0 to 1.5 V. All measurements were made at room temperature.

3. Results and Discussion

SW-ASV Behavior of Propranolol

Preliminary study indicates that the drug was accumulated effectively onto the solid gold electrode (Au) and it can be monitored by ASV approach after scanning the applied potential in the positive direction. For instance, the electrochemical collecting of 5×10^{-7} mol l^{-1} propranolol solution for 60 s in B-R supporting electrolyte (pH 2.0), yielded a single well-defined voltammetric peak at 1131 mV vs. Ag/AgCl reference electrode as can be seen in Figure 1, which illustrates a typical stripping voltammogram for the studied drug. This anodic voltammetric response is thought to have resulted from the oxidation process through the common active site of the N-alkyl-ethanolamine group, where the hydroxyl function is oxidized in two sequential steps, of which the second is the rate determining step, via the radical to ketone [23]. The suggested electrochemical oxidation mechanism is schematically shown in Figure 2.

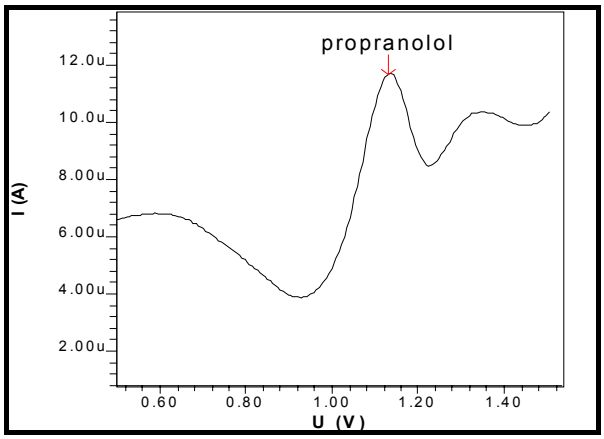

Figure 1: SW-ASV of propranolol in B-R buffer at pH 2.0. Experimental conditions:

T_{acc}= 180 s, E_{acc}= +0.8 V, scan rate 1000 mV s^{-1} and drug concentration 5 ×10^{-7} M.

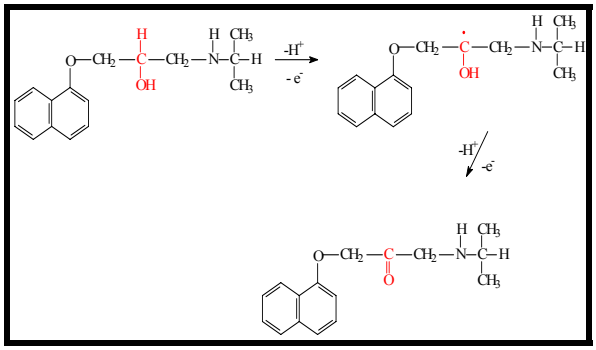

Figure 2: Structure and proposed oxidation mechanism of propranolol drug.

However, the resulted ketone form can be further undergoes quasi-reversible reductive reaction to give the initial alcoholic hydroxyl group. The quasi-reversible characteristic nature of this electrochemical process was confirmed by cyclic voltammetric measurement of propranolol solution at a scan rate of 50 mV s^{-1} in B-R buffer. Cathodic peak was observed for the measured cyclic voltammograms indicating the quasi-reversible characteristic of the investigated electroanalytical response.

Factors Affecting Adsorptive Stripping Response.

Effect of supporting electrolyte and pH

The choice of a suitable medium is an important parameter for the stripping voltammetric determination of the propranolol. Thus, 5×10^{-7} mol l^{-1} solutions of propranolol were studied by SW-ASV method in Britton-Robinson (B-R), carbonate, acetate, ammonia and phosphate buffers at different pH values (3, 7, and 10) after 60 s preconcentration times at 0.0 V accumulations potential.

The ideal adsorptive stripping response in terms of peak shape and current and the smoothness of the baseline was observed when utilizing B-R buffer, which was selected as an optimum buffer for subsequent works. In general, it was noticed that the peak height of the obtained ASV signal reached it maximum values in acidic media. The influence of the variation of pH over the range 2-6.5 on the peak height and potential of the drug signal was investigated further. This is exhibited in Figure 3, in which the stripping voltammetric peak height of 5×10^{-7} mol l^{-1} propranolol solution was plotted as a function of pH. Variations of pH values over the range 2-6.5 gradually decreased the monitored ASV peak current. For analytical purposes, the optimum pH value seems to be around pH 2.

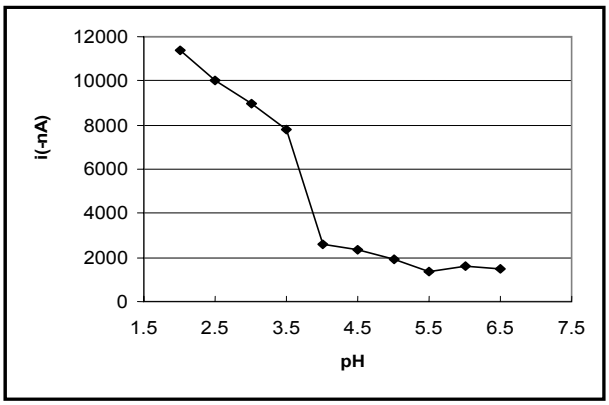

Figure 3: Effect of pH on the peak current of 5 ×10^{-7} M propranolol. Experimental conditions: supporting electrolyte B-R buffer, T_{acc}= 60 s and E_{acc}= 0.0 V .

Meanwhile, the peak potential of the propranolol drug was found to be dependent on the pH of the buffer solution. A gradual shift to a more positive potential was observed from 1137 mV to 1166 mV when increasing pH value over the range 2-6.5, shown involvement of hydrogen ions in the electrochemical process.

Effect of accumulation conditions

Preconcentration of the analyzed drug on the surface of the Au electrode is another essential condition for highly sensitive determination since the amount of the accumulated propranolol depends on the length of time over which accumulation process allowed to proceed, in addition to the intensity of stirring and applied accumulation potential. The oxidation current of 5×10^{-7} mol l^{-1} propranolol solution was measured as a function of accumulation time as shown in Figure 4. In a diluted solution, an almost linearly dependent between the ASV peak current and accumulation time was observed from 0.0 sec to 420 sec. For reducing experimental time, A 180 sec time collection was adopted as an optimum time for the following SW-ASV studies.

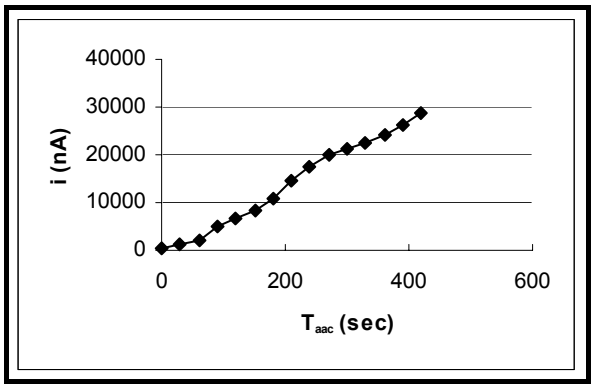

Figure 4: Effect of time accumulation on 5 ×10^{-7} M propranolol peak oxidation current. Experimental conditions: supporting electrolyte B-R buffer (pH = 2) and E_{acc} = 0.0 V .

On the other hand, a sharp effect on the peak current of the drug was recorded due to the variation of accumulation potential from +0.8 V to –0.8 V. The maximum voltammetric peak current value was obtained with an accumulation potential of +0.8 V, which was selected as an optimum potential in order to ensure adequate sensitivity. However, the alteration of accumulation time and potential did not cause significance shifts in the ASV peak potential.

Effect of potential sweep conditions

Generally, the SW-ASV response depends on various parameters related to the way the applied potential was scanned. For instance, the anodic peak current of propranolol was found to be proportional to the scan rate, particularly at high scan rate values. As can be seen from Figure 5, the alteration of scan rate between 100 and 1000 mV s^{-1}, caused the SW-ASV peak current to increase linearly. Furthermore, the effect of changing the pulse amplitude on the square-wave voltammetric current was also evaluated over the range 0.1-10 mV (see Figure 6).

The peak current of propranolol almost increased linearly with pulse amplitude over the range 0.1-10 mV. Accordingly, 10 mV pulse amplitude value was adopted as optimum value. In order to estimate the influence of square wave frequency on SW-ASV peak current, the value of this parameter was varied over the 10-120 Hz range. An initial proportional relationship was observed up to 100 Hz and approximately leveled off declined afterward. Hence, for further studies a 100 Hz frequency was chosen.

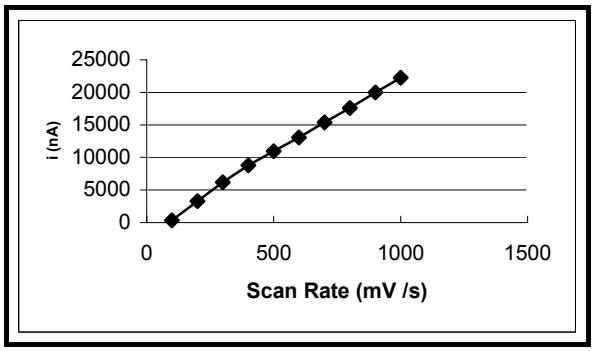

Figure 5: Effect of scan rate on 5 ×10^{-7} M propranolol peak current. Experimental conditions: supporting electrolyte B-R buffer (pH = 2), T_{acc}=180 s and E_{acc} = +0.8 V .

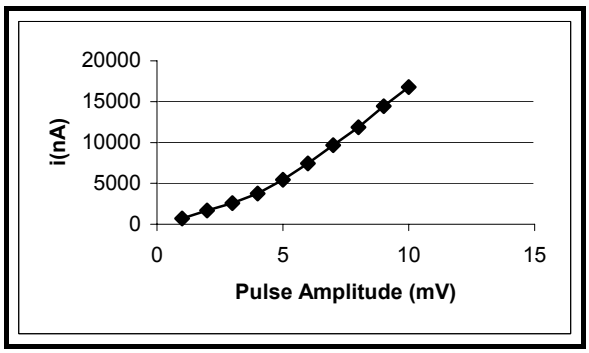

Figure 6: Effect of pulse amplitude on the peak oxidation current of 5 ×10^{-7} M propranolol. Experimental conditions: supporting electrolyte B-R buffer (pH = 2), T_{acc} = 180 s, E_{acc} = +0.8 V and scan rate = 1000 mV/s.

Effect of convection rate

The observed electrochemical signal can be further enhanced by optimizing other instrumental factors that can influence the accumulation process of propranolol. The voltammetric stripping peak current can be maximized by selecting faster stirring rate. In fact, the influence of convection rate on the monitored peak current was evaluated over the range 0 to 3000 rep. As expected, a linear enhancement in the analytical signal was observed with higher convection rate, hence, 3000 rpm stirring speed was chosen as optimum value.

3.3 Quantitative Utility.

3.3.1 Calibration graph.

Under the optimum experimental conditions a good linear correlation was obtained between propranolol electrochemical response and its concentration in the range 5×10^{-8}- 1×10^{-6} mol l^{-1} (see figure 7). The parameters of the drug concentration-current straight line were calculated by the least-squares method. The regression equation of the calibration line has the form:

i_p (nA) = 8.4 ×10^9 C (mol l^{-1}) + 925.2 r = 0.999 n = 7

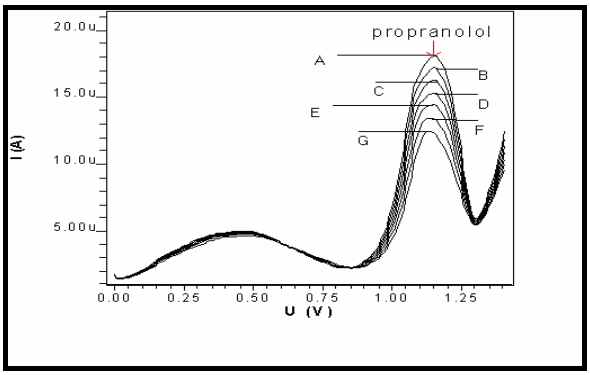

Figure 7: ASV voltammogram for propranolol in B-R buffer(pH = 2.0), T_{acc} =180 sec and E_{acc}= +0.8 V. Drug Conc. :- (A = 1x10^{-6} M, B = 8x10^{-7} M, C = 6x10^{-7} M, D = 4x10^{-7} M, E = 2x10^{-7} M, F =1x10^{-7} M, G = 5x10^{-8} M).

Where i_p is the SW-ASV peak current, C is the propranolol concentration, r is the correlation coefficient and n is the number of determinations.

Detection Limit

The detection limit, defined as three times the signal-to-noise ratio (S/N =3) reached in the optimum conditions for monitoring the drug was 1.36 ×10^{-9} mol l^{-1} (0.35 ppb). Such

remarkable sensitivity illustrates the preference of this electrochemical technique over the conventional analytical techniques such as HPLC, which only achieved 1.5 ppb detection limit [16], or spectrophotometric methods with 100 ppb detection limit [13] and conventional voltammetric methods with 2.1 ppm detection limit [12]. Obviously, the applied stripping voltammetric approach enhanced the sensitivity by 2-3 orders of magnitude in contrast to the cited analytical methods.

Reproducibility

The analytical precision of the developed method was verified from the reproducibility of ten determinations of 5×10^{-7} mol l^{-1} propranolol in B-R buffer at pH 2.0 . A relative standard deviation (RSD) of 3.8% was calculated, which indicates reproducible accumulation and monitoring of the studied propranolol compound.

Recovery

The recovery of the developed procedure, which reflects the accuracy of the method, was evaluated by analyzing spiked buffer solution containing 3×10^{-7} mol l^{-1} propranolol via the optimized SW-ASV procedure. The mean recovery of four measurements was found to be 99.75% ± 0.96.

Stability

The stability of the electroanalytical signal of 5×10^{-7} mol l^{-1} propranolol was investigated by monitoring the SW-ASV signal at the optimum analytical conditions. The signal was measured every ten minutes and the measured electrochemical response seemed to be increased slightly over the studied time period (0-90 minutes).

Interferences.

The effects of some possible interfering substances usually present as ingredients in pharmaceutical tablets (such as starch, lactose, sucrose, cellulose, and magnesium setearate) on the stripping voltammetric determination of propranolol were also investigated. The interferences by diverse materials were evaluated by adding appropriate amounts of these substance at different concentrations (1, 5- and 50-fold) higher than the concentration of propranolol in the test solution (10 ml of B-R buffer containing 5×10^{-7} mol l^{-1} propranolol). Although a moderate increases in the voltammetric signals were observed after the addition of most of these interferences, however, the presence of very high concentrations (50-folds) of these interferences did not enhanced the monitored ASV response by more than 30% of its original response.

Practical Applications.

The proposed SW-ASV method has been applied to the determination of propranolol in some real samples such as pharmaceutical tablets and human urine and plasma. The propranolol content of commercially available tablets [Inderal contain 40 mg of propranolol, Zeneca, UK] was determined directly by the optimized ASV method after the required dissolving and filtration steps. Five aliquot of the dissolved sample were diluted to the required concentration level and measured via the standard additions approach. For these studies, results obtained gave a recovery mean of 97.3 % with standard deviation of ±1.4%.

As can be seen from Table 1, these results achieved by the optimized ASV procedure were in good agreement with those obtained by the HPLC reference method. The agreement of the compared results was tested by the paired t-test and F-test statistical approach. The means of both analytical methods were found to be not differ significantly, since the calculated t-test value (0.784) was less than the critical value (2.776). In addition, the variances of the developed ASV procedure and the HPLC

reference method did not differ significantly, since the calculated F-test value (2.45) was less than the critical value (19), at the 95 % confidence level.

Table 1: comparative determination of propranolol in its commercial tablets by the proposed SW-ASV method and the reference HPLC method.

Tablet	SW-ASV		HPLC	
40 mg Propranolol	Recovery %	Found (mg)	Recovery %	Found (mg)
	38.4	96	39.2	98
	38.8	97	39.6	99
	39.5	98.8	98.8	97.22
	Mean	**38.9 mg**	**Mean**	**39.23 mg**
	S.D.	**±1.4**	**S.D.**	**±0.89**

Furthermore, the applicability of the ASV procedure for the analysis of propranolol in biological samples was also evaluated by estimating its recovery from spiked human urine and plasma samples. A simple and fast pretreatment (clean-up) procedure, which is in fact a slight modification of the sample preparation method developed for the determination of some antagonist drugs [24] was used. By adding a small amount of 5% $ZnSO_4.7H_2O$ solution, NaOH and methanol to the urine or plasma samples and centrifuging the mixture, most of the interfering substances (mainly proteins) were simply removed and eliminated by precipitation. As can be extracted from Table 2, this ASV method (after appropriate dilution and applying standard addition approach) allowed the determination of propranolol in spiked urine and plasma samples with mean recoveries ±SD 97 % ± 0.82 and 95.33 % ± 0.6, respectively.

Table 2 : Analytical results for propranolol recovery from biological fluids.

	Spiked Urine	**Spiked plasma**
	% Drug Recovery	% Drug Recovery
Added propranolol	96	95
3.0×10^{-7} mol l^{-1}	97	95
	97	96
	98	---
Mean	97	95.33
Standard Deviation	±0.82	±0.6

Acknowledgement

This work was supported by College Science Research Centre (project No **ST/Chem/2007/35**), and it was supported by King Abdulaziz City for Science and Technology (project No **15/28**).

References

[1] P. Ostapczuk, P. Valenta, H. Rutzel and H.W. Nurnberg, Sci. Total. Environm., **60,** 1-16 (1987).

[2] J.C. Vire, J.M. Kauffmann and G.J. Patriarche, J. Pharm. Biomed. Anal., **7**, 1323-1335 (1989).

[3] J.H. Liu, W.F. Lin and L Taylor, Forens. Sce. Inter., **16**, 43-52 (1980).

[4] A. Golcu, B. Dogan and S.A. Ozkan, Talanta, **67**, 703-712 (2005).

[5] T. Wahdan and N.A. El-Ghany, Farmaco, **60**, 830-833 (2005).

[6] A. Radi, J. Pharm. Biomed. Anal., **31**, 1007-1012 (2003).

[7] L. Gao, Y. Wu, J. Liu and B. Ye, J. Electroanal. Chem. **610**, 131-136 (2007).

[8] N. Erk, Anal. Biochem., **323,** 48-53 (2003).

[9] H. Zhang, L. Xu and J. Zheng, Talanta, **71**, 19-24 (2007).

[10] O.A. Farghaly, M.A. Taher, A.H. Naggar and A.Y. El-Sayed, J. Pharm. Biomed. Anal., **38**, 14-20 (2005).

[11] R. D. Joseph and A. Digregorio, Eds., Basic Pharmacology in Medicine, McGraw Hill, (1989).

[12] A. G. Al-Shammeri, Flow-Injection Determination of Some Essential Drugs Using Voltammetric Detection, M. Sc. Thesis, King Saud University, Riyadh. p. 34-81 (1998).

[13] A. A. El-Emam, F. F. Belal, M. A. Mustafa, S. M. El-Ashry, D. T. El-Sherbiny and S. H. Hansen, IL Farmaco, 58, 1179-1186 (2003).

[14] S. Khalil and N. Borham, J. Pharm. Biomed. Anal., 22, 235-240 (2000).

[15] G. Z. Jsogas, D. V. Stergiou, A. G. Vlessidis and N. P. Evmiridis, Anal. Chim. Acta., 541, 149-155 (2005).

[16] C. Pham-Huy, B. Radenen, A. Sahui-Gnassi and T. R. Cloude, J. Chromatogr. B, Biomed. Appl., 665, 125-132 (1995).

[17] W. Li and R. C. Lanman, Anal. Lett., 20, 603-615 (1987).

[18] A. A. Al-Warthan, Anal. Chim. Acta., 317, 233-237 (1995).

[19] Guiberteau-Cabanillas and Galeano-Diaz, Ann. Chim. (Roma), 83, 11-12 (1993).

[20] M. A. El-Ries, M. M. Abu-Sekkina and A. A. Wassel, J. Pharm. Biomed. Anal., 30, 837-842 (2002).

[21] F. Belal, O. A Al-Deeb, A. A. Al-Majed and E. A. Gd-Kariem, Il Farmaco, 54, 700-704 (1999).

[22] A. Ambrosi, R. Antiochia, L. Campanella, R. Dragone and I. Lavagnini, J. Hazard. Mater., 122, 219-225 (2005).

[23] E. Bishop and W. Hussein, Analyst, 109, 65-71 (1984).

[24] G. Stubauer and D. Obendorf, Analyst, 121, 351-356 (1996).

Arabian J. Chem. Vol. 1, No. 1, 47-59 (2008)

Hydroconversion of n-Heptane Over Modified H-ZSM-5 Zeolite Catalysts.

Abd EL-Wahed, M. G.[a*]; EL- Khatib, S. A.[a]; Mohamed, L. Kh.[b]and EL-Sadaany S. A.[b]

a)Chemistry Department, Faculty of Science, Zagazig University, Zagazig, Egypt.
b) Egyptian Petroleum Research Institute, Nasr City, Cairo, Egypt.
research@epri.sci.eg

Abstract

The hydroconversion of n-heptane over H-ZSM-5, Pt/H-ZSM-5, DH-ZSM-5 and Pt/DH-ZSM-5 catalysts was studied at temperatures 250-450˚C, using a pulse-microcatalytic reactor. The product distribution was determined employing gas chromatography.

Modification of H-ZSM-5, via dealumination and Pt-incorporation, as well as reaction temperature elevation, improves the total conversion of n-heptane from 22.21 to 100 wt %. The data obtained show that, the investigated solids seem to be excellent catalysts for hydrocracking reaction. Propane and butanes are the most predominant components in the products, indicating that C-C bond rupture is essentially centric (or near centric) rather than peripheral. Isomerization is also included as a substantial reaction in the transformation of n-heptane. Promotion of catalysts with 0.3 wt% Pt enhances the skeletal rearrangement of the alkane. A considerable amount of branched heptane once formed is cracked to lighter isoparaffins. Cyclization to methylcyclohexane and dehydrocyclization to aromatics are reactions of little significance on the metal-loaded H-ZSM-5 catalysts. However aromatization, particularly to toluene, is enhanced on alumina–deficient samples due to their pore widening as a result of the dealumination process.

Keywords: Hydroconversion, Zeolite catalysts, n-Heptane.

1. Introduction

The use of heavy petroleum cuts as jet fuel, diesel oil, or lubricants is limited by their characteristics at low temperatures and especially by their pour points. Such properties can be much improved chemically, by eliminating the long–chain paraffins having relatively high freezing points. This can be achieved through hydroisomerization or hydrocracking of n-paraffins on bifunctional catalysts [1, 2].

Bifunctional catalysts, consisting of a noble or transition metal loaded on an acidic support such as zeolites, are frequently used for these reactions [3-5]. High silica content acidic zeolites are attractive catalysts because of their hydrothermal and acidic stability, high resistance to the deposition of bulky coke molecules, and high activity and selectivity for a specific type of reactions [6, 7]. H-ZSM-5 type materials are the most important members of a new class of high silica zeolite, known as “pentasils”. Its least siliceous form has a higher SiO_2/Al_2O_3 ratio than naturally occurring and earlier synthetic zeolites [8]. It is characterized by large number of acid sites which acquire high strength. The zeolite possesses tridimensional channel system which consists of vertical channels with the size of 5.3 × 5.6 Å and

perpendicular to zigzag formed channel, whose dimension account to 5.1×5.5 Å [9, 10]. The medium pore zeolites have been proved to be a very important class of catalysts for a number of catalytic processes [11].The catalyst functionality can be significantly modified for refining types of reactions by balancing its acidic function, represented by the protonated zeolite, with its metal function represented mainly by the Pt sites [12, 13].

Although many papers have been already published dealing with studies on zeolites for various reactions systems [14, 15], it is still necessary to further investigate the properties and catalytic behavior of these catalysts. In the present work, the performance of H-ZSM-5 and metal loaded-H-ZSM-5 catalysts were studied using n-heptane as a model compound,where the reactant molecule can undergo variety of reactions such as cracking, isomerization, oligomerization, hydrogen transfer and aromatization reactions [16]. Moreover, n-heptane hydrocracking is much easier than n-pentane or n-hexane hydrocracking because it involves more stable carbenium ion intermediate [17]. The investigated H-ZSM-5 zeolite catalyst has been subjected to two modifications: 1) Dealumination to increase the SiO_2/Al_2O_3 ratio; 2) Promotion with Pt. The effect of these modifications on the catalytic behavior of H-ZSM-5 on the n-heptane hydroconversion was determined.

2. Experimental

All materials used in this work are highly pure.

Catalysts Preparation:

The catalysts studied in the present work were prepared according to the following procedures:

Preparation of H-ZSM-5, (HZ) Catalyst:

The Na^+ ions in Na-ZSM-5 were exchanged with NH_4 ions using ammonium chloride solution (3M).The catalyst was separated, washed with bidistilled water, till removal of all Cl^- ions and finally dried at 110˚C overnight. The hydrogen form of ZSM-5 zeolites was obtained by calcining NH_4-ZSM-5 in air at 530˚C for 4 hours.

Dealuminated H-ZSM-5, (DHZ) Catalyst:

H-ZSM-5 zeolite was dealuminated using (2N) HCl solution (1: 10). The mixture was refluxed at 150˚C for 12 hours till pH =7 were attained. The product was filtered, washed and dried overnight and calcined at 530˚C for 4 hours.

Catalysts Impregnation with Platinum:

H-ZSM-5 and dealumination H-ZSM-5 catalysts were impregnated with the required quantities of an aqueous solution of chloroplatinic acid ($H_2PtCl_6.6H_2O$) containing 0.4 gm Pt/gm such that the final catalysts contains 0.3 wt% Pt. The obtained catalysts were dried and calcined as described above.

Catalysts Characterization:

X-Ray Diffraction (XRD):

X-Ray powder diffraction was conducted on the various prepared catalysts using a Bruker Axs D8 diffractometer. All the samples were run with Nickel-filtered copper radiation (λ=1.5405Å) at 60 or 35 KV and 25 or 16 mA at a scanning speed of 2˚ in 2θ / min.

Textural Characteristics:

The specific surface areas and the pore volumes of HZ and DHZ catalysts were determined from nitrogen adsorption isotherms, measured at -196˚C using a conventional volumetric apparatus. The pore size of the investigated solids was estimated also from the desorption isotherm by using Kelvin equation.

IR Investigations:

IR transmission spectroscopic investigations were carried out using an ATI Mattson Genesis Series FTIR spectrometer. The

IR spectra were determined over the spectral range 4000 – 400 cm^{-1}.

Catalytic Activity Test:

The catalytic activity of the prepared zeolite samples was assessed by means of the test of hydroisomerization-cracking of n-heptane. This reaction was carried out under atmospheric pressure using a "pulse microcatalytic" unit. The experimental set-up is mainly composed of a micro-reactor directly attached to an on-line gas chromatograph, in order to provide immediate analysis of the reactor effluents. A detailed description of this method is given elsewhere [18].

0.2 gm of the catalyst was activated for 2 hours in a stream of hydrogen at 450˚C, thereafter; it was cooled stepwise to the desired reaction temperature. The hydroconversion runs were performed in the range of 250-450˚C with an interval of ≈ 50˚C. A dose of 0.5 µl of the reactant was passed over the catalyst in an H_2 carrier flowing at 30 ml/min. The peaks in the chromatogram of the individual components of the reaction were identified. The catalytic selectivity to a certain component was calculated according to the following equation:

$$Selectivity\% \ for\ component\ A = \frac{Wt\ component\ A \times 100}{Wt\ of\ total\ conversion}$$

3. Results and Discussion

Characterization:

X-Ray Diffraction:

The XRD diffractograms of the various catalysts were performed throughout 2θ range of 4-80. Figure (1a) shows all the intensive XRD lines characteristics for H-ZSM-5 zeolite. This identification was based on the corresponding data reported in reference [19]. The I/I_o value of the adsorption band at 2θ of 23 (d=3.85Å) is taken to represent the 100% peak of H-ZSM-5 sample. The obtained pattern reflects the high degree of crystallinity of this catalyst.

The effect of dealumination process on the crystalline stability of HZ was investigated. The XRD of H-ZSM-5 specimen subjected to dealumination process is depicted in Figure (1b). The 2θ adsorption peak (7.86) or (d=11.23Å), gives I/I_o values of 53.6 and 89.8 for HZ before and after dealumination, respectively. Also, the intensity of the diffraction line at 2θ = 8.8 and d-spacing of 10.03Å increased from 33.1 to 57.7 for HZ and DHZ samples, respectively. Moreover, the I/I_o value of the characteristic band of alumina at 2θ = 66.14 and d = 1.4Å, was 3.9Å for HZ compared to 2.4 for alumina-deficient HZ. Hence, the overall indication of XRD is partial dealumination of the zeolitic component. No shift in the 2θ values was observed, which means that the dimension of the unit cell does not change. No reflection due to Pt incorporation into the zeolite, (HZ and DHZ), was observed. The disappearance of the Pt diffraction lines suggests that the concentration of Pt crystallites is quite small which are not capable of detection via XRD method.

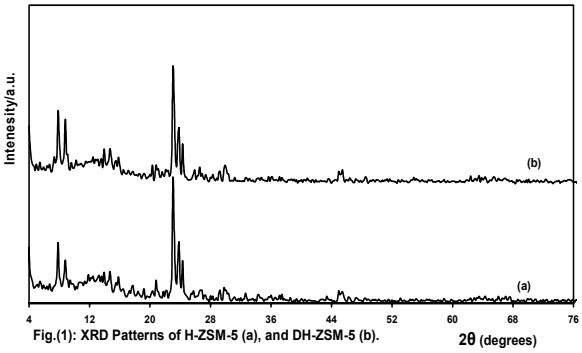

Figure (1) XRD Pattern of H-ZSM-5 (a), and DH-ZSM-5 (b) 2θ(degrees)

Textural Characteristics:

The values of specific surface area, total pore volume and mean pore size of HZ and DHZ samples were listed in Table

(1). The data demonstrate that, subjection of H-ZSM-5 to the dealumination process results in about 13% increase in the specific surface area of the investigated zeolite, associated with other increases in pore volume and size. The widening of pores has been attributed essentially to the partial removal of alumina.

Table (1): Textural Properties of HZ and DHZ samples:

Sample	Surface area, (S_{BET}) m^2/g	Pore volume, cc/gm	Average Pore size, Å
H-ZSM-5	393.39	0.219	11.95
DH-ZSM-5	444.49	0.315	15.04

Fourier Transform Infrared Studies, FTIR:

The FTIR spectrum of H-ZSM-5 catalyst Figure (2), shows three OH bands. The strong and sharp band at 3741 cm^{-1}, is attributed to the OH stretching of terminal silanol groups located at the external zeolite surface. The smaller band at 3620 cm^{-1}, is associated with the stretching of the acidic bridging Si(OH)Al groups located at the internal zeolite surface. Additionally, a pronounced component near 3673 cm^{-1}, likely corresponding to non-framework alumina, is also detected. The positions are in accordance with those reported previously for the same type of zeolite [20, 21].

The FTIR spectra of DHZ catalyst is shown in Figure (3). It is obvious from these Figures that, the band of the bridging OH's near 3620 cm^{-1}, has a small intensity (which has actually the lower Al content), compared to the virgin HZ sample. This result agrees with that published by Armaroli et al [22]. It is well known that the presence of the bridging OH's is due to the charge unbalance associated to the Al for Si substitution in the bulk of the zeolite structure.

In the lower frequency region when the skeletal spectra of the bulk HZ is observed, bands at 550, 850, 1100, 1225, 1400, 1650 and 3340 cm^{-1}, were detected for the HZ catalysts. The presence of the IR band at 550 cm^{-1}, has been assigned to the five-membered ring of the pentasil zeolite structure [23].

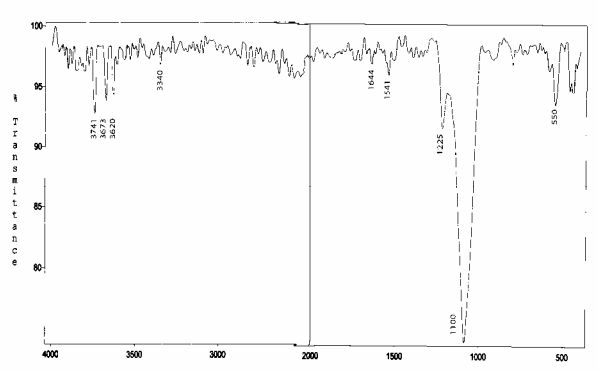

Figure (2): FTIR Spectrum of H-ZSM-5 Catalyst.

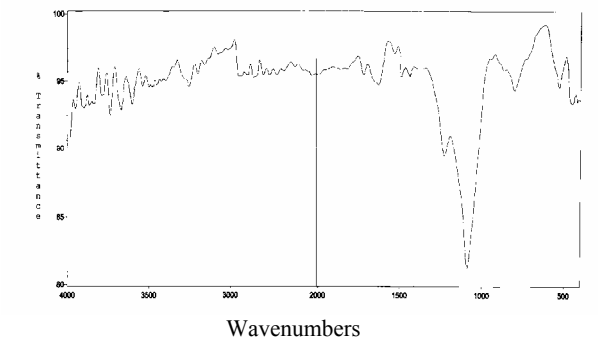

Figure (3): FTIR Spectrum of DH-ZSM-5 Catalyst.

Catalytic activity:

Unloaded H-ZSM-5 (HZ) Catalyst:

The reactions with n-heptane were carried out at various temperatures in 250-450˚C range, using H-ZSM-5 zeolite catalyst. The results depicted in Figure (4) show that, in the temperature domain studied, the transformation is of a moderate level. The total conversions of 22.2 to 70.1 wt % are achieved, a fact that points to the remarkable activity of this catalyst.

Complete analysis of the obtained products has been accomplished using the gas liquid chromatographic (GLC) technique. The data represented in Table (2) and Figure (5) reveal the abundance of components lighter than C_7 which comprise 85.5 - 90.4 % of the converted yield, indicating that the principal reaction using HZ is hydrocracking. Although this catalyst does not contain metals, the produced alkanes are mainly saturated. This behavior suggests that HZ zeolite possesses a self-hydrogenating activity which is accomplished via hydrogen transfer [24].

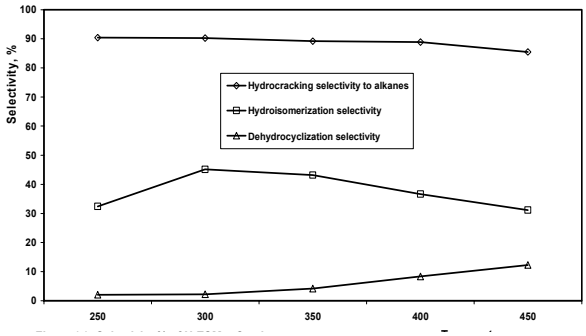

Figure (5) : selectivity,% of H-ZSM-5 catalyst

The catalytic hydroconversion of n-C_7 is characterized by the prevalence of C_3 and C_4 hydrocarbons in the cracked products. It assumes that, the most preferential position of C-C bond scission is that located between the third and the fourth carbon atoms. The percentage of hexanes in the product is always lower than that of pentanes, denoting that splitting of a methyl group from a heptane molecule on HZ catalyst is more difficult than the splitting of an ethyl group. With temperature ascending, butanes, pentanes and hexanes concentrations diminish as a results of further hydrocracking. This can be supported by a relative increase of the percentages of C_1-C_3 in the products.

HZ catalyst exhibits a considerable selectivity for n-heptane isomerization, particularly at 300˚C. The maximum selectivity for iso-heptane formation is 6.2%, whereas the ratios of i-C_4/n-C_4 ranges from 1-2.4 at reaction temperatures between 250-450˚C. It reveals that the catalyst is relatively active for isomerization, but, that the heptane isomers produced are simultaneously cracked mainly to isobutane and propane.

On the other hand, HZ catalyst possesses some activity towards dehydrocyclization reaction. Transformation to aromatics is more favourable at elevated temperatures, and represents ≈11.9% of the converted product at 450˚C. Selectivity for aromatization to benzene and toluene comprises 5.8 and 3.9%, respectively, at such temperature. This proves that HZ unloaded with metal has a particular activity for dehydrocyclization. Negligible amounts of methylcyclohexane, formed via direct ring closure of linear heptane, have appeared in the products, particularly at lower temperatures. Traces of C_8 resulted as a by-product from oligomerization of the cracked fragments was also detected.

Table (2): Hydroconversion of n-Heptane on H-ZSM-5 Catalyst:

selectivity , % / Components	Reaction Temperature , ˚C				
	250	300	350	400	450
Conversion , %	22.21	41.78	55.36	64.46	70.11
$C_1 + C_2$	0.70	1.20	1.90	4.12	7.30
C_3	29.72	31.54	32.95	35.50	36.70
i-C_4	26.00	32.50	31.70	30.40	26.57
n-C_4	27.01	15.10	14.43	13.60	11.20
i-C_5	1.36	3.58	3.06	2.17	1.47
n-C_5	2.70	2.24	1.47	0.74	0.58
i-C_6	0.36	2.87	2.61	1.77	1.24
n-C_6	2.52	1.22	0.92	0.57	0.43
i-C_7	4.68	6.15	5.78	2.33	1.80
MCH	1.62	1.32	0.98	0.50	0.40
Benzene	0.43	0.63	2.55	4.54	5.76
C_8	2.90	1.44	0.98	0.57	0.46
Toluene	0.00	0.21	0.40	1.51	3.84
Ethyl benzene	0.00	0.00	0.02	0.58	1.00
Xylenes	0.00	0.21	0.27	1.10	1.25
Hydrocracking selectivity to alkanes	90.37	90.25	89.18	88.87	85.49
Hydroisomerization selectivity	32.40	45.10	43.15	36.67	31.08
Dehydrocyclization selectivity	2.05	2.16	4.20	8.32	12.25
To cycloparaffins	1.62	1.32	0.98	0.50	0.40
To aromatics	0.43	0.84	3.22	7.73	11.85
i-C_4/n-C_4	0.96	2.15	2.20	2.23	2.37
$\sum C_1,C_2,C_5$ and C_6/C_3+C_4	0.09	0.14	0. 13	0.12	0.14
$C_1+C_2 / \sum C_1 - C_6$	0.007	0.013	0.020	0.050	0.086
$\sum C_1,C_2,C_5$ and $C_6 / \sum C_1 - C_6$	0.084	0.123	0.112	0.110	0.129

Pt-Loaded H-ZSM-5 (Pt /HZ) Catalyst:

The influence of Pt incorporation in HZ zeolite on n-heptane hydroconversion as a function of reaction temperature is illustrated in Figure (4). A significant change in the catalytic activity of HZ occurs on its loading with a low concentration of 0.3 wt% Pt. Such modification enhances the activity from 22.2 to 42.3 wt % at 250˚C, and from 55.4 to 92.1 wt % at 350˚C Tables as shown (2 and 3). This enhancement is undoubtedly attributed to the bifunctionality [25], where Pt catalyses the dehydrogenation of the alkane which is then protonated at a BrÖnsted acid site to form an alkylcarbenium ion that rearranges and/or cracks. This ion migrates as an alkene to be hydrogenated on a metal site giving a saturated product [26]. The distribution of the individual hydrocarbons in the converted products of n-heptane demonstrates the predominance of hydrocracking reaction over Pt/HZ catalyst, Table (3) and Figure (6).

The concentration of components lighter than C_7 commences with ≈ 87.4 % at 250˚C to attain 93.5 % at 450˚C. The dissociation of heptane is slightly lower in magnitude

than that of HZ catalyst, particularly at 250˚C, beyond which this amount is shifted to higher values (compared with the unloaded sample). The major hydrocracked constituents are propanes and butanes, which implies that chain splitting occurs very frequently near the center of the molecule.

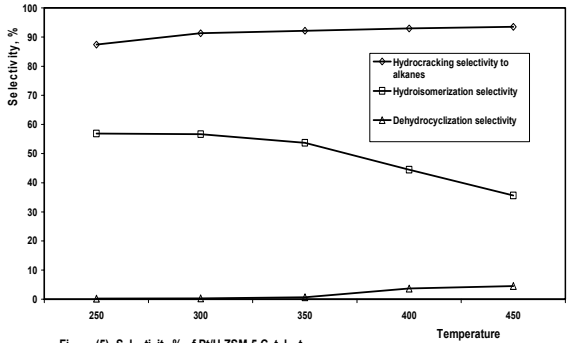

Figure (6) selectivity, % of Pt/H-ZSM-5 catalyst

However, hydrocracking selectivity for centric fission is lower than that for HZ, since higher amounts of C_1, C_2, C_5 and C_6 are achieved too, indicating that the terminal C-C bond cleavage are also included . Therefore, promotion of the catalyst with Pt increases the inclination to peripheral bond rupture, which can be ascribed to hydrogenolysis. Hydrogenolysis takes place principally on Pt crystallites rather than on acid sites. The relative higher acceleration of C_1 and C_2 formation over Pt containing catalyst substantiates the role of Pt content for enhancing hydrogenolysis. In the hydroconversion of n-heptane, it is recognized that hydrogenolysis is favored by the presence of large Pt particles [27].

Pt/HZ possesses hydroisomerization activity surpasses that of the parent HZ catalyst. Total isomerized components amount to 56.9 % from the transformed yield was obtained at 250˚C, on the former sample, compared to 32.4 % on the latter catalyst. The presence of metal has inhibited the catalytic cracking activity, to some extent, at the lower temperature, i.e., 250˚C, and directed the activity towards the skeletal rearrangement. This reflects the importance of bifunctionality for n-alkane isomerization. From the data in Tables (2 and 3), it is obvious that, maximum selectivity for branched heptane production was as high as 12.2 % with Pt - containing zeolite, whereas only 6.2 % was attained on HZ catalyst. Isomerization reaction is favoured at mild temperatures (between 250 and 300˚C). More intensive temperature leads to a decrement in the yield of C_7 isomers due to the destruction of the formed species. At 350˚C more than 92% of the heptanes are hydrocracked with an i-C_4 /n-C_4 ratio of 5.1 compared to 2.3 with HZ at the same reaction temperature.

The data reflects substantial paucity of dehydrocyclized products on Pt/HZ compared to HZ catalyst. The weight of the cyclic constituents in the converted yield started with a value of 0.2 % at 250˚C and ascended to 4.6 % at 450˚C over the Pt metal-loaded catalyst, whereas they comprised 0.1 and 12.3 % for the unmodified HZ, at the same reaction temperature, respectively. These components consist mainly of aromatics, particularly benzene.The difficulty of cyclic compounds formation in the presence of metal-containing HZ can be ascribed to their relatively narrow pores. Insignificant amounts of polymerized constituents, represented by octane, were appeared as a by-product.

Dealuminated H-ZSM-5 (DHZ) Catalyst:

A second modification of H-ZSM-5 catalyst has been carried out for raising the SiO_2:Al_2O_3 ratio, by reducing the alumina content. The dealuminated catalyst, DHZ, has been found to exhibit significantly different catalytic performance for n-heptane hydroconversion than the catalysts mentioned before. It has resulted in appreciable improvement in the overall catalytic activity, particularly at lower temperature, i.e., 250˚C, to be 74.3 wt % compared with 22.2 and 42.5 wt % for HZ and Pt/HZ samples, respectively. By further increase, of

temperature up to 450˚C, most of the reactant, i.e., 99.5 wt %, has been hydroconverted can be seen in Figure (4).

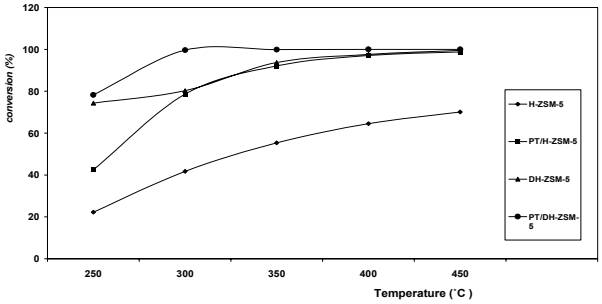

Figure(4) : Hydroconversion percent n-Heptane on H-ZSM-5, Pt/H-ZSM-5, DH-ZSM-5 and Pt/DH-ZSM-5 catalysts

Alumina-deficient HZ zeolite has slightly higher selectivity levels towards hydrocracking and hydroisomerization reactions than the original HZ catalyst particularly at 250-350˚C. More intensive temperatures inhibit the ability of the catalyst for these reactions, to a certain degree, and directed its activity to aromatic production Table (4) and Figure (7).

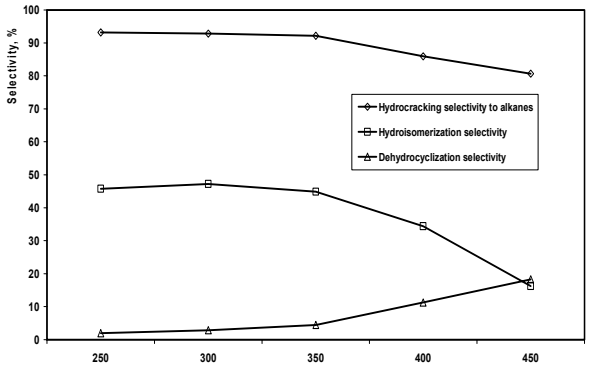

Figure (7) selectivity, % of DH -ZSM-5 catalyst

The increases in aromatic content at higher temperatures are attributed principally to the endothermic dehydrocyclization and dehydrogenation of n-paraffins and the intermediate cycloparaffins, respectively. Aromatics, (which are mainly benzene resulted essentially from toluene cracking), are formed in a significant amount at 450˚C and comprise 18.1%. Nevertheless, methylcyclohexane is found in the product in very low concentrations (not exceed than o.5 %) at 250˚C.

Hence, it can be considered that DHZ is the most selective catalyst towards dehydrocyclization reaction amongest all catalysts investigated in this study. The formation of aromatics (even with molecular weight higher than toluene) is facilitated as a result of pore-widening via dealumination that associated with diffusion limitation reduction [28].

Pt–Loaded Dealuminated H-ZSM-5 (Pt / DHZ) Catalyst:

The last modification has been accomplished by impregnating the alumina-deficient hydrogen ZSM-5 zeolite with 0.3 wt % Pt. Such promotion rendered the catalyst quite efficient for n-heptane transformation. A total conversion of 78.2 wt % is achieved at 250˚C, beyond which this value jumped to approach 100 % at elevated temperatures. The improvement in catalytic activity of Pt/DHZ compared with the corresponding unloaded sample is definitely ascribed to the dual functionality of the catalyst.

The product distribution results represented in Table (5) and Figure (8), reveal that the hydroconverted yields composed essentially from components lighter than heptane, in addition to considerable amounts of isomers and modest proportions of aromatics. Hydrocracking selectivities varying from 91.0 to 92.6 % have been realized during the applied temperature range. The abundance of hydrocracked iso-components, namely i–C_4, i–C_5 and i–C_6, donates that isomerization of the intermediate n-heptane to iso-heptane precedes hydrocracking under the investigated conditions . It is widely accepted that carbocation rupture is very slow for a

linear olefin. Therefore, a linear carbocation probably undergoes skeletal rearrangement before cracking can take place. The high yield of isomerates confirms the high hydroisomerization capability of Pt/DHZ catalyst, in as much as 51.9 % selectivity has been acquired at high conversion of 99.6 wt %, compared to 47.2 % at 80.3 wt % conversion on using DHZ catalyst. Actually, the differences in activity and selectivity between both catalysts can be attributed to the dual functionality of Pt-containing DHZ catalyst.

It is also obvious from the data obtained that, upon ascending the reaction temperature, the concentration of the light fraction (C_1-C_3) in the hydrocracked product increases whereas the level of the relatively heavier components declines. Evidently, these heavier hydrocarbons suffer from secondary hydrocracking at such higher severity of the conditions. A remarkable drop in the dehydrocyclization selectivity occurred upon loading the DHZ catalyst with Pt. This resulted from the partial blocking of the pores with the metal particles.

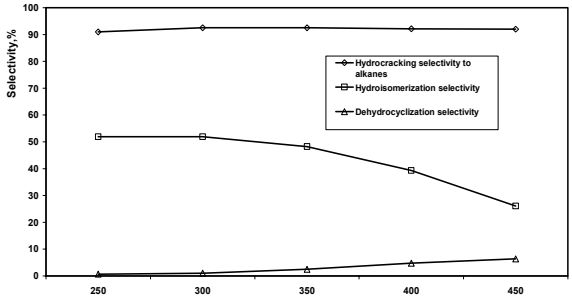

Figure(8) selectivity, % of Pt/DH -ZSM-5 catalyst.

Conclusions

(1) The efficiency of evaluated catalysts for hydroconversion of n-heptane can be arranged ascendingly in the following manner:

HZ < Pt / HZ < DHZ < Pt / DHZ

(2) Modified H-ZSM-5 zeolites are found to be excellent catalysts for hydrocracking reactions.

(3) Pt incorporation in HZ, whether modified or unmodified, is greatly effective, particularly for enhancing the hydroisomerization selectivity of n-heptane.

(4) The unloaded alumina-deficient H-ZSM-5 is the most selective catalyst in this study towards dehydrocyclization reaction.

Table (3): Hydroconversion of n-Heptane on Pt/H-ZSM-5 Catalyst:

selectivity , % / Components	Reaction Temperature , ˚C				
	250	300	350	400	450
Conversion , %	42.46	78.64	92.10	97.10	98.81
$C_1 + C_2$	0.80	1.30	2.22	6.70	13.06
C_3	25.10	29.70	33.59	37.00	40.10
i-C_4	32.10	38.08	36.99	34.31	29.54
n-C_4	10.69	8.73	7.21	6.80	5.96
i-C_5	7.77	7.10	6.80	4.78	3.04
n-C_5	4.33	2.25	1.90	0.95	0.51
i-C_6	4.80	3.20	2.84	1.94	1.08
n-C_6	1.80	0.94	0.60	0.44	0.24
i-C_7	12.19	8.24	7.03	3.40	1.91
MCH	0.15	0.10	0.08	0.05	0.03
Benzene	0.07	0.20	0.58	2.14	2.78
C_8	0.20	0.16	0.14	0.03	0.01
Toluene	0.00	0.00	0.02	0.46	0.51
Ethyl benzene	0.00	0.00	0.00	0.40	0.50
Xylenes	0.00	0.00	0.00	0.60	0.73
Hydrocracking selectivity to alkanes	87.39	91.30	92.16	92.92	93.53
Hydroisomerization selectivity	56.86	56.62	53.66	44.43	35.57
Dehydrocyclization selectivity	0.22	0.30	0.68	3.65	4.55
To cycloparaffins	0.15	0.10	0.08	0.05	0.03
To aromatics	0.07	0.20	0.60	3.60	4.52
i-C_4 / n-C_4	3.00	٤.36	5.13	5.05	4.96
$\sum C_1,C_2,C_5$ and C_6 / C_3+C_4	0.29	0.22	0.18	0.19	0.24
C_1+C_2 / $\sum C_1 - C_6$	0.009	0.014	0.024	0.072	0.140
$\sum C_1,C_2,C_5$ and C_6 / $\sum C_1 - C_6$	0.22	0.16	0.156	0.159	0.190

Table (4): Hydroconversion of n-Heptane on DH-ZSM-5 Catalyst:

selectivity , % / Components	Reaction Temperature , ˚C				
	250	300	350	400	450
Conversion , %	98.44	98.98	99.06	99.13	99.41
$C_1 + C_2$	22.47	24.23	32.55	39.82	46.03
C_3					
i-C_4	34.07	38.54	35.71	32.82	30.25
n-C_4	21.57	19.15	15.51	11.67	9.08
i-C_5	4.51	3.23	2.43	1.80	1.65
n-C_5	5.19	4.85	3.40	1.57	0.65
i-C_6	2.53	1.99	1.21	0.56	0.16
n-C_6	1.73	1.23	0.88	0.32	0.16
i-C_7	2.02	1.15	0.77	0.34	0.17
n- C_7	1.32	0.58	0.41	0.10	0.04
MCH	0.95	0.56	0.47	0.16	0.15
Benzene	0.00	0.23	0.34	0.51	0.72
i-C_8	2.00	1.54	1.07	0.70	0.54
Toluene	1.23	1.56	3.03	6.83	6.9
Ethyl benzene	0.31	0.66	1.47	1.55	1.7
Xylenes	0.10	0.50	0.75	1.22	1.80
Hydrocracking selectivity to alkanes	95.41	94.95	92.87	89.03	88.19
Hydroisomerization selectivity	45.13	46.45	41.19	36.25	32.77
Dehydrocyclization selectivity	2.59	3.51	6.06	10.27	11.27
To cycloparaffins	0.95	0.56	0.47	0.16	0.15
To aromatics	1.64	2.95	5.59	10.11	11.12
i-C_4/n-C_4	2.61	4.14	5.18	4.64	4.25
$\sum C_1,C_2,C_5$ and C_6 / C_3+C_4	0.175	0.161	0.171	0.210	0.675
C_1+C_2 / $\sum C_1 - C_6$	0.020	0.034	0.048	0.084	0.341
$\sum C_1,C_2,C_5$ and C_6 / $\sum C_1 - C_6$	0.150	0.140	0.146	0.172	0.400

Table (5): Hydroconversion of n-Heptane on Pt/DH-ZSM-5 Catalyst:

selectivity , % / Components	Reaction Temperature , ˚C				
	250	300	350	400	450
Conversion , %	78.23	99.62	99.95	99.99	100
$C_1 + C_2$	2.41	3.58	4.04	7.79	17.30
C_3	30.03	33.04	37.02	42.01	45.50
i-C_4	34.02	37.70	35.72	30.31	20.87
n-C_4	11.60	7.80	6.65	5.02	4.23
i-C_5	6.60	6.02	5.90	4.62	2.90
n-C_5	2.16	1.85	0.99	0.67	0.17
i-C_6	3.48	2.01	1.81	1.44	0.86
n-C_6	0.70	0.55	0.42	0.34	0.22
i-C_7	7.82	6.20	4.78	2.93	1.45
MCH	0.32	0.29	0.16	0.04	0.02
Benzene	0.36	0.68	1.75	3.17	4.75
C_8	0.50	0.20	0.16	0.13	0.12
Toluene	0.00	0.08	0.18	2.96	1.11
Ethyl benzene	0.00	0.00	0.12	0.21	0.20
Xylenes	0.00	0.00	0.30	0.40	0.30
Hydrocracking selectivity to alkanes	91.00	92.55	92.55	92.20	92.05
Hydroisomerization selectivity	51.92	51.93	48.21	39.30	26.08
Dehydrocyclization selectivity	0.68	1.05	2.51	4.74	6.38
To cycloparaffins	0.32	0.29	0.16	0.04	0.02
To aromatics	0.36	0.76	2.35	4.70	6.36
i-C_4 / n-C_4	2.93	4.83	5.37	6.04	4.93
$\sum C_1,C_2,C_5$ and C_6 / C_3+C_4	0.200	0.180	0.166	0.190	0.300
C_1+C_2 / $\sum C_1 - C_6$	0.026	0.039	0.044	0.084	0.19
$\sum C_1,C_2,C_5$ and C_6 / $\sum C_1 - C_6$	0.17	0.15	0.14	0.16	0.23

References

[1] Giannetto, G.E.; Perot, G.R. and Guisnet, M.R., Ind.Eng. Chem. Prod. Res. Dev., **25**, 481, (1986).

[2] Noordhoek, N.J.; Schuring, D.; de Gauw, F.J.M.M.; Anderson, B.G.; de Jong, A.M.; de Voigt, M.J.A. and Van Santen R.A., Ind. Eng. Chem. Res., **41**, 1973, (2002).

[3] Kinger, G.; Majda, D. and Vinek, H., App. Catal. A: **225**, 301, (2002).

[4] Aljandre, A.; González, M. and Ramirez, J., Ind. Eng. Chem. Res., **40**, 3484, (2001).

[5] De Lucas, A.; Valverde, J.L.; Sánchez, P.; Dorado, F. and Ramos, M.J., App. Catal. A: **282**, 15, (2005).

[6] Zhang, W. and Smirniotis, P. G., App. Catal. A: **168**, 113, (1998).

[7] Scherzer, J., ACS Symp. Scr., **248**, 157, (1984).

[8] Armaroli, T.; Simon, L.J.; Digne, M.; Montanari, T.; Bevilacqua, M.; Valtchev, V.; Patarin, J. and Busca, G., App. Catal. A: **306**, 78, (2006).

[9] Niu F. and Hofman, H., App. Catal. A: **128**, 107, (1995).

[10] Meier, W.M. and Olson, D.H., Atlas of zeolite Structure Types, Butterworth-Heinemann, 3rd Edn, (1992).

[11] Roldán, R.; Romero, F.J.; Sanchidrian, C.J.; Marinas, J.M. and Gómez, J.P., App. Catal. A: **288**, 104, (2005).

[12] Smirniotis, P.G. and Ruckenstein, E., App. Catal. A: **117**, 75, (1994).

[13] Smirniotis, P.G. and Ruckenstein, E., Catal. Lett; **25**, 351, (1994).

[14] Sen, S.; Wusirika, R.R. and Youngman, R.E., Microporous and Mesoporous Materials, **87**, 217, (2006).

[15] Cheng, Y.; Wang, L.J.; .Li; J.S. Yang, Y.C. and Sun, X.Y., Mat. Lett; **59**, 3427, (2005).

[16] Swanadham, N.V.; Muralidhar, G. and Rao, T.S.R.P., J. Mol. Cat. A: Chem., **223**, 269, (2004).

[17] Guisnet, M.; Alvarez, F.; Lannetto, G.G. and Perot, G., Catalysis to Day, **1**, 415, (1987).

[18] Mohamed, L.Kh., M.Sc. Thesis, Fac. of Eng., Cairo Univ,1992).

[19] Foger, K.; Sanders, J. and Sedon, D., zeolites, **4**, 337, (1984).

[20] Jentys, A.; Tanaka, H. and Lercher, J.A., J. Phy. Chem. B **109**, 2254, (2005).

[21] Triantafyllidis, K.S.; Nalbandian, L.; Trikalitis, P.N.; Ladavos, A.K.; Mavromoustakos, T. and Nicolaides, C.P., Micropor.- Mesopor. Mater. , **75,** 89, (2004).

[22] Armaroli, T.; Simon, L.J.; Digne, M.; Montanari, T.; Bevilacqua, M.; Valtchev, V., Patarin, J. and Busca, G., App. Catal. A: G. **306**, 78, (2006).

[23] Kirschhock, C.E.A.; Ravishankar, R.; Verspeurt, F.; Grobet, P.J.; Jacobs, P.A. and Martens, J.A., Plup. Chem. B **103**, 4965, (1999).

[24] Platteeuw, J.C.; de Ruites, H.; Zoonen, D.V. and Kouwenhoven, H.W., Ind. Eng. Chem., Prod. Res. Dev., **6**, 76, (1967).

[25] Blomsma, E.; Martens, J.A. and Jacobs, P.A., J. Catal., **165**, 241, (1997).

[26] Weitkamp, J., Ind. Eng. Chem. , Prod. Res. Dev., **21**, 550, (1982).

[27] Abul-Gheit, A.K.; Menoufy, M.F.; EL-Fadly, A.M.; EL-Din, O.I.S. and Sultane, S.A., J. Chem. Tech. Biotech., **32**, 1000, (1982).

[28]EL-Morsi, A.K., Ph.D. Thesis, Cairo Univ. Cairo, Egypt, (1983).

Arabian J. Chem. Vol. 1, No. 1, 47-59 (2008)

Arabian J. Chem. Vol. 1, No. 1, 61-66 (2008)

Pharmacological Activity Of The New Compound { 5, 5````-Dipropyl - 2,2`: 5`,2`` : 5``,2```: 5```,2````-Pentathienyl (1) and Octocosanoic Acid, 28-Hydroxy-2`, 3`-Dihydroxy Propylester (2) } Isolated From *ALHAGI MAURORUM* Roots

M. S. Marashdah[1*], H. M. AL- Hazimi, M. A. Abdallah[1], B. M. Mudawi [2]

Department of Chemistry, Faculty Of Science, King Saud University, Riyadh-11451, P.O.Box 2455, Saudi Arabia
[2]Department of Chemistry, Faculty of Science, Khartoum University, Khartoum, Sudan

الملخص

قمنا حديثاً بدراسة مكثفة على خلاصات متنوعة لجذور نبات العاقول (الذي ينمو في فلسطين) من أجل فصل المكونات الكيميائية الفعالة في الخلاصات. وقد تمت دراسة الخواص الطبية للمركبين (1) و (2)، اللذين فصلا بشكل نقي، ليعطيا النتائج التالية: i) أدى حقن المركب (1)، بطريقة الاعتماد على الجرعة، في صفاق بطن الفئران إلى خفض درجة حرارة الجسم بمعدل ٩,٦ درجة مئوية. ii) لم تؤد معالجة العضلات البطنية لمستقيم الضفادع بجرعات ٤ ملغـم /مـل مـن المركب (1) إلى التأثير سلباً على الانقباض الناتج عن الأستيلين كولين المحثوث. iii) لم ينتج عن المركـب (1) تـأثير ملحوظ على القلب. iv) للمركب (2) تأثير منبه ومثبط لعضلة القلب. v) أدى المركب (1) و (2) إلى استرخاء حالب خنازير غينيا وثبطا التقلصات الناتجة عن الهيستامين المحثوث، مما يجعلهما يساعدان على التخلص من حصوات الكلـى و تخفيف الألم المصاحب لذلك.

Abstract

Various extracts of *Alhagi maurorum* (growing in Palestine) roots were recently subjected to an extensive study to isolate its chemical constituents [1-3]. Compounds (**1**) and (**2**) – which were isolated as pure compounds - were investigated for their pharmacological activity to give the following results: 1- Administration of compound (**1**) intraperitoneally into mice decreased the body temperature in a dose dependent manner. The decrease was about 9.6 ^{o}C. 2- Treatment of the frog rectus abdominis muscle with compound 1 in doses of 4 mg / ml bathing fluid did not antagonise Acetyl Colin (Ach) (neurotransmitter) – induced contraction. 3- Compound (**1**) did not produce significant effects on the heart. 4- Compound (**2**) possessed a heart rate stimulant action and a myocardial depressant action. 5- Compound (**1**) and compound (**2**) induced relaxations to the guinea – pig ureter and suppressed histamine – induced spasms. Both compounds seemed to possess an anticolic action and a ureter relaxing action that can enhance getting ride of renal stones and relieve of the accompanying pain (contraction of the ureter). 6- None of the compounds possessed the property of enhancing dissolution of oxalate celculi.

Keyword: Alhagi maurorum ; Leguminosae; Thiophenol derivatives; Octacosanoic acid ester; Biological tests.

[*] ms_marashdah@yahoo.com

1. Introduction

Alhagi maurorum is used in folk medicine as a purgative, laxative, diaphoretic, expectorant and diuretic [4, 5]. Its flowers are used to treat piles, migraine, and warts. Oil from the leaves is used in the treatment of rheumatism [6]. Locally, water extracts of its roots are used to enlarge the ureter and to remove kidney stones.

2.Experimental

Plant material

The plant was collected from an internal plane in Palestine in February 2004, and identified by Department of Botany and Microbiology, Faculty of Science; King Saud University, Saudi Arabia. The roots were taken out, cleaned and dried in the shade for two weeks and then powdered. The powdered roots were extracted by different solvents of increasing polarity. The various extracts were separated by column chromatography and the compounds were isolated and purified by thin layer chromatography. The structures of the compounds were elucidated mainly by spectroscopic methods in addition to chemical reactions. A good yield was obtained of compound 1 and compound 2 (1.1486 % and 0.5142%), respectively), Therefore their pharmacological activity was examined.

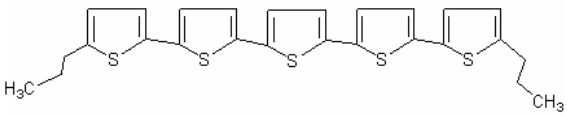

Compound 1

$HO\text{-}CH_2\text{-}CH\ (OH)\text{-}CH_2\text{-}O\text{-}CO\text{-}(CH_2)_{26}\text{-}CH_2\text{-}OH$

Compound 2

Standard procedures for biological activity tests

The effects of the extracts on mice rectal temperature were studied following the method described by Gray et al, 1987 [7] .

The effects of the different extracts on the rectus abdominis muscle were studied following the method described by Fleisher et al, 1960 [8].The effects of the different extracts on the heart using the ECG (Electro - cardio gram) were studied following the method described by Bakheet et al,1999 [9].Also, The effects of the different extracts on the guinea – pig ureter were studied using the method described by Yoshiaki, 1968 [10].

Preparation of test samples

The compounds were used in form of suspension in 0.25 % aqueous sodium carboxy methyl cellulose. After suspension, the mixture was emulsified by vortexing (shaking). A glass rode is usually inserted inside a tube containing the suspension to facilitate emulsification during vortexing in the vortex mixer.

Biological activity tests

1- Effect on rectal temperature: Rectal temperature of mice was measured using an Aplex rectal thermometer (Haly) fitted with thermistor probes. The probe was inserted to a depth of 2.5 cm into the rectum of each mouse and temperature reading was allowed to stabilize, recorded and the probe then removed. The temperature was taken at interval of 30 minutes.

2- Effect on the rectus abdominis muscle of the frog: Initially, each frog was decapitated and then pithed by inserting a needle into the spinal cord. The frog was then fixed to a wooden board with its abdomen facing upwards. The outer skin of the frog was cut longitudinally and horizontally to expose the abdominal wall. The two rectus abdomini muscles were located and the two muscles were cut and removed completely from the animal and placed in Krebs` solution. Then, each muscle was suspended vertically in the chamber of an organ bath containing Krebs` solution and aerated using (95 % O_2 + 5 % CO_2).

The temperature of the bathing fluid was adjusted to 37 ^{o}C. Each tissue was allowed to equilibrate with the bathing fluid for 30 minutes. Each dose of the drug was allowed to contact the tissue for a time to obtain the

maximum response. Each compound was allowed to contact the tissue for 5 minutes before addition of the nicotine agonist. The percentage inhibition induced by the compounds on the agonist submaxional dose was then calculated.

3- Effect on the Electro-Cardio Gram (ECG) of rats: Male Wister rates (250 g) were anesthetized with urethane and prepared for measurement of the ECG waves. The limbs of the animal were fastened to a dissection board with the animal lying on its back. The ECG lead II was recorded by the aid of subcutaneous needle electrodes and the record was displayed in chart of the instrument. The recording speed was adjusted to 25 mm /sec. The compounds were injected intraperitoneally and the effect was then followed for twenty minutes to observe any disturbances in the cardiac rhythm. The heart rate before and after the compound injection was recorded and the percentage changes were then calculated.

4- Effect on the ureter: Guinea-pigs were killed by blows on the neck, and the abdominal cavity of each animal was opened. The kidney and the ureters were located and the whole length of the ureter (from the kidney to the urinary bladder) was cut and placed in Krebs` solution. The ureter was then prepared for the study of the effect of the compounds. 2 cm length of each ureter was suspended in an organ bath containing oxygenated (95 % $O_2$ + 5 % $CO_2$) Krebs` solution. Each tissue was connected to an isometric transducer connected to a physiograph (Narco Biosystems, USA). Each tissue was allowed to equilibrate with the bathing fluid for 30 minutes.

Initially the effects of different doses of the compounds were determined. Then the effect of the compounds on the standard agonists (Histamine, Acetyl Colin (ACh)) were then determined. Each compound was allowed to contact the tissue for 5 minutes before the addition of the agonist. The percentage inhibition induced by the compound on the selected dose of the agonist was then calculated.

3. Results

General screening of compound 1 in conscious mice

Intraperitoneal administration of compound **1** into conscious mice in doses of 1.6 g / kg produced a moderate sedation following its administration. The compound also decreased the locomotion activity of the animals and skeletal muscle relaxation suggesting an action at the skeletal muscles neuromuscular junctions. The compound also decreased the rectal temperature of the animals 5.8 ^{o}C. These results directed the attention to study the effects of the compound on the rectal body temperature of the mice and on the skeletal muscle of the frog. The compound produced changes in the heart rate and this directed the attention to study its effects on the heart rate via registering the electro-cardio gram (ECG).

Effect on Mice Rectal Temperature

Administration of compound **1** in doses of 0.25 and 0.5 g/kg into mice (I.P) induced dose and time dependent decreases in the rectal temperature. Significant decreases were observed 15 minutes following injection of the extract. Maximum decreases of rectal temperature were observed two hours following administration of the extract. At this time the observed decreases were 6.1 and 9.6 ^{o}C at doses of 0.25 and 0.5 g/kg, respectively. Administration of higher doses e.g. 1 g/kg induced death of the animals within twenty minutes. The results are shown in Table 1.

Table 1: Effect of compound 1 on Mice Rectal Temperature.

	Before injection	**Temperature After injection** (min.)				
Dose mg/kg)	0	15	30	60	90	120
250	38.5±0.3	36.5±0.3*	36.3±0.5*	35.4±0.2*	34.3±0.4*	32.4±0.5*
500	39.2±0.7	36.9±0.4*	35.5±0.3*	34.6±0.2*	32.8±0.3*	29.6±0.2*

* ($p < 0.05$), p = statistic factor.

Effect on the Frogs Rectus Abdominis Muscle (Skeletal Muscle).

Exposure of the muscle to compound **1** in a concentration of 1, 2 and 4 mg /ml of bathing fluid did not induce any contraction. However, exposure of the tissue to the same compound in concentration of 10 and 20 mg/ml bathing fluid induced contraction of the tissue.

Effect on ACh-induced Contraction of the Frogs Rectus Abdominis Muscle

1- Exposure of the frog's rectus abdominis muscle to the nicotinic receptor stimulant ACh in concentration of 1 – 4 µg/ml induced concentration – dependent contractions.
2- Exposure of the tissue to compound **1** in concentrations of 4 mg/ml of bathing fluid for 5 minutes did not antagonized ACh – (3µg/ml) – induced contraction.

Effect of the Nicotinic Receptor Blocker.

Atracurium (standard medicine relaxes the skeletal muscles) on compound **1** induced contractions on the frog's rectus abdominis muscle.

Treatment of the Frog's Rectus abdominis muscle atracurium in doses of 100 or 200 µg/ml of bathing fluid for 5 minutes did not block the stimulant action of compound **1**.

Effect on the Rat heart

When rats were anaesthetized with urethane and the ECG was monitored to investigate the effects of the compounds on the heart rate and force of contraction, the results revealed that compound **2** at a dose of 0.2 g/kg (i.p) was myocardial depressants. But compound **1** induced bradycardia while compound **2** induced tachycardia. The results are shown in Table 2

Effect on Calcium oxalate solubility

When 1 g calcium oxalate was added to 5 ml of 20 % solution of the compound **1** and **2** and the mixture was mixed and left to stand for 3 days, there was no solubilization of the calcium oxalate crystal. The weight of undissolved calcium oxalate was not changed compared with the initial weight.

Effect on the Guinea – pig ureter.

Addition of histamine in doses of 3 µg/ml bathing fluid to the isolated guinea – pig ureter induced continuous contractions. But addition of compound **1** in doses of 5 mg/ml bathing fluid completely suppressed histamine induced contractions. Also, it was found that addition of another dose of histamine did not reverse the inhibition, while compound **2** at a dose of 3 mg/ml completely suppressed histamine contractions. Results are shown in Table 3.

Table 2: Effect of compounds 1 and 2 on the rat heart

Extract & Dose	Normal Heart Rate	% change in heart rate after 20 min	% in force of contraction after 20 min	Remarks
5) compound **2** 0.2g/kg (i.p)	330 /min	↑ 27.2 (420 /min)	28.5	Myocardial depressant
2) compound **1** 1g/kg (i.p)	480 /min	↓ 6.25% (450 /min)	No effect	

Table 3: Effect of compounds 1 and 2 on the guinea – pig ureter

Extract and Dose	% inhibition of Histamine – induced contraction
2) Compound **1** 5mg/ml	100%
5) Compound **2** 5mg/ml	100%

Acknowledgment

We are indebted to the staff of the research center, Faculty of Pharmacy, King Saud University, Riyadh, Saudi Arabia, for their contribution in carrying out the biological tests.

References

[1] M. S. Marashdah, B. M. Mudawi, H. M. Al-Hazimi and M. A. Abdallah, New Triglyceride and New Alephatic Ester from the Roots of *Alhagi maurorum* medik, J. Saudi Chem. Soc., (2006), 10 (**2**), 367.

[2] M. S. Marashdah, B. M. Mudawi, H. M. Al-Hazimi and M. A. Abdallah, New Aliphatic Ketone and New Alephatic Ester from the Roots of *Alhagi maurorum* medik, J. Saudi Chem. Soc.,(2006)10 (**3**), 509.

[3] B. M. Mudawi, H. M. AL- Hazimi, M. A. Abdallah and M. S. Marashdah, New Aliphatic Ester and New Theophene Derivative from the Roots of *Alhagi maurorum* medik, J. Saudi Chem. Soc., 11 (**1**) 87.

[4] J. C. Th. Uphof. Ed.,. Dictionary of Economic Plants, Weinheim (1959).

[5] A. Chakravarty, The plant Wealth of Iraq (a dictionary of economic plants). Botany Directorate, Ministry of Agriculture &Agrarian Reform (1976), England.

[6] D. Brown, Encyclopaedia of Herbs and their Uses. Dorling indersley, London (1995), ISBN 0-7513-020-31.

[7] J. A. Gray, G. M. Goodwin, D. J. Hcal and A. R. Green, (1987).

Hypothermia induced by baclofen, a possble index of GABAB receptor function in mice, is enhanced by antidepressant drugs and ECS. Br. J. Pharmacol., (1987) **92**,863.

[8] J. H. Fleisher, L. P. Corrigan and J. W. Howard , Reciprocal Potentiating action of depolarizing drugs on the isolated frog rectus abdominis muscle, Br. J. pharmacol. Chemother, (1960) **15**, 23.

[9] M. Bakheet, K. E. H. El Tahir, M. I. AL-Sayed, H. A. EL-Obeid and K. A. Al-Rashood, Studies on the cardiovascular depressant effects of N-ethyl – and N-benzyl – diphenyl ethanolamine. Elucidatoin of the mechanisms of action. Pharmacol. Res. **37**,(1999) 463.

[10] Yoshiaki Washizu, Epinephrine on potential, tension and ionic content of guinea– big ureter, Eur. J. Pharmacol, (1968) **4**, 411.

Arabian J. Chem. Vol. 1, No. 1, 67-78 (2008)

Diphosphine Compounds : Part 1. Synthesis and Electrochemistry of $(Ph_2P)_2C= CH_2$ and Cis-$Ph_2PCH=CHPh_2$ When Chelated to $M(CO)_6$(M=Cr, Mo, W) and $CuCl_2$

Fatma S. M. Hassan[1], Mahmoud A. Ghandour[2], Adila E. Mohamed[3] and Ahmed F. Al- Hossainy[1,4]

[1, 3, 4]Department of Chemistry, Aswan Faculty of Science, South Valley University, Aswan ,P.O.Box 81528 Egypt
E-mail-al_hossainy@yahoo.com
[2]Department of Chemistry, Faculty of Science, Assiut University, Assiut, Egypt

Abstract

Treatment of hexametal carbonyl $M(CO)_6$ (where M= Cr, Mo, W) and bivalent transition metal $CuCl_2$ in n-decane with one mole of free ligands $(Ph_2P)_2C=CH_2$ **[Vdpp]**[I] and Ph_2**P**(CH=CH)**P**Ph_2[II], gave $[(OC)_4M(Vdpp)]$ [III], $[(OC)_4M\{Ph_2PCH=CHPPh_2\}]$ [IV], $[Cl_2Cu(Vdpp)]$ [V] and $[Cl_2Cu\{Ph_2PCH=CHPPh_2\}]$ [VI]. The redox properties of vinylidine [I] and cis-$(Ph_2PCH=CHPPh_2)$ [II] as ligands and their complexes ([III]-[VI]) have been studied using cyclic voltammetry in an aqueous solvent (Methanol/ H_2O 20%).

The structures of free ligands [I],[II]and their complexes([III]-[VI] have been characterized by using elemental analysis, IR spectra, ^{1}HNMR, ^{1}H-{^{31}P}NMR and Mass spectra .

Keywords*:* Organometallic;; Vinylidine diphenyl phosphine (Vdpp); cis 1,2-bis (diphenyl phosphine) ethene ; Transition metals; Cyclic voltammetry.

1. Introduction

Although tertiary phosphines and anion $[Ph_2PCHPh_2]^-$ are important ligands in coordination and organometallic chemistry and essential components in many catalytic systems, relatively, little has been reported with functionalised phosphines [1-3]. Phosphorus- phosphorus nuclear spin-spin coupling has been studied in a series of symmetrical bis(diphenylphosphino)-compounds with aliphatic, olefinic and acetylenic carbon groups linking the two phosphorus atoms. The synthesis of the new and reactive ligand of tetraphenyl carbon or carbonyl group diphosphine and their complexes with pt(II) or pt(IV) to give activated complexes as $[(Me)_2pt(Vdpp)]$ [4,5] in toluene solvent. Although vinylidine double and cis-diphenylphosphino ethylene is not active to nucleophilic attack but complexes of [III]-[VI] are highly active to type Michael additions when complexed with $M(CO)_6$ [6,7]. The electrode mechanism of trans-dicarbonyl phosphine complexes of molybdenum(I), trans-$[Mo(CO)_2(P\text{-}P)_2]PF_6$ (where P-P=$ph_2PCH_2CH_2Pph_2$ or $ph_2PCH=CHPph_2$) was investigated by cyclic voltammetry in 0.1 mol. dm^{-3} TBAP/CH_2Cl_2 solution at a platinum electrode. The complexes are both oxidized and reduced in one-electron processes. The oxidation and reduction processes are following a well-defined EC_{irrev} mechanism. Digital simulation and comparison with the experimental cyclic voltammetric results was used for the determination of homogeneous and heterogeneous rate constants values [8].

2. Experimental

Apparatus

Electrochemical studies:

The cyclic voltammograms were obtained using an EG&G Princeton Applied Research Corporation (PAR) 264A Polarographic analyzer/stripping voltammeter, coupled with PAR Model 303A Static Mercury Drop Electrode (SMDE),

(drop size, medium), (area of the drop 0.014 cm^2). The polarographic cell (PAR Model K0060) was fitted with Ag/AgCl saturated KCl and used as a reference electrode and a platinum wire as an auxiliary one. A PAR 305 stirrer was connected to the 303A SMDE. A PAR model RE – 0089 X-Y recorder was used to collect the experimental data.

Analysis studies:

Spectroscopic analysis was studied by using Perkin–Elmer 599B spectrophotometer. An infrared spectrum (IR) was carried out by Shimadzu Corporation Chart 200-91527, in KBr pellets. ^{1}HNMR spectra was recorded on a Varian Em-390-90 MHz spectrometer using $CDCl_3$ as a solvent and TMS as an internal standard (chemical shifts in δ ppm). Microanalysis was performed on a Perkin-Elmer 240E microanalysis. Mass spectra were recorded on a Mass JEOL JMS600.

Preparation of organometallic compounds:

Synthesis of Olefinic Diphosphine Ligands:

The olefinic diphosphines, 1,1-*Bis*-(diphenylphosphino)-ethene [I] and/ or 1,2-*cis*-(diphenylphosphino)ethene [II], were prepared according to the following procedure [2]: Triphenylphosphine (86.8 g , 0.33 mol) and lithium (4.6 g 0.66 mol) in tetrahydrofuran ,THF, (750 cm^3) were stirred overnight under dinitrogen. The solution was treated with 2-chloro-2-methylpropane (36.5 cm^3 , 0.33 mol) to remove phenyl-lithium and was then decanted, under dinitrogen, into a large dropping funnel. The resulting of $LiPPh_2$, was slowly added to 1,1-dichloro-ethane and/or 1,2-cis-dichloro-ethane (16.1 g, 0.165 mol) in dry benzene (60 cm^3). Then dilute HCl (250 cm^3) was added most of the THF solvent was removed by rotary evaporator, the organic was extracted and separated using dry ether. After removal of the solvents oil remained which was crystallized on addition of absolute methanol. [I] and/or [II] ligands (colorless, air-stable crystals) were recrystallized from dry ethanol. Yield 35 g (31%); m.p (114 ^oC and/or 85 ^oC).

Preparation of $[(OC)_4M\{(Ph_2P)_2C=CH_2\}]$ and cis-$[(OC)_4M(Ph_2P)CH=CH(PPh_2)]$

1,1-Bis(diphenylphosphine)ethane (Vdpp) and cis[(Ph_2P) $CH=CH(PPh_2)$] had been synthesized. The complexes of the type $[(OC)_4M\{(Ph_2P)_2C=CH_2\}]$ and cis-$[(OC)_4M(Ph_2P)CH=CH(PPh_2)]$ were prepared by reflux of free ligand [I] (0.396 mole) and ligand [II] (0.396 mole) with $M(CO)_6$ (M=W, Cr, Mo) (0.352, 0.219, 0.266, mole, respectively) and $CuCl_2$ (0.133 mole) in *n*-decane under 80^{o}C and for 6 hours. The compounds were recrystallised from ethanol, giving yields for all over 74%.

Reagents used in electrochemical studies:

Stock solution of $1x10^{-3}$ M free ligand and their complexes of compounds [I] and [II] were prepared by dissolving the appropriate amounts of each in double distilled water Solution of 0.1M potassium nitrate was prepared and used as the supporting electrolyte. 0.01M KNO_3 was transferred into the voltammetric cell (10 ml) used as the supporting electrolyte.

The free ligand or their complexes were added using an automatic pipettor (10-100 µl). The cell content was degassed by passing pure nitrogen for 16 min. The accumulation potential was varied by the variation of the complexes and free ligands and selected to a fresh mercury drop, the scan rate was 100 mVs^{-1}. The voltammogram was recorded (quiescent solution) and a potential was terminated at -1.3 V. All results were obtained at room temperature (25±1)^{o}C with a nitrogen atmosphere maintained over the solution surface.

3. Results and Discussion

^{1}H NMR and ^{1}H-{^{31}P} NMR Spectrum (400 MHz) and Mass Spectrum.

^{1}H and ^{1}H-{^{31}P}NMR spectrum of [Ph_2**P**C(=CH_2)**P**Ph_2] and [Ph_2**P**CH=CH**P**Ph_2] ligands were established by 400 Hz [a "virtual triplet" with the extremely large splitting as appears in Fig. (1)]. Splitting of [^{3}J(P-C=C-H)(cis)] in Fig. (1) is equal to splitting of [^{3}J(P-C=C-H) (trans)] in Fig. (2) [9,10].

Cis and/or trans of 1,2-ethylene diphosphine complexes [$(CO)_4$M{(Ph_2P)CH=CH(PPh_2)}] was prepared by treatment of trans and /or 1,2 diphenyl phosphino ethylene with hexacarbonyl metal in *n*-decane under reflux in oil bath at 25°C, (M= Cr and W), in 73 % yield. A remarkable feature of the ^{1}H-NMR spectrum of these complexes was confirmed by the presence of a single band at δ = 4.83 ppm. This separation is equal to [^{3}J(P-CH=C-H)(*cis*)+^{3}J(-CH=CH-P)(*trans*)]

^{3}J(PCCP) Coupling [10]Studies of vicinal P-H [11] and P-C [12] coupling make it reasonable to Fig. (2) expecting a Karplus type of dependence of ^{3}J(^{31}PCC^{31}P) coupling on dihedral angle ψ, defined as in V,(see below) and this is indeed so for the ^{3}J(^{31}PvCC^{31}Pv) coupling, for example, for the ethylenic derivatives it is found that $J_{trans} > J_{cis}$. For the ethane derivative the value of ^{3}J(^{31}P-^{31}P) is even greater than in the trans ethylene compound.

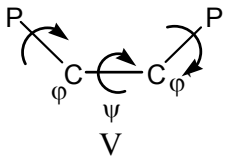

V

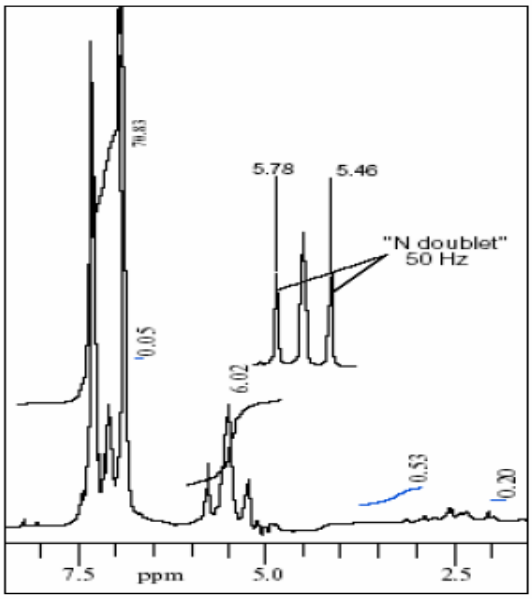

Fig. 1 ^{1}H-{^{31}P} n.m.r.[Ph_2PC(=CH_2)PPh_2]

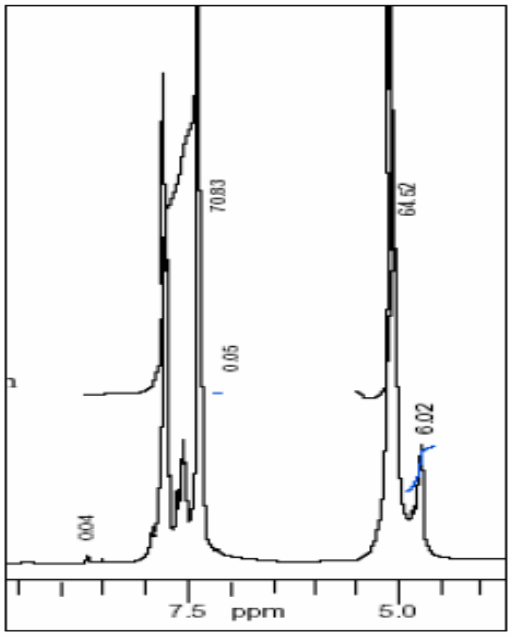

Fig. 2 ^{1}H-{^{31}P} n.m.r.[Ph_2PCH=CH)PPh_2]

This is a rather surprising if the observed coupling constant is a result of averaging over different conformation [cf. vicinal (H, H) coupling in ethane and ethylene [13] and suggests that there is a preponderance of the conformer with phosphorus atoms mutually trans. In the diphosphines the conventional dependence of coupling constant on dihedral angle [14] does not hold, as demonstrated by the result $J_{cis} >> J_{trans}$. This can be accounted for in terms of Ion-pair (I.p) orientation effects (i.e the Ione pair –P-C-C dihedral angle φ and φ`) and has previously been obtained [15, 16] experimentally for the coupling $^{3}J(^{31}PCCH)$. By analogy with these results it is to be expected that large positive values of $^{3}J(^{31}P\text{-}^{31}P)$ will arise, when the angles φ and φ` are both small. Therefore, a conformation equal ($^{3}J = 105Hz$).

Molecular models suggest that the need to minimize interactions between the phenyl groups is responsible for the adoption of this conformation, but in the trans isomer, the two diphenylphosphino-groups are sufficiently far apart to allow essentially free rotation about the two olefin C-P bounds. The mass spectra of these complexes showed a molecular ion peak , the isotopic distribution patterns of which were in agreement with the assigned molecular formula. In addition to the molecular ion, intense patterns were observed consistent with the consecutive loss of up to three carbonyl ligands as shown Scheme (1).

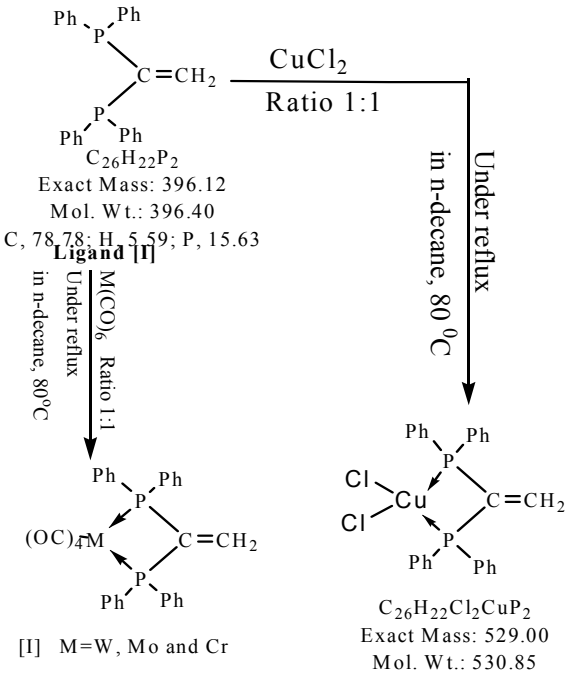

[I] M=W, Mo and Cr

The structure of complexes for ligand [I] with metals]

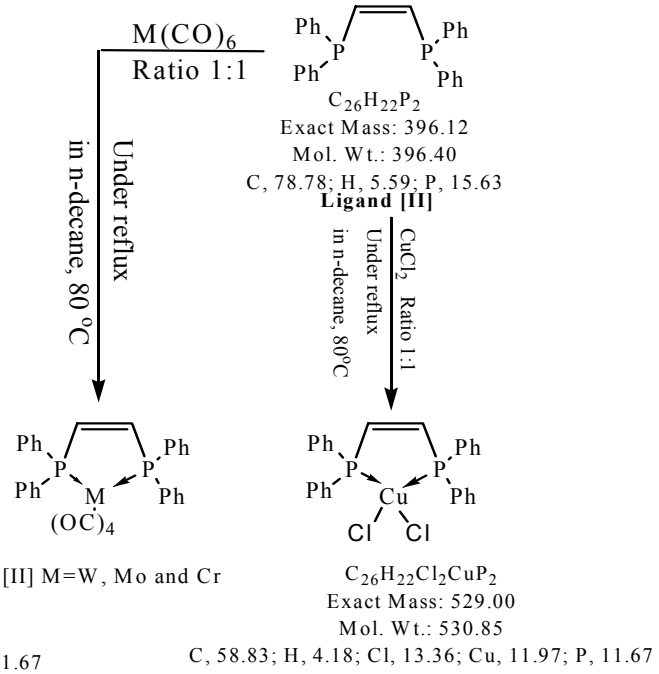

[II] M=W, Mo and Cr

The structure of complexes for ligand [II] with metals]

Scheme (1)

Cyclic voltammetry investigation

Cyclic voltammetric studies for free ligands

Cyclic voltammetric measurements for free ligand (I and II) ($1x10^{-3}$ M) were studied in the presence of 0.01M KNO_3, at initial potential -0.5V and final potential -1.25V, scan rate 100 mVs^{-1}. It is worthily to mention that the two ligands give the same cyclic voltammograms. The cyclic voltammogram for ligand [I] is shown in Fig.(3), where a single reversible cathodic peak was obtained at -0.66V , while the anodic one observed at -0.63V. The effect of scan rate ν (from 10 – 100 mVs^{-1}) on the peak current and the peak potential for the cathodic one was studied . The log ip vs. log ν gives a straight line with a slope =0.7688. This value is expected for an ideal reaction of surface species [17]. A 10 mV negative shift in the peak potential was observed upon increasing the scan rate in the range given. This is a further evidence for the adsorption of the ligand onto the electrode surface [18]. The value of the linear correlation coefficient is 0.998.

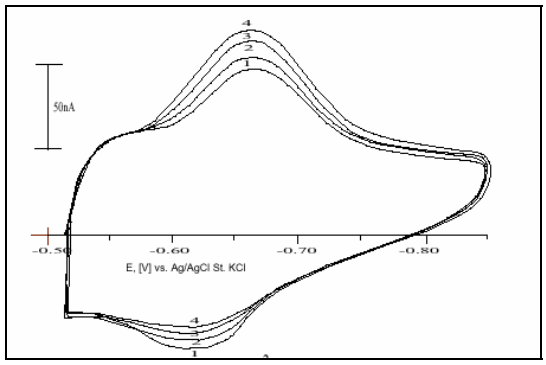

Fig.3 Cyclovoltammograms of 1x 10^{-3} M free ligand [I] in 0.01M KNO_3 At scan rate = 100 mVs^{-1} and initial potential = -0.5V

The electroreduction mechanism of the free ligand [I] and II can be expressed as [19]:

$$[(Ph_2P)_2C{=}CH_2\}]+ 2e^- + 2H_2O \rightleftharpoons [(Ph_2P)_2CH\text{-}CH_3]+2OH^-$$

$$[(Ph_2PCH{=}CHPPh_2]+2e^- + 2H_2O \rightleftharpoons [Ph_2PCH_2\text{-}CH_2PPh_2] + 2OH^-$$

From Table (1) where the value of (i_{pa}/ i_{pc}) ratio is (0.42) at scan rate value (100 mVs^{-1}) which indicates the irreversibility of the electrode process, the difference ($\Delta E_p = E_{pa}-E_{pc} \cong 0.059/n$) gradually increases from 20 mV at 10 mVs^{-1} to 30 mV at 100 mVs^{-1}, where n is equal to approximately two. This indicates that two electrons involve in this chemical reaction and the calculated formal electrode potential ($E`_0$)= –0.645V(corrected for the reference electrode being used) [20-21].

Cyclic voltammetric studies for complexes $[(OC)_4M(Ph_2P)_2C{=}CH_2]$ where[M= W(VI), Mo(VI) and Cr(VI)]and $[Cu(Ph_2P)_2C{=}CH_2]$

Cyclic voltammetric measurements for ($1x10^{-3}$M) $[(OC)_4M(Ph_2P)_2C{=}CH_2]$ was studied in presence of 0.01M KNO_3, at initial potentials +0.05, +0.05,-0.05 and ±0.00V for Cu, W, Mo and Cr, respectively, and final potentials -0.18,-0.68, -0.40 and -0.85 V in the same order and scan rate 100 mVs^{-1}. Figs.(4-7) give the cyclic voltammograms for ($1x10^{-3}$) complexes of ligand (I) with Cu(II), W(VI), Cr(VI) and Mo(VI), respectively. In Fig.(4) for ligand [I] with Cu(II), the first cycle shows distorted peak in both sides. In repetitive cycles well defined cathodic and anodic peaks (-0.056 and –0.024V) are observed with enhancement in the peak current. This peak is due to the reduction of Cu(II) complex and the reaction mechanism of ligand [I] with Cu(II) explained in the following equations:

$$[(Ph_2P)_2C{=}CH_2]CuCl_2 + 2e^- \rightleftharpoons [(Ph_2P)_2C{-}CH_2] + Cu^0(Hg)$$

$$Cu^{++} + 2e^- \rightleftharpoons Cu^0$$

Table (1) Dependence of i_p on scan rate and concentration and of E_p on scan rate for some common classes of electrode process in cyclic voltammetry of $[(CO)_4M\{(Ph_2P)_2C{=}CH_2\}]and[Cl_2Cu\{(Ph_2P)_2C{=}CH_2\}]$ (M= Cr, Mo or W) complex.

Complex	ν	Ipa	Ipc	Ipa/ipc	-Epc	-Epa	ΔEp	n	E`^{0}
Free ligand	100	25.0	60.0	0.420	0.66	0.63	0.03	1.97	-0.645
$C_{26}H_{22}CuP_2$	10	10	10	1.00	0.0477	0.0163	0.0314	1.879	-0.032
	20	14.5	11.5	1.26	0.0498	0.0175	0.0323	1.826	- 0.034
	50	20	15	1.33	0.0510	0.0201	0.0309	1.909	- 0.036
	100	27.5	20	1.375	0.0560	0.0240	0.032	1.844	-0.040
$C_{30}H_{22}WO_4P_2$	10	22.5	22.5	1.00	0.110	0.089	0.021	2.809	- 0.099
	20	35	37.5	0.93	0.116	0.094	0.022	2.681	- 0.105
	50	50	55	0.91	0.121	0.101	0.020	2.950	- 0.111
	100	59	65	0.91	0.129	0.109	0.020	2.950	- 0.119
$C_{30}H_{22}CrO_4P_2$	10	2.04	2.00	1.02	0.428	0.410	0.018	3.278	-0.419
	20	4.28	4.01	1.07	0.452	0.433	0.019	3.105	-0.443
	50	5.96	6.02	0.99	0.482	0.462	0.020	2.950	-0.472
	100	7.12	7.01	1.01	0.500	0.480	0.020	2.950	-0.490
$C_{30}H_{22}MoO_4P_2$	10	0.240	0.254	0.9449	0.248	0.200	0.048	1.229	- 0.224
	20	0.261	0.272	0.9595	0.271	0.222	0.049	1.204	- 0.2465
	50	0.274	0.288	0.9514	0.299	0.242	0.057	1.035	- 0.2705
	100	0.289	0.300	0.9633	0.310	0.261	0.049	1.204	- 0.2855

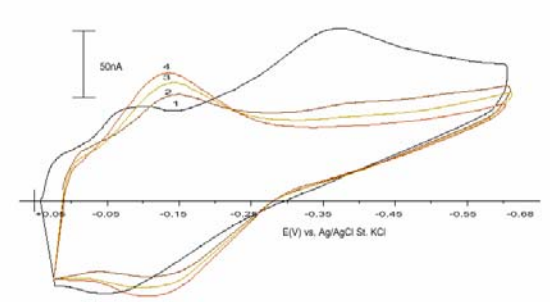

Fig. 4 Cyclovotammograms of 1 × 10^{-3} M { Cl_2Cu[Vdpp]} in 0.01 M KNO_3 at scan rate = 100 mVs^{-1} and initial potential = + 0.05 V.

The effect of scan rate ν (10-100 mVs^{-1}) on the cathodic peak was studied. The log ip vs. log ν gave a straight line with a slope equal 0.6995. This indicates that the reaction is controlled by adsorption, with a correlation coefficient of 0.9804.

From Table (1) it can be seen that the value of (i_{pa}/ i_{pc}) ratio is approximately constant at unity at all scan rate values. This indicates that the reversibility of the redox change, the difference ($\Delta E_p = E_{pa} - E_{pc} \cong 0.059/n$) is about 32 mV, where (n) is equal to two which indicates that two electrons are involved in the electrode process and the calculated formal electrode potential ($E`_0$) equal –0.04V (corrected for the reference electrode being used).

In the case of the 1x10^{-3}M complex from W(VI) with ligand [1] in presence of 0.01M KNO_3, distorted peak was observed in both sides, in repetitive cycles well defined cathodic and anodic peaks (-0.13 and – 0.11V) are observed with enhancement in the peak current as shown in Fig.(5). This peak is due to the reduction of W(IV) complex to W(III) complex. The reaction mechanism of ligand [I] with W(VI) explained in the following equation:

$$[\{(OC)_4W\}(Ph_2P)_2C{=}CH_2] + 3e^- \rightleftharpoons [(Ph_2P)_2C = CH_2\}] + \mathbf{W(III)}$$

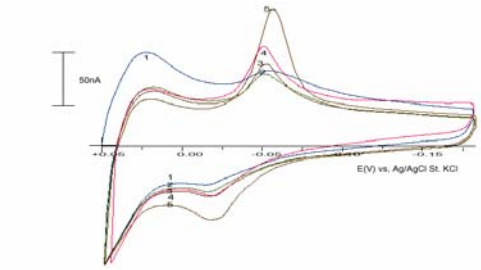

Fig. 5 Cyclovotammograms of 1 × 10^{-3} M { $(CO)_4W$[Vdpp]} in 0.01 M KNO_3 at scan rate = 100 mVs^{-1} and initial potential = + 0.05 V.

The effect of scans rate ν (from 10-100 mVs^{-1}) on the cathodic peak current and the peak potential was studied. The log ip vs. log ν gave a straight line with a slope equal 0.681 indicated that the reaction is controlled by adsorption, with a correlation coefficient of 0.9928.

From Table (1) the value of (i_{pa}/ i_{pc}) ratio is approximately constant at unity at all scan rate values indicate the chemical reversibility of the redox change, the difference ($\Delta E_p = E_{pa} - E_{pc} \cong 0.059/n$) is about 0.02 for 10 mVs^{-1} to 100 mVs^{-1}, where (n) is equal to three which indicated that three electrons are involved in the reduction mechanism and the calculated formal electrode potential ($E`_0$) equal –0.12V (corrected for the reference electrode being used).

Fig.(6) gives the cyclic voltammogram for 1x 10^{-3}M ligand [I] with Cr(VI) in presence of 0.01M KNO_3, two cathodic (- 0.50 and –0.58 V) and one anodic peaks (–0.48V) were obtained. The first peak (-0.50) may be due to the reduction of Cr(VI) complex to Cr(III) complex (adsorptive peak) and the second peak (-0.58V) is for the free ligand. The effect of scan rate ν (from 10-100 mVs^{-1}) on the first cathodic peak was studied. The log i_p vs. log ν gives straight line with a slope equal 0.64. This

indicated that the reaction is diffusion controlled with adsorption component, with a correlation coefficient of 0.987. The reaction mechanism of ligand [I] with Cr(VI) could be explained as in the following equation:

$$[\{(OC)_4Cr\}(Ph_2P)_2C{=}CH_2]+3e^- \rightleftharpoons [(Ph_2P)_2C = CH_2\}] + \mathbf{Cr(III)}$$

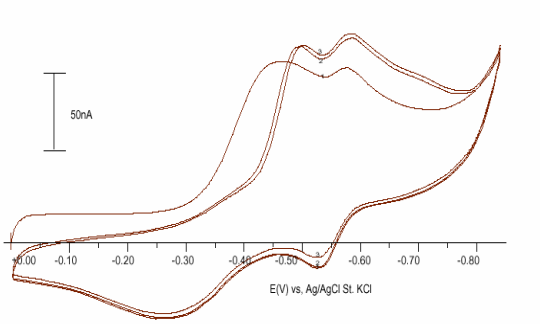

Fig. 6 Cyclovotammograms of 1 × 10^{-3} M { $(CO)_4Cr[Vdpp]$} in 0.01 M KNO_3 at scan rate = 100 mVs^{-1} and initial potential = + 0.05 V.

From Table (1) the value of (i_{pa}/ i_{pc}) ratio is approximately constant at unity at all scan rate values. This indicates that the chemical reversibility of the redox change, the difference ($\Delta E_p = E_{pa} - E_{pc} \cong 0.059/n$) gradually increased from 11 mV at 10 mVs^{-1} to 19 at 100 mVs^{-1}, where (n) is equal to three which indicates that three electrons are involved in the reaction mechanism and the calculated formal electrode potential ($E`_0$) equals –0.12V (corrected for the reference electrode being used).

Fig.(7) shows the cyclic voltammogram for ($1x10^{-3}$M) complex from ligand (I) with Mo(VI) in presence of 0.01M KNO_3. One cathodic peak was obtained at (-0.31V) and one anodic peak at (-0.25V). This may be due to the reduction of Mo(VI) complex to Mo(V) complex. The log i_p vs. log ν gave a straight line with a slope equal 0.3795 and this indicated that the reaction is controlled by diffusion, with a correlation coefficient of 0.9804. The reaction mechanism of ligand [I] with Mo(VI) could be explained as in the following equation[22].

$$[\{(OC)_4Mo\}(Ph_2P)_2C{=}CH_2]+3e^- \rightleftharpoons [(Ph_2P)_2C \text{---} CH_2] + \mathbf{Mo(V)}$$

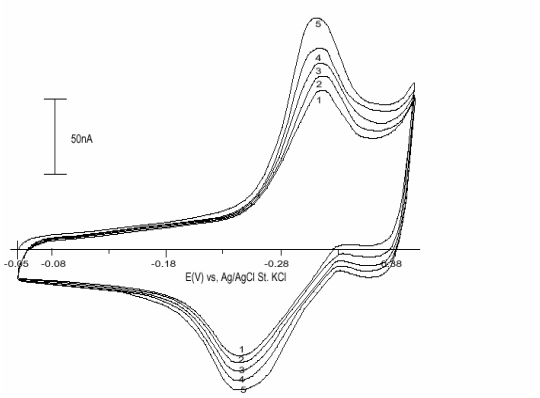

Fig.7 Cyclovotammograms of 1 × 10^{-3} M { $(CO)_4Mo[Vdpp]$} in 0.01 M KNO_3 at scan rate = 100 mVs^{-1} and initial potential = + 0.05 V.

Table (1) summarizes the value of (i_{pa}/ i_{pc}) ratio which is approximately constant at unity at all scan rate values. This indicates that the reversibility of the redox change, the difference ($\Delta E_p = E_{pa} - E_{pc} \cong 0.059/n$) is 48 mV, where (n) is equal to one which indicates that one electron is involved in the reaction mechanism and the calculated formal electrode potential ($E`_0$) equal –0.28 V (corrected for the reference electrode being used).

Cyclic voltammetric studies for complexes $[(OC)_4M(Ph_2PCH=CHPPh_2)]$ where[M=W(VI), Mo(VI) and Cr(VI)]and $[Cu(Ph_2PCH=CHPPh_2]$

Table (2) summarized the cyclic voltammetric parameters obtained for free ligand [II] and their complexes with metals {Cu(II), Mo(IV), W(IV) and Cr(IV)}. By comparison with data obtained from ligand [I] and their complexes in Table(1). It was observed that all the cyclic voltammetric parameters, which obtained from ligands [I] and [II] are the same. However, when free ligand [11] formed complexes with the metals under study the cathodic peak potential for the complex is shifted to more negative value than that for ligand [I] complexes as shown in Table(1). This may be attributed to the fact that ligand [II] when chelated with metals form five membered ring which is more stable than the four membered ring which is formed from the reaction of ligand [I] with the metals, therefore the E_{pc} is being shifted to a more negative potential.

Table (2) Dependence of i_p on scan rate and concentration and of E_p on scan rate for some common classes of electrode process in cyclic voltammetry of $[(CO)_4M\{Ph_2PCH=CHPPh_2\}]and[Cu\{Ph_2PCH=CHPPh_2\}]$ (M=Cr, Mo or W) complex.

Complex	ν	Ipa	Ipc	Ipa/ipc	Epc	Epa	ΔEp	n	E^0
$C_{26}H_{22}CuP_2$	10	9.02	8.93	1.01	0.087	0.058	0.029	2.03	0.072
	20	13.5	12.52	1.07	0.089	0.057	0.032	1.84	0.073
	50	22.21	19.11	1.16	0.091	0.059	0.032	1.84	0.075
	100	28.11	24.21	1.16	0.095	0.061	0.034	1.73	0.078
$C_{30}H_{22}WO_4P_2$	10	11.3	10.9	1.036	0.124	0.104	0.02	2.95	0.114
	20	14.78	13.58	1.088	0.128	0.107	0.021	2.81	0.117
	50	20.58	19.18	1.073	0.131	0.114	0.017	3.47	0.122
	100	25.14	23.81	1.05685	0.132	0.113	0.019	3.11	0.122
$C_{30}H_{22}CrO_4P_2$	10	14.51	14.01	1.036	0.647	0.628	0.019	3.11	0.637
	20	18.78	17.89	1.049	0.657	0.632	0.025	2.36	0.644
	50	21.15	20.09	1.053	0.66	0.641	0.019	3.11	0.650
	100	25.14	24.17	1.040	0.662	0.643	0.019	3.11	0.652
$C_{30}H_{22}MoO_4P_2$	10	17.14	16.54	1.036	0.198	0.104	0.094	0.62	0.151
	20	19.45	18.23	1.066	0.201	0.125	0.076	0.78	0.163
	50	24.02	21.98	1.092	0.231	0.132	0.099	0.59	0.181
	100	27.84	26.35	1.056	0.246	0.158	0.088	0.67	0.202

Table (3) Elemental analysis of complexes of the types $[(CO)_4M\{(Ph_2P)_2C=CH_2\}]$ (M=W, Mo, Cr) and $[(Cl)_2Cu\{(Ph_2P)_2C=CH_2\}]$.

Complex	Elemental analysis %			i.r data		Physical properties	
	C%	H%	P %	ν(CO)	ν(C=CH_2)	Yield % (Color)	m.p °C
$(CO)_4W\{(Ph_2P)_2C=CH_2\}$ Mol. Wt=692.05	52.05(A) 52.11(B)	3.02 3.00	8.95 9.04	2000s, 1980w, 1890w, 1860b	1656m 887s	77 Yellow	215
$(CO)_4Mo\{(Ph_2P)_2C=CH_2\}$ Mol. Wt=606.38	59.62 59.17	3.67 3.71	10.25 10.41	2020, 1942, 1850, 1850	1650m 892s	89 White	201
$(CO)_4Cr\{(Ph_2P)_2C=CH_2\}$ Mol. Wt=560.44	64.29 63.87	3.96 3.99	11.05 11.10	2000s,1980w,1890w,1860sb	1652m 890s	82 White	195
$(Cl)_2Cu\{(Ph2P)_2C=CH_2\}$ Mol. Wt= 530.85	58.83 58.11	4.18 4.09	11.67 11.51	2002s,1980w,1890w,1855sb	1650m 894s	94 Green	205

Elemental analysis: (A) the calculated values, (B) the found values, IR spectra: Strong(s), Weak (w), Board (b), medium (m)

Table (4) Elemental analysis and IR spectra of $[(CO)_4M\{(Ph_2P\text{-}CH=CH\text{-}PPh_2\}]$ (M= Cr, Mo, W and Cu)complex.

Compound	Elemental Analysis			i.r data		Physical properties	
	C%	H%	O%	ν(CO)	Trans (CH=CH)	Yield % (Color)	m.p °C
$(CO)_4Cr\{(Ph_2PCH=CHPPh_2\}$ Mol. Wt=560.44	64.21(f) 63.87(c)	3.92 3.99	11.48 11.54	2000s,1980w, 1890w,1860sb	1673(v) 974(s)	87 White	198
$(CO)_4W\{(Ph_2PCH=CHPPh_2\}$ Mol. Wt=692.05	52.25 52.11	3.02 3.00	9.34 9.21	2000s, 1980w, 1890w, 1860b	1670(v) 978(s)	74 White	230
$(CO)_4Mo\{(Ph_2PCH=CHPPh_2\}$ Mol. Wt=606.38	59.22 59.17	3.69 3.71	10.50 10.51	2020, 1942, 1850, 1850	1669(v) 968(s)	68 Yellow	209
$(Cl)_2Cu\{(Ph_2PCH=CHPPh_2\}$ Mol. Wt=529.00	58.98 58.83	4.21 4.18	-	2000s, 1980w, 1890w, 1860b	1672(v) 978(s)	94 Blue	187

Elemental analysis Found (f) Calculation (c) IR spectra Strong(s),Weak(w), Board(b), variable(v)i.r data in KBr discs.

References

[1] Cooper, G. R., Mecwan, D. M., Shaw, B. L., Inorganica. Chimica, Acta, 76 (1983) L165.

[2] Colquhoun, I. J., Mc Farlane, W., Journal Chem. Soc. Dalton. Trans., (1982) 1915.

[3] Ibrahium, M. A. A., Fatma, S. M. H., Adila, E. M., and Al-Hossainy, A. F. Phosphorus, Sulfur, and Silicon, (2004) 1251.

[4] Hassan, F. S. M., Higgins, S. J., Jacobsen, G. B., Shaw, B. L., Thoronton-pett. M., Journal Chem. Soc., Dalton Trans., (1988) 3011.

[5] Hassan, F. S. M., Shaw, B. L. Thoronton-pett., Journal Chem. Soc., Dalton Trans (1988) 89.

[6] Cooper, G. R., Hassan, F. S. M., Shaw, B. L., Fatma, S. M. H., Bernard, L. S. Thoronton-pett., M., Journal Chem. Soc., Chem. Commun., (1985) 614.

[7] Fontaine, X. L. R., Hassan, F. S. M., Higgins, S. J. Jacobsen, G. B., M., Shaw, B. L., Thoronton-pett, Chem. Soc., Chem. Commun., (1985) 1635.

[8] Abdel-Hamid, R., El-Samahy, A. A., Rabia, M. K. M., Taylor, N., shaw, B. L., Bull. Chem. Soc., Jpn. (1994) 321.

[9] Anderson, W. A., Freeman, C. A., Reilly, R., J. Chem. phys., (1963)1518.

[10] Samitov, Y. Y., Berdnikov, E. A., Tantasheva, F. R., Margulis, B. Y., Kataev, E. G., Zhur. Obschei Khim., (1975) 2130.

[11] Mavel., G. A. Ann. Rep. NMR Spectrosc., 5B (1972) 1.

[12] Quin, L. D. Ed., The Heterocyclic Chemistry of Phosphorus, John Wiley, New York. (1981) 280.

[13] Murrell, J. N., Prog. NMR Spectrosc., 6 (1971) 1.

[14] Quin, L. D. Ed., The Heterocyclic Chemistry of Phosphorus, John Wiley, New York, (1981) 327.

[15] Bushweller, C. H., Brunelle, J. A., Anderson, W. A., Bilotsky, H. S., Tetrahedron Lett., (1972) 3261.

[16] Bond, A. M. Ed., Modern Polarographic Methods in Analytical Chemistry, Marcel Dekker, New York, (1980) 196.

[17] Wang, J., Tolzhi, P., Lin, M. S., Tapia, T., Talanta (1986) 707.

[18] Kolthoff, I. M., James, J. L.Eds., Polarography, second addition, (1952) 634.

[19] Kissinger, I., peter, T., H., Willian, R., Laboratory techniques in electroanalytical chemistry. (1884) 89.

[20] Bard, A. J., Faulkner, L.R., Eds., Electrochemical Methods: Fundamentals and applications, Wiley, New York, 1980.

[21] Azza M. M. A., Mahmoud, A. G., Salah, A. E., Seddique, M. A., Electroanalysis. (2000) 155.

Arabian J. Chem. Vol. 1, No. 1, 79-82 (2008)

Microwave-Assisted Reactions: A convenient and Efficient Synthesis of 4-Aryl-3,4-Dihydropyrimidine-2(1*H*)-ones under Microwave Irradiation

Kamal U. Sadek* **and Ramadan A. Mekheimer**

Chemistry Department, Faculty of Science, El-Minia University, El-Minia 61519, A. R. Egypt

Tel. : 2086-2364806 ; E-mail : kusadek@yahoo.com

Abstract

A convenient and efficient synthesis of the Biginelli 4-aryl-3,4-dihydropyrimidine-2(1*H*)-ones in acetic acid solvent and under microwave irradiation was reported.

Key words: Biginelli reaction, Microwave-assisted, Acetic acid

Although Biginelli reaction [1] is more than one hundred years old but it has received a great deal of attention in very recent years because of the wide range of biological, pharmaceutical and therapeutic properties associated with the 3,4-dehydropyrimidine-2(1*H*)-ones (DHMPs) produced by this reaction [2]. The one-pot three component Biginelli condensation provides certainly the most efficient access to (DHMP) derivatives due to it's atom economy feature and the availability and the diversity of the starting components.

The simple and direct method for the synthesis of DHMP involves the one-pot condensation of an aldehyde, β-ketoester and urea under strong acidic conditions which was first reported in 1983. However, the yields of the products were very low (20-25%). From then on, many new techniques such as the use of Lewis acids[3], for example: $LiAlO_4$, $LaCl_3$-$7H_2O$, $InCl_3$, $Bi(OTf)_3$, $BiCl_3$, $Mn(OAc)_3$, $Cu(OTf)_2$, $FeCl_3$-$6H_2O$, $PhB(OH)_2$. Other workers have been devoted to the use of solventless microwave technique in the presence of a suitable catalyst[4], ionic liquids[5], solid phase reagents[6], polymer supported catalysis[7] and grindstone technique [8]. In spite of their potential utility, many of these methods involve expensive reagents, strong acidic conditions, long reaction times and unsatisfactory yields.

In continuation to our interest [9] in investigating new, simple and high yield synthesis of five and six-membered heterocycles we report herein our preliminary investigations dealing with the synthesis of (DHMPs) in acetic acid solvent and under reflux in microwave lab. station. Conducting the reaction in a solvent under microwave irradiation ensured complete homogeneity of the reaction mixture and effective microwave heating as well as avoiding the possible sharing of the reaction mixture under solvent-free microwave irradiation.

A test experiment was conducted [10] by mixing together equivalent amounts of benzaldehyde, ethyl acetoacetate and excess urea in acetic acid solvent and heating under reflux in a microwave lab. station at 120°C for five minutes after which the reaction mixture was poured on ice-cold water and isolating the (DHMPs) solid formed.

In order to examine the substrate effect on the reaction rate overall yield, various aromatic aldehydes with different substituents were used under the above reaction conditions (table 1). From the results it can be seen that all reactions proceeded smoothly to afford the corresponding DHMPs in

high yields, with a little bit increase when R is an electron-donating group.

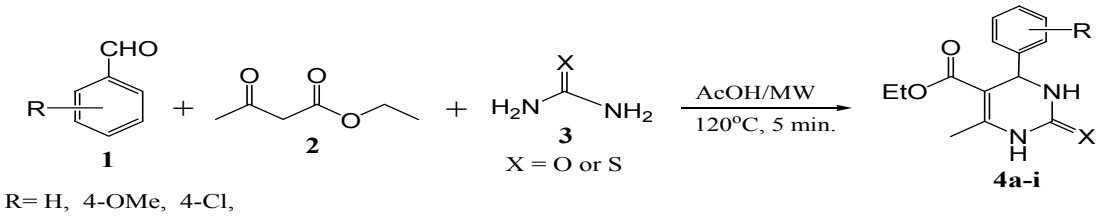

R= H, 4-OMe, 4-Cl, 4-Me, 4-NO_2, 3-Cl, 2-Furyl

There are several useful aspects of this approach. The procedure is simple either in conducting the reaction or isolation of the products. We avoided the several attempts to select the optimium molar ratio of catalyst to the starting materials in addition acid sensitive aldehydes such as 2-furan carboxaldehyde reacted without the formation of any side products.

In conclusion, we have developed a simple and efficient method for a one-pot three component synthesis of 3,4-dihydropyrimidinone derivatives using acetic acid as solvent and MW heating technique

Table 1. Synthesis of dihydropyrimidinones (4a-i) using acetic acid as a solvent and MW as a heating technique

Compound	R	X	Yield (%)	Mp (^{o}C)	[Lit.]
4a	H	O	90	210	209-210
4b	4-OMe	O	91	200-201	199-201
4c	4-Cl	O	88	211	210-212
4d	4-Me	O	90	213-214	215-216
4e	4-NO_2	O	80	206	205-207
4f	4-Cl	O	87	194	193-195
4g	2-Furyl	O	95	222-224	
4h	H	S	87	207	206-207
4i	4-OMe	S	88	151	150-152

Acknowledgement

K. U. Sadek is grateful to the Alexander *von* Humbolt Foundation for their donation of a start Milestone Microwave Lab. Station which was of great help in finishing this work.

References and notes

[1] Biginelli, P. *Gazz. Chem. Ital*., **1983**, *23*, 360.

[2] (a) For a review on DHMPs, see: Kappe, C. O., *Tetrahedron*, **1993**, *49*, 6937; (b) Atwal, K. S.; Rovnyak, G. C.; Kimball, S. D.; Floyd, D. M.; Moreland, S.; Swanson, B. N.; Gougoutas, J. Z.; Schwartz, J.; Smilie, K. M.; Malley, M. F., *J. Med. Chem*. **1990**, *33*, 2629; (c) McCarthy, J. R.; Zhary, R.; Moreland, S., *J. Med. Chem*. **1995**, *38*, 119; (d) Srinivas, K. V. N. S.; Das, B. *Synthesis* **2004**, 2091; (e) Kappe, C. O., *Eur. J. Med. Chem*. **2000**, *35*, 1043.

[3] (a) Kumar, K. A.; Kasthuraiah, M.; Reddy, C. S.; Reddy, C. D., *Tetrahedron Lett.* **2001**, *42*, 7873; (b) Ramalinga, K.; Vijayalakshmi, P.; Kaimal, T. N. B., *Synlett* **2001**, 863; (c) Paraskar, A. S.; Dewkar, G. K.; Sudalai, A., *Tetrahedron Lett*. **2003**, *44*, 3305; (d) Reddy, C. V.; Mahesh, M.; Raju, P. V. K.; Babu, T. R.; Reddy, V. V. N., *Tetrahedron Lett*., **2002**, *43*, 2657 ; (e) Lu, J.; Ma, H. R., *Synlett.,* **2000**, 63; (f) Russowsky, D.; Lopes, F. A.; Da Silva, V. S.; Canto, K. F. S.; Montes Doca, M. G.; Godoi, M. N., J. *Brazil Chem. Soc*., **2004**, *15,* 165; (g) Maiti, G.; Kundu, P.; Guin, C., *Tetrahedron Lett*., **2003**, *44*, 2757; (h) Gohain, M.; Prajapati, D.; Sandhu,

[4] J. S., *Synlett.* **2004**, 235; (i) Khodaei, M. M.; Khosropour, A. R.; Jowkan, M., *Synthesis* **2005**, 1301, (j) Han, X.; Xu, F.; Luo, Y.; Shen, Q., *Eur. J. Org. Chem.*, **2005**, 1500; (k) Debache, A.; Boumoud, B.; Amimour, M.; Belfaitah, A.; Rhouati, S.; Carboni, B. *Tetrahedron Lett*., **2006**, *47*, 5697; (l) Laing, B.; Wang, X.; Wang, j. X.; Du, Z., *Tetrahedron Lett*., **2007**, *63*, 1981; (m) Suzuki, I.; Suzumura, Y.; Takeda, K., *Tetrahedron Lett*., **2006**, *47*, 7861; (n) Jiany, C.; You, Q. D., Chinese *Chemical Lett*., **2007**, *18*, 647.

[5] Kappe, C. O.; Kumar, D.; Varma, R. S., *Synthesis* **1999**, 1799.

[6] Peng, J.; Deng, Y., *Tetrahedron Lett*., **2001**, *42*, 5917.

[7] Wipf, P.; Cunningham, A., *Tetrahedron Lett*., **1995**, *36*, 7819.

[8] Dondoni, A.; Massi, A., *Tetrahedron Lett*., **2001**, *42*, 7975.

[9] Bose, A. K.; Pednekar, S.; Ganguly, S. N.; Chakraborty, G.; Manhas, M. S., *Tetrahedron Lett*., **2004**, *45*, 8351.

[10] (a) Barsy, M. A.; Abdel Latif, F. M.; Aref, A. M.; Sadek, K. U., *Green Chemistry* **2002**, *4*, 196; (b) Mekheimer, R. A.; Abdel Hameed, A. M.; Sadek, K. U., *Molecules,* **2007** (in press)

[11] Typical procedure for the synthesis of tetrahydropyrimidinones: A mixture of an aromatic aldehyde (0.1 mol), ethyl acetoacetate (0.1 mol) and

urea or thiourea (0.2 mol) in acetic acid (10 ml) was heated under reflux at 120^{o}C in a microwave lab. station for 5 min. The reaction mixture poured onto ice cold water and the solid product that formed on standing was collected by filtration and crystallized from the proper solvent. All the known products were characterized by comparison of their charactristics with those of authentic samples. New products were characterized by ^{1}H NMR spectroscopy.

Arabian J. Chem. Vol. 1, No. 1, 83-92 (2008)

Nanoparticles: Promising Tools for Genomic Application

A.M. Alenad[1] and M. S. Alokail*[2]

[1]Department of Biochemistry and Molecular Biology, School of Biological Sciences, University of Southampton, Bassett Crescent East, Southampton, SO16 7PX, UK,

[2]Department of Biochemistry, College of Science #5, King Saud University, P.O. Box 2455, Riyadh 11451, Saudi Arabia*

Tel. 4675943, Fax. 4675931.

e-mail msalokail@yahoo.com

Abstract

Nanotechnology is the study, design, creation, manipulation, and synthesis through control of matter at the nanometer scale, and the utilization of novel phenomena and properties of matter at that scale. Manipulation at the tiny scale of atoms and molecules exhibits novel phenomena and properties. Nanoparticles (NPs) have a promising future in the design of functional materials, devices, but their use will be driven by the need for smaller detection platforms with lower limits of detection. Thus, scientists are harnessing nanotechnology to create new, inexpensive materials, devices, and systems with unique properties to be used in many important fields including chemistry, physics, biochemistry, biology, pharmaceuticals, and medical sciences. In this review we concentrate on research that is leading towards the benefits of nanobiotechnology applications for DNA biomolecules which is expected to open up new opportunities for DNA techbiology in biochemical systems.

KEYWORDS: Nanoparticles, DNA, Gene Transfer, genomagnetic, single nucleotide polymorphism

Introduction

Nanotechnology is a new field of applied science that involves dealing with materials and devices that are at the nanoscale level (10^{-9} of a meter) which is about ten times the diameter of a hydrogen atom [1]. Nanotechnology manipulates the chemical and physical properties of a substance on molecular level. In life sciences, nanobiotechnology is the fusion of biotechnology and nanotechnology [1]. This hybrid discipline can also mean making atomic-scale machines by imitating or incorporating biological systems at the molecular level, or building tiny tools to study or change natural structure properties atom by atom [1]. Nanobiotechnology can have a combination of the classical micro-technology with a molecular biochemical approach to create new applications knowledge to manipulate molecular, genetic, and cellular chemical processes to develop products. It's outstanding potential opportunities to overlap of biotechnology, nanotechnology and information technology to achieve many important applications in life sciences (Figure 1).

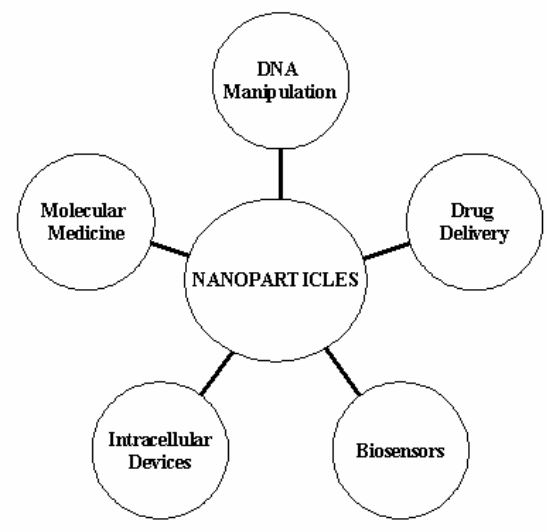

Figure 1. Application approaches of nanoparticles (NPs) in biomolecules technology.

Biochemical Nanotechnology is expected to create innovations with fundamentally new properties and functions in various biochemical and molecular applications, like DNA manipulation, drug delivery, gene therapy, molecular imaging, molecular diagnosis, biomarkers and biosensors [2]. The recent developments of nanotechnology approaches are offering novel materials such as nanoparticles (NPs) with special interest for molecular basis analysis.

This review will bring together the current applications of NPs to DNA technology. The integration of nanotechnology with DNA biochemistry is expected to produce major advances in the field of molecular targeting with low cost of analytical systems for analysis of biomolecules, such as proteins and nucleic acids.

DNA Nanoparticles

The discovery of the polymerase chain reaction (PCR) cemented the way to a new era of biochemical research [3]. The impact can be felt not only in the field of molecular biology, but also in many other related sciences. Novel classes of semi-synthetic DNA-protein conjugates, self-assembled oligomeric networks consisting of streptavidin and double-stranded DNA, which can be converted into well-defined supramolecular nanocircles have been developed [4]. In order to produce new immunological reagents for the ultrasensitive trace analysis of proteins and other antigens as immuno-PCR technology, the DNA-streptavidin conjugates are applicable as building blocks model [5-7]. Immuno-PCR is a combination of the specificity of an antibody-based immuno-assay with the exponential power of the amplification of PCR.

Nanotechnology application has been recently used in application of self-assembled DNA-streptavidin conjugates. As nanometre-scale 'soft material' calibration standards, the conjugates are used as model systems for ion-switchable nanoparticle networks for scanning probe microscopy [8,9], or as programmed building blocks for the reasonable construction of complex biomolecular structural design, which may be used as templates for the growth of nanometre-scale inorganic devices [10]. Moreover, application as solid substrates for nucleic acid hybridization with covalent conjugates of single-stranded DNA and streptavidin are used as biomolecular adapters for the immobilization of biotinylated macromolecules [11]. This directed immobilization of nucleic acid allows for reversible and site-selective occupation of solid substrates with metal and semiconductor NPs. Direct DNA also occupied by gold NPs with proteins, such as immunoglobulins and enzymes. The manufacture of practical biometallic nanostructures from gold NPs and antibodies are design as diagnostic tools in bioanalytics [11].

Furthermore, the DNA biosensor field has significantly affected the development of sensitive nonisotopic detection [12]. Based on enzyme labeling electrochemical biosensors affinity solved the problems of

radioactive detection (e.g. health hazards and short lifetimes) and opened up new possibilities in ultrasensitive and automated biochemical assays[13]. The DNA-recognition event can be detected using different strategies, including intrinsic electroactivity of the nucleic acid, DNA duplex intercalators, electroactive markers, and enzyme labeling [14-17]. Fluorescent labeling of biological materials with small organic dyes is also widely used in the life sciences and has been used in a variety of DNA-sensing systems based on optical detection [18]. However, classical organic fluorophores have many limitations including narrow excitation bands, broad emission bands with red spectral tails and many organic dyes exhibit low resistance to photodegradation [19]. Recently, the electrochemical properties of NPs make organic fluorophores extremely easy to be detected with simple instrumentation, long life time, multiplexing capability and high sensitivity [20-22]. These electrochemical properties may also allow simple and inexpensive electrochemical systems to be designed for detection of ultrasensitive, multiplexed assays.

In addition, there are many advantages of electrochemical labeling for DNA sensing by making the DNA/NPs detection system more integrated. The related technique – stripping voltammetry – is cheaper, faster and easier to use in field analysis than optical ones [19]. Because of the distinct voltammetric waves produced by different electrochemical tracers, this application also offers the possibility of simultaneous detection of several biochemical molecules in the same sample using a unique sensor. The electrochemical techniques require the development of novel NP-detection strategies that avoid dissolution of NPs before detection thereby integrating the whole assay which is highly advantageous in several biosensing systems [19].

A novel gold NPs based protocol for detection of DNA hybridization using magnetically trigged direct electrochemical detection of gold quantum dot tracers has been reported [23]. This technology based on binding target DNA with Au(67) quantum dot in equal ratio followed by a genomagnetic hybridization assay between Au(67)-DNA and another DNA called complementary probe DNA marked paramagnetic beads. Differential pulse voltammetry is used for a direct voltammetric detection of resulting Au(67) quantum dot-DNA/ complementary probe DNA-paramagnetic bead conjugate on magnetic graphite-epoxy composite electrode. Then the Au(67) NP tag is directly detected after the DNA hybridization event, without the need for acidic dissolution [19]. The feature, optimization, and advantages of the direct electrochemical detection assay for target DNA were applied. The two main highlights of this novel genosensor are (1) the direct voltammetric detection of metal quantum (QDs) dots obviates their chemical dissolution and (2) the Au(67) QD-DNA probe/DNA target-paramagnetic bead conjugate does not create the interconnected three-dimensional (3D) network of Au-DNA duplex-paramagnetic beads as previously designed as DNA-NPs assays [23]. Thus, the sensitivity of the assay is not decreased by the sharing of one gold tag by several DNA strands, achieving lower detection limits.

In very recent cancer NPs application, gold NPs-based genomagnetic sensors have used by designing two assays [24]. *Castañeda et al* (2007) have designed first strands assay format consisting of the hybridization between a capture DNA strand which is linked with paramagnetic beads and another DNA strand related to breast cancer gene 1 (BRCA1). This hybridization was used as a target to coupl with streptavidin-gold NPs. Then they designed the genomagnetic sensor as the second assay to work as a sandwich format with more application possibilities[24]. The target DNA for this application was a cystic fibrosis related DNA strand and sandwiched between the paramagnetic beads and modified gold NPs via biotin-

streptavidin reactions. The electrochemical detection of gold NPs by differential pulse voltammetry was performed in both cases. The developed genomagnetic sensors provide a reliable discrimination against noncomplementary DNA as well as against one and three-base mismatches [24,-26].

Gene Delivery

One of the key issues in bio-availability is cell transfection in DNA gene therapy. Current methods have considerable limitations, including the risk of inadvertent transmission of disease by viral vectors. This has led researchers to discover polymer-DNA complexes and liposome-DNA complexes for gene delivery [27]. It has been shown in postmitotic cells transfection that the compacted DNA can be used in the form of NPs [28].

Gene transfection of DNA-NPs composed of polylysine–polyethylene glycol (PEG) and DNA, colocalization of the NPs and nucleolin protein was observed [29]. Although nucleolin is well known to shuttle between nucleus and cytoplasm, in some cells it reaches the plasma membrane as well, only the cells that expressed nucleolin on the cell surface took up the DNA-NPs. Purified nucleolin binds to DNA-NPs with low nanomolar range by surface plasmon resonance, and deplete surface nucleolin also reduce expression of reporter genes from DNA-NPs. On the meantime, transfection of tagged nucleolin that migrates to the surface increases gene expression from DNA-NPs. Particles preincubated with exogenous nucleolin results in dose-dependent reduction in gene expression. Hence, nucleolin is an excellent candidate for the receptor for the DNA-NPs [29]. The nucleolin shuttle pathway to the nucleus is nondegradative, bypassing lysosomes, and endosomal release mechanisms are not required. Even if the nonviral vector escapes the lysosomal compartment or enters the cells via a nondegradative pathway, the journey to the cell nucleus is difficult, since free DNA molecules greater than 2000 base pair in length are essentially immobile in the cytoplasm [30]. This surveillance may explain why microinjection studies have shown that lipid-DNA complexes injected into the cytoplasm do not access the nucleus for gene expression. It is well documented that the typical plasmid DNA payloads likely required carrier-mediated transport to the nucleus [26,31,32]. The site of action of short interfering RNA (siRNA) is the cell cytoplasm, although short-hairpin RNA expression plasmids must enter the nucleus to be active.

The DNA-NPs vigorously transfect nondividing cells. This observable fact was first studied by comparing the ability of naked or compacted DNA encoding enhanced green fluorescent protein (EGFP) to transfect cells following intracytoplasmic or nuclear injection [28]. Cells receiving intracytoplasmic injections of DNA were chased for cell division by coincided high-molecular-weight rhodamine-labeled dextran, which is unable to pass the nuclear membrane unless the cell divides. Gene transfer enhancement in nondividing cells was noticed for compacted DNA compared with naked DNA following an intracytoplasmic injection, however only for NPs having a minimum diameter less than 25 nm, which is about the size of the nuclear membrane pore. Wheat germ agglutinin blocked all gene transfer that believed to block the nuclear membrane pore. This microinjection study correlates well with *in vivo* transfection results with a several postmitotic target cells with 30%-99% transfection efficiency [33-35]. DNA-NPs gain an entry into these cell types by binding to cell surface nucleolin which facilitates nuclear transport and uptake in a nondegradative pathway [36]. *Kube and Davis* (2003) results provide a great knowledge in measuring device of how these DNA-NPs are able to tackle the various physiologic barriers.

The current generation of lipid-mediated gene transfer technology has encountered significant and

limitations like inflammatory toxicity in human. This toxicity appears to be the consequence of CpG sequences in the plasmid and the depletion of CpG sequences in the plasmid greatly reduces the toxicity and improves the therapeutic index [37]. However, the DNA-NPs, even those that retain CpG sequences, appear not to display the toxic consequences of proinflammatory cytokines activation [38,39]. This may be due to one of several mechanisms. First, it is likely that the NP remains compacted as it enters the nucleus, and so free DNA is never available to the cytoplasmic inflammatory factors. In addition, it is likely that the DNA-NPs enter only cells with surface nucleolin. Avoiding the CpG response gives greater flexibility in plasmid design, since at least one excellent eukaryotic promoter, ubiquitin C, has CpG sequences that cannot be eliminated without additional eliminating promoter function [39]. In cystic fibrosis little excess of inflammation appears in lungs of animal models by DNA-NPs over that induced by saline alone. Animal treated with 100 μg of DNA in PEG-polylsine (polyK)-DNA-NPs displayed some modest accumulation of mononuclear cells about the pulmonary veins [39]. One possible mechanism for such a response is that if the DNA-NPs separate into their component parts, the polycation might be available to activate complement [38]. Nevertheless, there were no complement consumption detected either in animal models or human studies, so the mechanism of the modest mononuclear cell accumulation remains unclear and there was, however, no systemic inflammatory response.

Additionally, gene transfer by nanoscale polymer capsules can be designed to break down and release drugs at controlled rates, to allow differential release in certain environments, such as an acid medium, and to promote uptake in tumours versus normal tissues[40]. Scientists focused now on creating novel polymers and exploring specific drug-polymer combinations. Nanocapsules can be synthesized directly from monomers or by means of nanodeposition of preformed polymers[41]. Nanocapsules have also been formulated from albumin and liposomes. Implantable drug delivery systems that are being developed will make use of nanopores to control drug release.

Single Nucleotide Polymorphisms

Single nucleotide polymorphisms (SNPs) analysis of map variation in the human genome sequence have shown to contain over two million SNPs.[42]. Microfluidic devices enable SNPs detection through very rapid fragment separation using capillary electrophoresis and high-performance liquid chromatography, together with mixing and transport of reagents and biomolecules in integrated systems[43]. The basic objectives in the development of a DNA extraction and purification system that will be compatible with high-throughput SNPs genotyping requires several steps such as DNA release from the cells without enzymatic or mechanical DNA breakdown [44]. Removing cellular proteins may interfere with DNA amplification or hybridization assays and avoidance of hazardous chemical requirements as much as possible to minimize handling and disposal costs. At this point, DNA quantification is unnecessary with high class of reproducibility of subsequent DNA amplification and/or hybridization, and assays anticipation is highly efficient [44,45].

The potential contribution of nanotechnology in SNPs analysis is mainly evident with smart biochip platforms. The development of an electronically addressable microarray chip has been described previously [46,47]. Differences of SNPs occurring in close proximity to each other on the genome are normally correlated due to linkage during the process of replication, and the extent of this correlation is termed linkage disequilibrium. Where a significant association occurs between the genetic variation observed at specific SNPs and the presence of a disease, susceptible genes can be identified [48]. McCarthy and Hilfiker (2000) suggested every order of magnitude increase in the number of markers tested requires a linear

increase in sample size. Therefore, susceptible gene with positive identification from a screening programme including 1 Million SNPs would require a minimum sample size of 1000.

As mentioned above, aggregation of DNA-modified gold NPs in a non-cross-linking configuration has extraordinary selectivity against terminal mismatch of the surface-bound duplex [49]. The ultrasensitive electrochemical SNPs biosensor using the conducting polyaniline (PANI) nanotube array as the signal enhancement element has been documented previously [50]. The PANI nanotube array of a highly organized structure was fabricated under a well-controlled nanoscale dimension on the graphite electrode using a thin nanoporous layer as a template, and oligonucleotide probes were immobilized on these PANI nanotubes. The PANI nanotube array-based DNA biosensor could achieve similar sensitivity without catalytic enhancement, purification, or end-opening processing [50]. The electrochemical results showed that the conducting PANI nanotube array had a signal enhancement capability, allowing the DNA biosensor to readily detect the target oligonucleotide at a concentration as low as 1.0 fM. In addition, this biosensor demonstrated good capability of differentiating the perfect matched target oligonucleotide from one-nucleotide mismatched oligonucleotides even at a concentration of 37.59 fM. This detection specificity indicates that this biosensor could be applied to the SNPs analysis and single-mutation detection [50].

Recently, *Liu and Lin* (2007) have introduced a new approach for electrochemical quantification of SNPs using NPs based on DNA polymerase I [51]. They applied magnetic beads through a biotin-avidin affinity reaction and magnetic separation of DNA after liquid hybridization for biotinylated DNA probes, mutant DNA, and complementary DNA. Modified cadmium phosphate-loaded apoferritin NPs with complementary sequence to the mutant site probe was designed to couple to the mutant sites of the formed duplex DNA in the presence of DNA polymerase [50]. Following electrochemical stripping analysis of the cadmium-NPs offered a means to quantify the concentration of mutant DNA. The method of SNP detection enable the quantitative analysis of nucleic acid without PCR preamplification, which was possible to determine SNPs with frequencies as low as 0.01 with accurate, sensitive, rapid, and low-cost method [50].

Conclusion

Nanotechnology research is anticipated to lead to the development of novel, sophisticated, multifunctional applications which can provide real-time assessment of molecular mechanism efficacy, and most importantly, monitor intracellular changes. The requirement for repeat dosing has focused attention on nonviral vectors, and the requirement to minimize toxicity for lipid/DNA complexes has driven the biochemists to design plasmid DNA to reduce inflammatory sequences.

Two vector types appear to meet these criteria: DNA-NPs composed of both PEG-poly K-DNA and lipid-DNA complexes have achieved some success and are under intensive development. Modification of the plasmid DNA is achieving less toxicity and longer duration of transgenic expression, and the vectors themselves appear to be sufficient for partial and possibly therapeutic correction of the genetic disorders.

Nevertheless, improvements in vector design may permit lower doses to be administered, thereby reducing dose-related toxicities. DNA-NPs, complexes may improve the specificity of gene transfer to life cell systems with low doses to be effective. Finally, Two types of DNA-NPs aggregation assays were summarized. One of the methods relies on the gold nanoparticle (GNP) by hybridization. The other method is the GNP non crosslinking system. This approach shows high performance in the detection of SNP.

These methods do not need special equipment and open up a new era of molecular diagnoses.

References

[1] Ernest. H., Shetty. R., Merkoçi. A., FEBS Journal (2007), 274(2), 310-316.

[2] Sahoo. K. S., Labhasetwar. V., DDT (2003), 8(24), 1112-1120.

[3] Mullis. K., Faloona. F., Scharf. S., Saiki. R., Horn G., Erlich. H., Quant. Biol. (1986), 51, 263-273.

[4] Niemeyer. C.M., Adler. M., Gao. S., Chi. L.F., Chem. Int. Ed. Engl. (2000), 39, 3055-3059.

[5] Niemeyer. C.M., Wacker. R., Adler. M., Chem. Int. Ed. Engl. (2001), 40, 3169-3172.

[6] Adler. M.: Langer. M., Witthohn. K., Eck. J., Blohm. D., Niemeyer. C.M., Biochem. Biophys. Res. Commun. (2003), 300, 757-763.

[7] Adler. M., Wacker. R., Niemeyer. C.M., Biochem. Biophys. Res. Commun. (2003), 308, 240-250.

[8] Gao. S., Chi. L.F., Lenhert. S., Anczykowsky. B., Niemeyer. C.M., Adler. M., Fuchs. H., Chem. Phys. Chem. (2001), 2, 384-388.

[9] Pignataro. B., Chi. L.F., Gao. S., Anczykowsky. B. Niemeyer. C.M.: Adler. M.: Fuchs. H., Apply. Phys. (2002), A74, 447-452.

[10] Niemeyer. C.M., Science. (2002), 297, 62-63.

[11] Niemeyer. C.M., Biochem. Soc. Transac. (2004), 32Pt (1), 51-3.

[12] Bath. J., Turberfield. A.J., Nature Nanotech. (2007), 2, 275-284.

[13] Merkoçi. A., Aldavert. M., Tarrasón. G., Eritja. R.: Alegret. S., Anal Chem. (2005), 77, 6500–6503.

[14] Jelen. F., Yosypchuk. B., Kourilova. A., Votny. L.: Palecek. E., Anal Chem. (2002), 74, 4788–4793.

[15] Kara. P., Kerman. K., Ozkan. D., Meric. B., Erdem. A., Ozkan. Z., Ozsoz. M., Electrochem Commun. (2002), 4, 705–709.

[16] Wang. J., Polsky. R., Merkoçi. A., Turner. K. L., Langmuir. (2003), 19, 989–991.

[17] Caruana. D. J., Heller. A., J. Am. Chem Soc., (1999), 121, 769–774.

[18] Bauer. M., Haglmuller. J., Pittner. F., Schalkhammer. T., J Nanosci Nanotechnol. (2006), 6(12), 3671-3676.

[19] Merkoçi. A., FEBS Journal. (2007), 274, (2), 310-316.

[20] Wang. J., Kawde. A-N., Electrochem Commun. (2002), 4, 349–352.

[21] Katz. E., Willner. I.: Wang. J., Electroanalysis. (2004), 16, 19–44.

[22] Merkoçi. A., Aldavert. M., Marín. S., Alegret. S., Trends Anal Chem. (2005), 24, 341–349.

[23] Pumera. M., Castañeda, M. T., Pividori. M. I., Eritja. R., Merkoçi. A., Alegret. S., Langmuir. (2005), 21, 9625–9629.

[24] Castañeda M T, Merkoçi A, Pumera M, Alegret S. Biosens. Bioelectron. (2007), 15, 1961-1967.

[25] Bertram. J., Matra. M., Curr Pharm Biotechnol. (2006), 7(4), 277-285.

[26] Torchilin. V.P., AAPS J. (2007), 11, E128-E147.

[27] Xu. L., Frederik. P., Pirollo. K.F., Hum. Gene Ther. (2002), 13, 469-481.

[28] Liu. G., Li. D., Pasumarthy. M.K., Pasumarthy. M. K., Kowalczyk. T. H.: Gedeon. C. R., Hyatt. S. L., Payne. J. M., Miller. T. J., Brunovskis. P., Fink. T. L., Muhammad. O., Moen., R. C., Hanson. R. W., Cooper. M. J., J. Biol. Chem.(2003), 278, 32578-32586.

[29] Chen. X., Davis. P.B., Mol Ther. (2006), 13, S152.

[30]kacs. G.L., Haggie. P., Seksek. O., Lechardeur. D., Free dman. N., VerkmanA.S., J Biol Chem.(2000), 275, 1625-1629.

[31] Suh. J., Wirtz. D., Hanes. J., Biotechnol Prog. (2004), 20, 598-560.

[32] Jestin. E., Mougin-Degraef. M., Faivre-Chauvet. A., Remaud-LeSaec. P., Hindre. F., Benoit. J.P., Chatal. J.F., Barbet. J., Gestin. J.F., Q J Nucl Med Mol Imaging. 2007, 51(1), 51-60.

[33] Ziady. A.G., Gedeon. C.R., Miller. T., Quan.W., Payne. J. M., Hyatt. S. L., Fink. T. L., Muhammad. O., Oette. S., Kowalczyk. T., Pasumarthy.: M. K., Moen. R. C., Cooper. M. J., Davis. P. B., Mol Ther.(2003), 8, 936-947.

[34] Farjo. R., Skaggs. J., Quiambao. A. B., Cooper. M.J.: Naash. M.I., Mol Ther. (2005), 11, 258.

[35] Yurek. D.M., Fletcher-Turner. A., Cooper. M. J., Mol Ther.(2005), 11, 253.

[36] Kube. D., Davis. P. B., Mol Ther. (2003), 7, 371.

[37] Yew. N.S., Zhao. H.: Wu. I. H. Song. A., Tousignant. J. D., Przybylska. M., Cheng. S. H., Mol Ther. (2000), 1, 255-262.

[38] Konstan. M.W., Davis. P. B., Wagener. J. S. Hilliard. K. A., Stern. R. C., Milgram. L. J., Kowalczyk. T. H., Hyatt. S. L., Fink. T. L., Gedeon. C. R.: Oette. S. M., Payne. J. M., Muhammad. O., Ziady. A. G., Moen. R. C., Cooper. M. J., l. Hum Gene Ther. (2004),15,1255-1269.

[39]Ziady. A.G.: Gedeon. C.R.: Muhammad. O.: Stillwell. V.: Oette. S. M., Fink. T. L., Quan. W., Kowalczyk. T. H., Hyatt. S.L., Payne. J., Peischl. A., Seng. J.E., Moen. R. C., Cooper. M. J., Davis. P. B., Mol Ther. (2003), 8, 948-956.

[40] Na. K., Bae. Y. H., Pharm. Res. (2002), 19, 681-683.

[41] Couvreur. P., Barratt. G., Fattal. E., Legrand. P., Vauthier. C., Crit. Rev. Ther. Drug. Carrier Syst. (2002), 19, 99-134.

[42] The International SNP Map Working Group. Nature. (2001), 409, 928-933.

[43] Galvin. P., Psychiatric Genetics.(2002), 12, 75-82.

[44] Qin. W.J., Yung. L. Y., Nucleic Acids Res. (2007), 35(17), e111.

[45] Baron. R., Willner. B., Willner. I., Chem Commun (Camb). (2007), 28, 323-332.

[46] Heller. M. J., Forster. A. H.: Tu. E., Electrophoresis, (2000), 21, 157-164.

[47] Wang. L., Lofton. C., Popp. M., Tan. W., Bioconjug Chem. (2007), 18, 610-613.

[48] McCarthy. J. J., Hilfiker. R., Nat. Biotechnol. (2000), 18, 505-508.

[49] Sato. K., Hosokawa. K.: Maeda. M., Anal Sci. (2007), 23(1):17-20.

[50] Chang. H., Yuan. Y.: Shi. N., Guan. Y., Anal Chem. (2007), 1(13), 5111-5115.

[51] Liu. G., Lin. Y., J Am Chem Soc. (2007), 129(34), 10394-10401.

Arabian J. Chem. Vol. 1, No. 1, 93-110 (2008)

Synthesis, Characterization and Reactivity of Diamine-*bis*(triphenylphosphine)ruthenium(II) Complexes as Catalysts for Selective and Direct Hydrogenation of Cyanamid Aldehyde

Ismail Warad*[1], Nizam Diab[2], Saud Al-Resayes[1], Refaat Mahfouz[1], Yahia Mabkhoot[1], Ibraheem Mkhalid[3]

[1]*Department of Chemistry, King Saud University P.O Box 2455, Riyadh-11451, Saudi Arabia*

[2]*Department of Chemistry, Arab American University-Jenin, P.O. Box 240, Jenin, Palestine.*

[3]*Department of Chemistry, King Abulaziz University, P.O. Box 80203, Jeddah-21589, Saudi Arabia*

Abstract

The diamine-*bis*(triphenylphosphine)ruthenium(II) complexes using 1,4-butanediamine and N^1-(2-aminoethyl)-1,2-ethanediamine as co-ligands has been made available for the first time. These complexes were characterized by NMR, IR, and mass spectroscopy in addition to the elemental analysis. The chemical behavior of the phosphine and diamine ligands during the complexation reactions was manipulated by $^{31}P\{^1H\}$ NMR spectroscopy at room temperature. In case of using triamine as bidentate co-ligand one of the chloride ligand in dichloromethane solvent was self-abstracted from the coordination sphere of the ruthenium center atom to the outer sphere which permitted monocationic complex with one chloride and three nitrogen bonds formation. This hemilabile of N^1-(2-aminoethyl)-1,2-ethanediamine has been confirmed step by step, by $^{31}P\{^1H\}$ NMR as well as FAB-MS, additionally only 1,4-butanediamine ligand in complex **3** was totally exchanged by CH_3CN ligand when complex **3** and **4** were dissolved in CH_3CN solvent which confirmed that: seven membered diamines-ruthenium(II) complexes are less stable than the others. Complexes **3** and **4** showed a high degree of catalytic activity and selectivity in the direct hydrogenation of the α,ß-unsaturated aldehyde substrate (cyanamid aldehyde) under mild hydrogenation condition, additionally the role of different co-catalysts are shortly investigated in this process.

Keywords: Ruthenium(II) complexes, phosphine, diamine ligand and hydrogenation.

* Corresponding author. Tel.: 00966501485303; Fax 0096614675992, warad@ksu.edu.sa.

1. Introduction

Transition-metal catalyzed transfer hydrogenation using 2-propanol as a hydrogen source has become an efficient method in organic synthesis as illustrated by several useful applications reported in recent years [1-5]. The reaction conditions for this important process are economic, relatively mild and environmentally friendly. The most commonly used catalysts for this reaction are ruthenium(II) complexes, but some rhodium, iridium and samarium derivatives have also been used [6-10]. Considerable effort has been made to establish an empirical relationship between catalysis potential and structural behavior following the $^{31}P\{^{1}H\}$ NMR chemical shift of the phosphine ligand during reaction processes. Small changes in structure may lead to dramatic changes in selectivity and activity of the catalysts [11-15]. Highly active and selective catalysis involving transition metal complexes often requires well-designed structural and electronic features of the coordination sphere around the metal [16, 17]. It has long been recognized that changing substituents on phosphorus or nitrogen ligands can cause marked changes in the behavior of the free ligands and their transition metal complexes. By now, nearly everything was rationalized in terms of electronic effect or/and steric effect properties of the ligands [18]. Several complexes of (diphosphine)/(diamine)-$RuCl_2$ with different phosphine or diphosphine and diamine ligands were made available and tested as hydrogenation catalysts [1-5, 14, 19-26] Moreover, many efforts have been made to achieve this target, after what had been reported by R. Noyori (Nobel prizzer 2001) that such systems in the presence of strong bases, as co-catalysts, and 2-propanol as solvent, proved to be an excellent catalyst for the hydrogenation of prochiral ketones under mild conditions [1, 6-10].

We have already reported an open procedure to synthesize neutral diamine-(diphosphine)ruthenium(II) complexes by what is called later ligands exchanged technique [19, 27-29]. In addition, several neutral and cationic diamine–*bis*(ether–phosphine)ruthenium(II) complexes using hybrid ligand were made available [4]. The cleavage of Ru-O or Pd-O bond in O,P chelate complexes required a minimum donor ability of incoming ligand, such as the diamines [4, 20, 22] which under certain selected reaction conditions were found to be very suitable ligands. Compounds of this type can be easily supported, by the introduction of **T**-silyl functions into the ether–phosphine ligands, several polysiloxane sol-gel matrixes were prepared and tested as xerogels catalysts [14, 15]. Our current research portfolio is focused at the extension of methodology to related system, namely the reduction of the C=O function group in the presence of the C=C groups. These complexes in both homogenous and heterogonous phase showed a high degree of catalytic activity toward selective hydrogenation of functionalized carbonyl compounds [14-19].

Searching literature reveals the need for analysis an hydrogenation catalysts using *bis*(triphenylphosphine)-Ru(II) complexes containing N^1-(2-aminoethyl)-1,2-ethanediamine and 1,4-butanediamine co-ligands. Herein, we report on the preparation, characterization and application of new diamine-*bis*(triphenylphosphine)-*trans*-dichloro-ruthenium(II) (**3**) and (**4**) complexes as an active direct hydrogenation catalysts under mild condition.

2. Experimental

General remarks, materials, and instrumentations

All reactions were carried out in an inert atmosphere (argon) by using standard high vacuum and Schlenk-line techniques unless otherwise stated. Prior to use, CH_2Cl_2, *n*-hexane, and Et_2O were distilled from CaH_2, $LiAlH_4$, and from sodium/ benzophenone, respectively.

The diamines were purchased from Acros, and Merck and were purified. Triphenylphosphine and 2-propanol from Fluka, were used without a need for purification. [$RuCl_2.xH_2O$] is available from Chempur.

$[Cl_2Ru(PPh_3)_3]$ complex **2** was prepared by the published method [4]. Elemental analysis was carried out on an Elementar Varrio EL analyzer. High-resolution ^1H, $^{13}C\{^1H\}$, DEPT 135, and $^{31}P\{^1H\}$ NMR spectra were recorded on a Bruker DRX 250 spectrometer at 298 K. Frequencies are as follows: ^1H NMR 250.12 MHz, $^{13}C\{^1H\}$ NMR 62.9 MHz, and $^{31}P\{^1H\}$ NMR 101.25 MHz. Chemical shifts in the ^1H and $^{13}C\{^1H\}$ NMR spectra were measured relative to partially deuterated solvent peaks which are reported relative to TMS. ^{31}P chemical shifts were measured relative to 85% H_3PO_4 ($\delta_p = 0$). Mass spectra: FAB-MS; Finnigan 711A (8kV), modified by AMD and reported as mass/charge *(m/z)*. Infrared spectra of the solid complexes were recorded on a Bruker IFS 48 FT-IR spectrometer using KBr disk. The analyses of the hydrogenation experiments were performed on a GC 6000 Vega Gas 2 (Carlo Erba Instrument) with a FID and capillary column PS 255 [10 m, carrier gas, He (40 kPa), integrator 3390 A (Hewlett Packard)].

General procedure for the preparation of complexes 3 and 4.

A solution of the corresponding diamine ligand (10% excess) in 25 ml of CH_2Cl_2 was added dropwise to $Cl_2Ru(PPh_3)_3$ solution (while stirring) in 25 ml of CH_2Cl_2 placed in 100 ml Schlenk tube. The reaction mixture was stirred approximately for 15 min at room temperature; during that time the color changed from deep brown to the light yellow. The volume of the solution was concentrated to about 5 ml under reduced pressure. Addition of 40 ml of diethyl ether caused the precipitationo of the product which was filtered (P4) and washed out 4 times with 50 ml of *n*-hexane each and dried under vacuum.

2.2.1 **Complex 3**: Complex **2** $[Cl_2Ru(PPh_3)_3]$ (500 mg, 0.522 mmol) was treated with 1,4-diaminobutane (0.050 ml, 0.57 mmol) to give complex **3** with 61% yield. ^1H NMR (CD_2Cl_2): δ (ppm), 1.62 (m, 4H, NCH_2CH_2), 2.97 (m, 4H, NCH_2), 3.88 (s, 4H, NH_2), 7.20-7.70 (m, 20H, C_6H_5). $^{31}P\{^1H\}$ NMR (CD_2Cl_2): δ (ppm) 45.57 (s). $^{13}C\{^1H\}$ NMR (CD_2Cl_2): δ (ppm) 29.34 (d, 2C, $NCH_2\underline{C}H_2$), 44.21 (s, 2C, $N\underline{C}H_2CH_2$), 128.22-134.42 (m, 36C, C_6H_5). FAB-MS: *m/z*: 784.2 $[M^+]$; elemental *Anal.* Calc. (%) from $C_{40}H_{42}Cl_2N_2P_2Ru$ (784.7): C, 61.22; H, 5.39; N, 3.57; Cl, 9.04; Found: C, 61.06; H, 5.31; N, 3.23; Cl, 9.43%.

2.2.2 **Complex 4**: Complex **2** $[Cl_2Ru(PPh_3)_3]$ (500 mg, 0.522 mmol) was treated with N^1-(2-aminoethyl)-1,2-ethanediamine (0.057 ml, 0.58 mmol) to give complex **4** with 92% yield. ^1H NMR (CD_2Cl_2): δ (ppm), 2.48-4.21 (br, m, 13H, $H_2NCH_2CH_2HNCH_2CH_2NH_2$), 7.24-7.78 (m, 20H, C_6H_5). $^{31}P\{^1H\}$ NMR (CD_2Cl_2): δ (ppm) 40.16 and 43.94 (dd). $^{13}C\{^1H\}$ NMR (CD_2Cl_2): δ (ppm) 39.71 (s, C_1, $H_2N\underline{C}H_2CH_2$-$HNCH_2CH_2NH_2$-Ru, 43.02 (s, C_4, $H_2NCH_2CH_2$-$HNCH_2\underline{C}H_2NH_2$-Ru), 48.92 (s, C_2, $H_2NCH_2\underline{C}H_2$-$HNCH_2CH_2NH_2$-Ru), 53.72 (s, C_3, $H_2NCH_2CH_2$-$HN\underline{C}H_2CH_2NH_2$-Ru), 126.31-135.52 (m, 36C, C_6H_5). FAB-MS: *m/z*: 799.2 $[M^+]$; elemental *Anal.* Calc. (%) from $C_{40}H_{43}Cl_2N_3P_2Ru$ (799.71): C, 60.08; H, 5.42; N, 5.25; Cl, 8.87; Found: C, 60.42; H, 5.24; N, 4.98; Cl, 8.86%.

General procedure to prepare complex 6

Amount of complex **3** was placed in 100 ml Schlenk tube enough volume of CH_3CN was added, the reaction mixture was stirred for approximately 50 min at room temperature; during that time samples were taken and checked by $^{31}P\{^1H\}$ NMR, the reaction was completed when all the material singed at δp 45.57 ppm i.e. complex **3** had been exchanged by bread δp 31.3 ppm resonated to complex **6**. The volume of the solution was concentrated to about 5 ml under reduced pressure. Addition of 60 ml of *n*-hexane caused the precipitation of the product which was filtered (P4) and washed well with petroleum ether and dried under vacuum.

2.3.1 **Complex 6**: Complex **3** (250 mg, 0.27 mmol) was treated by dissolving in 100 ml of CH_3CN to give complex **6** with 56% yield. ^1H NMR (CD_2Cl_2): δ (ppm), 1.78 (b, 6H, CH_3), 7.10-7.60 (m, 20H, C_6H_5). $^{31}P\{^1H\}$ NMR (CD_2Cl_2): δ

(ppm) 31.30 (b). $^{13}C\{^{1}H\}$ NMR (CD_2Cl_2): δ (ppm) 1.71 (s, 2C, CH_3), 117.88 (s, 2C, CN), 126.42-134.52 (m, 36 C, C_6H_5). FAB-MS: *m/z*: 778.2 [M^+]; elemental *Anal.* Calc. (%) from $C_{40}H_{36}Cl_2N_2P_2Ru$ (778.80): C, 61.70; H, 4.66; N, 3.60; Cl, 9.11; Found: C, 61.26; H, 4.38; N, 3.43; Cl, 9.21%.

General Procedure for the Catalytic Study

The respective diamine*bis*(tri-phenylphosphine) ruthenium(II) complexes **3** or **4** [0.01 mmol, Ru(II)] was placed in a 100 ml Schlenk tube and solid KOH, *t*BuOK and Na_2CO_3 [0.10 mmol each] were added individually as co-catalysts. The entire apparatus was evacuated and filled back with argon three times to establish an inert atmosphere. The solid mixture was stirred and warmed room temperature for about 1 h. During the hydrogenation process samples were taken from the reaction by a special glass syringe then directly inserted into a gas chromatography to control the conversion and selectivity. during the evacuation process to remove traces of oxygen and water. Subsequently the Schlenk tube was filled with argon and 10 ml of 2-propanol. The mixture was vigorously stirred, degassed by two freeze-thaw cycles, and then sonicated for 30 min (to ensure complete dissolving of components and remove trace of remained gases). A solution of Cyanamid aldehyde compound (10.0 mmol) in 30 ml of 2-propanol was subjected to a freeze-thaw cycle in a different 100 ml Schlenk tube and was added to the catalyst solution. Finally the reaction mixture was transferred to 200 ml pressure Schlenk tube the entire apparatus was evacuated and filled back with hydrogen gas three times to wash out argon inert sphere then pressurized with 1 bar of hydrogen. The reaction mixture was vigorously stirred at
The kind of the reaction products was compared with authentic samples.

3. Results and Discussion

Complexes Synthesis and NMR Investigations

Dichloro-*bis*(triphenylphosphine)-ruthenium(II) complex was prepared from $RuCl_3.xH_2O$ according to literature methods [4], (Scheme 1). $Cl_2Ru(PPh_3)_3$ (**2**) was found to be a rigid compound in solid state, it revealed by CP/MAS P NMR only one broad peak at 42.1 ppm (Figure 1, a).

Dissolving this complex in dichloromethane showed another new P sharp peak at δ_p 30.6 ppm as well as free PPh_3 at δ_p -4.3 ppm (as in eq1 and Figure 1, b).

$$Cl_2Ru(PPh_3)_4 \rightleftharpoons Cl_2Ru(PPh_3)_3 + PPh_3 \text{.....eq1}$$

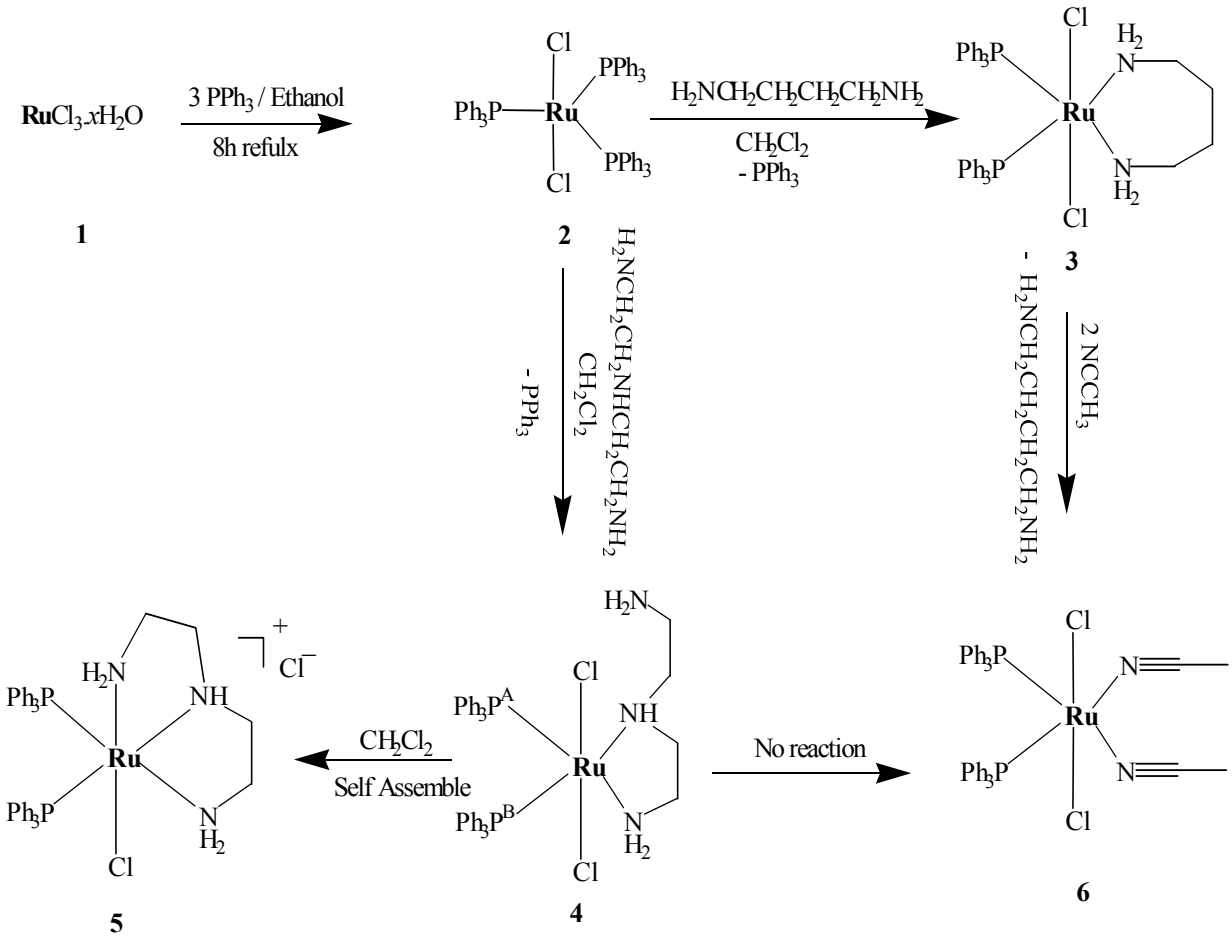

Scheme 1. Synthetic scheme of ruthenium(II) complexes.

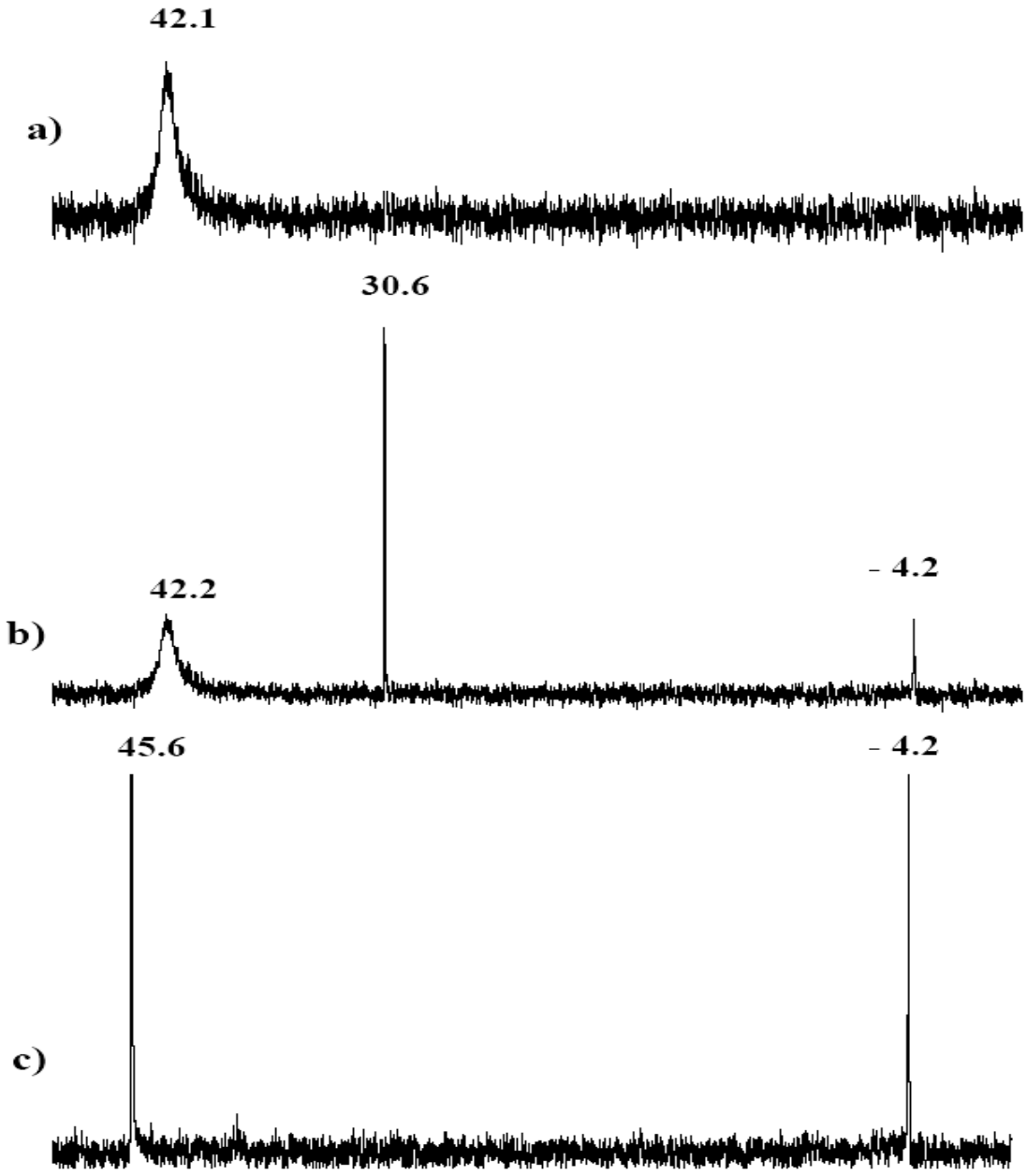

Figure 1. $^{31}P\{^{1}H\}$ NMR spectroscopic of ruthenium(II) complexes a) Solid state CP/MAS ^{31}P NMR of $[Cl_2Ru(PPh_3)_3$, δ_p =42.1 ppm], b) The same matrix dissolved in CD_2Cl_2, free PPh_3, δ_p = - 4.2 ppm in addition to another isomer, δ_p = 30.6 ppm were recorded, c) Liquid $^{31}P\{^{1}H\}$ NMR of the same matrix after 10 min from 1,4-butanediamine co-ligand addition, complex 3, δ_p = 45.6 ppm was formed.

The liquid $^{31}P\{^{1}H\}$ NMR spectrum gave these two sharp and broad singlets at δ_p 30.6 and δ_p 42.2 ppm respectively, indicates the presence of two non-equivalents phosphorous. If these two non-equivalents phosphorous are present in the same complex, one should get two doublets due to the presence of two non-equivalents phosphorous with P–P coupling. As $^{31}P\{^{1}H\}$ NMR spectra gave only two singlets, it is inferred that these two $^{31}P\{^{1}H\}$ singlets were originating from two different complexes. Together the CP/MAS P NMR and liquid $^{31}P\{^{1}H\}$ NMR results revealed an equilibrium formation [between $Cl_2Ru(PPh_3)_4$ and $Cl_2Ru(PPh_3)_3$] as in equation 1. Both these two $^{31}P\{^{1}H\}$ NMR singlets were replaced by one sharp peak at δ_p 45.6 ppm when 1,4-diaminobutane was added, which permitted complex **3** preparation see (Figure 1, C).

It also noteworthy that, complexes **3** and **4** can be prepared by treating complex **2** with slight excess equivalent amount of 1,4-butanediamine and N^1-(2-aminoethyl)-1,2-ethanediamine respectively, when one equivalence of the corresponding diamine is mixed with precursors $Cl_2Ru(PPh_3)_3$, one triphenylphosphine ligand was replaced by two nitrogen donors (see Figure 1) to synthesize the 18 electron octahedral diamine-*bis*[triphenylphosphine]*trans*-dichlororuthenium(II) complexes in a good yields. This fact was confirmed in addition to $^{31}P\{^{1}H\}$ NMR by X-ray crystallography [25].

To establish the unrestrictive structural behavior of the incorporation active site during the reaction, $^{31}P\{^{1}H\}$ NMR as a power tool was investigated, together the multiplicity, the chemical shifts and the coupling constant of these complexes confirmed the expected *trans*-configured dichloro-$RuCl_2$ **B** isomer formations [4, 27-30]. The three possible isomers were charted in Chart 1.

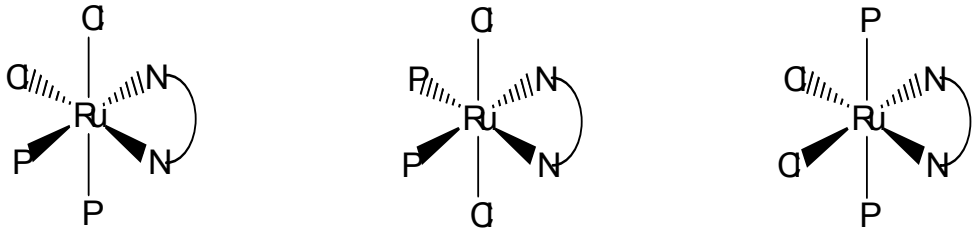

Chart 1. The possible geometries of $RuCl_2(PPh_3)_2$(diamine) complexes.

The stoichiometry of five and six-coordinate complexes **4** and **3** respectively, is supported by elemental analysis FAB-MS, IR, $^{31}P\{^{1}H\}$ ^{1}H, $^{13}C\{^{1}H\}$NMR spectroscopy (see experimental section for details), which are also consistent with a chelate coordination of diamine ligands at room temperature, in the $^{31}P\{^{1}H\}$ NMR spectrum of complex **3** at

room temperature is very simple, it exhibited a singlet with (δ_p = 45.6 ppm) revealing that the chemical equivalence of phosphine groups in solution due to the C_{2v} symmetry of the $RuCl_2(PPh_3)_2$diamine complex are equivalent. While in complex **4** and due to loss of C_2 symmetry by N^1-(2-aminoethyl)-1,2-ethanediamine ligand $^{31}P\{^1H\}$ NMR in dichloromethane exhibit the **AB** pattern. Two doublets at around 40.1 and 43.9 ppm attributable to different chemical environments P^A and P^B which in other hand revealed J*pp* = 35.3 Hz as in Figure 2, confirming the **B**-isomer formation.

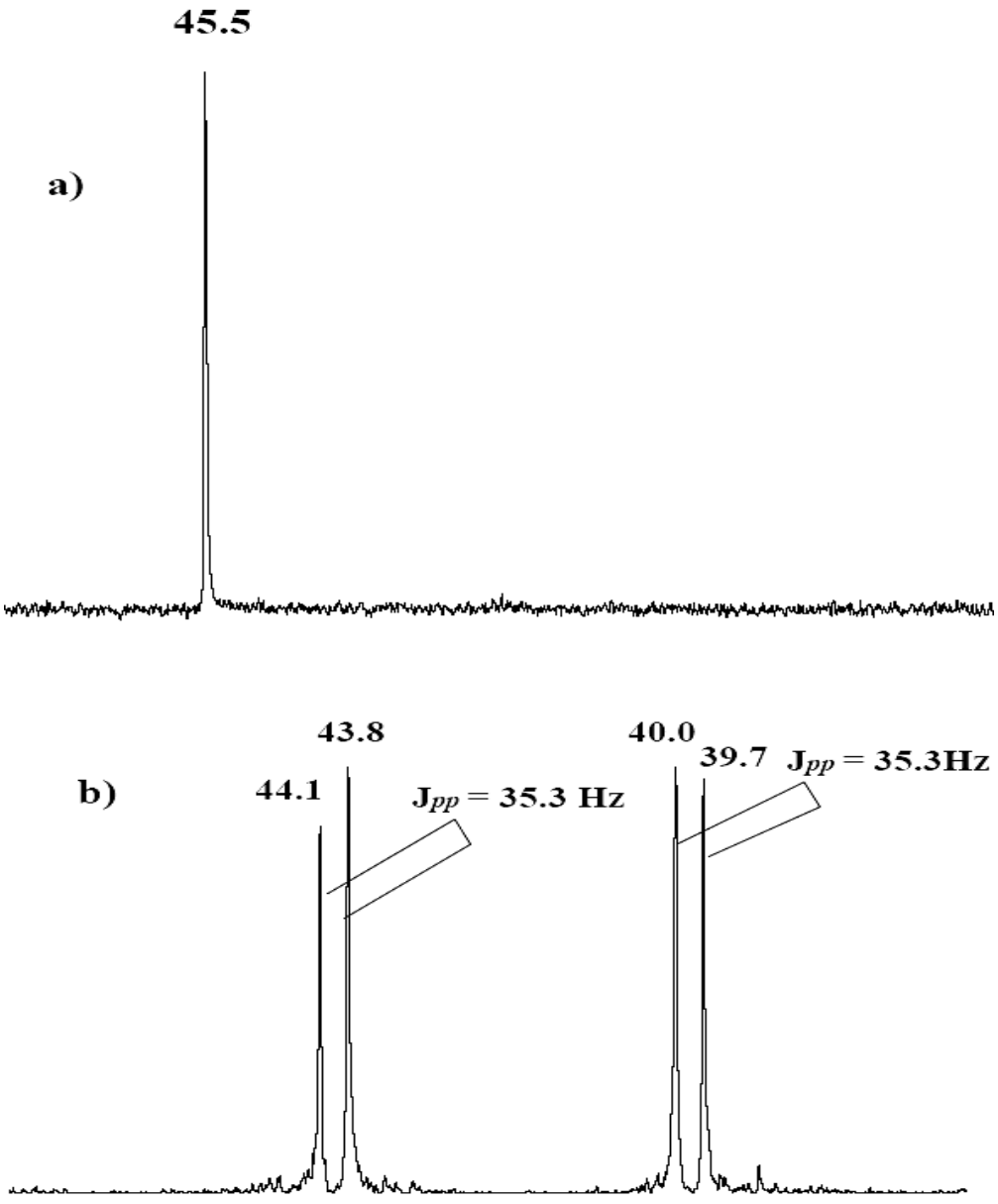

Figure 2. a) Liquid $^{31}P\{^1H\}$ in ppm of complex 3 in CD_2Cl_2. b) Liquid $^{31}P\{^1H\}$ of complex 4 in CD_2Cl_2.

In the ^{1}H NMR spectra of the diamine-*bis*(triphenylphosphine)ruthenium(II) complexes **3** and **4** characteristic sets of signals are observed, which are attributed to the aliphatic diamine as well as phenyls of phosphine ligands. In case of complex **4** due to closed chemical shifts of the backboned function groups of the diamine ligand, multi-broadness peaks were observed even in free ligand studies.

The $^{13}C\{^{1}H\}$ NMR spectra also corroborate the structures given in Scheme 1. Characteristic ^{13}C signals are due to the carbons of phenyls and carbons of the diamine ligands in both **3** and **4** complexes, respectively. The 135 Dept $^{13}C\{^{1}H\}$ NMR spectra of complex **4** as atypical example to differentiate the C, CH and CH_2 carbon types represented in Figure 3. The chemical shifts of the corresponding fragments are in agreeing with the free ligands studies.

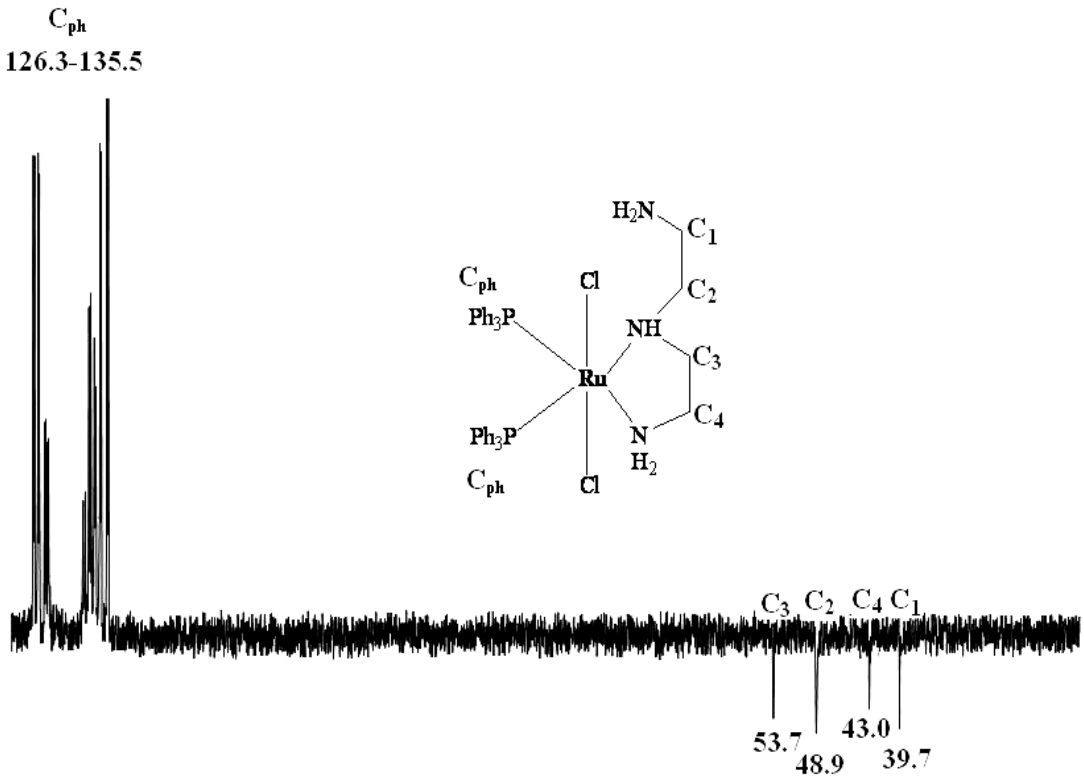

Figure 3. The 135 Dept $^{13}C\{^{1}H\}$ NMR spectrum corroborates the structure of complex 4.

Of interest, the self rearrangement reaction of complex **4** in dichloromethane to give monocationic complex **5**. It was observed that leaving complex **4** under stirring in dichloromethane lead to form the unstable [$RuCl(PPh_3)_2$diamine]Cl monocationic complex. One chloride around the coordination sphere of the ruthenium

center atom was abstracted to outer sphere position. This abstraction was confirmed by FAB-Mass spectrophotometric as in Figure 4. Octahedral complex with one chloride bond and three coordination bonds *via* the nitrogen of N^1-(2-aminoethyl)-1,2-ethanediamine ligand was detected.

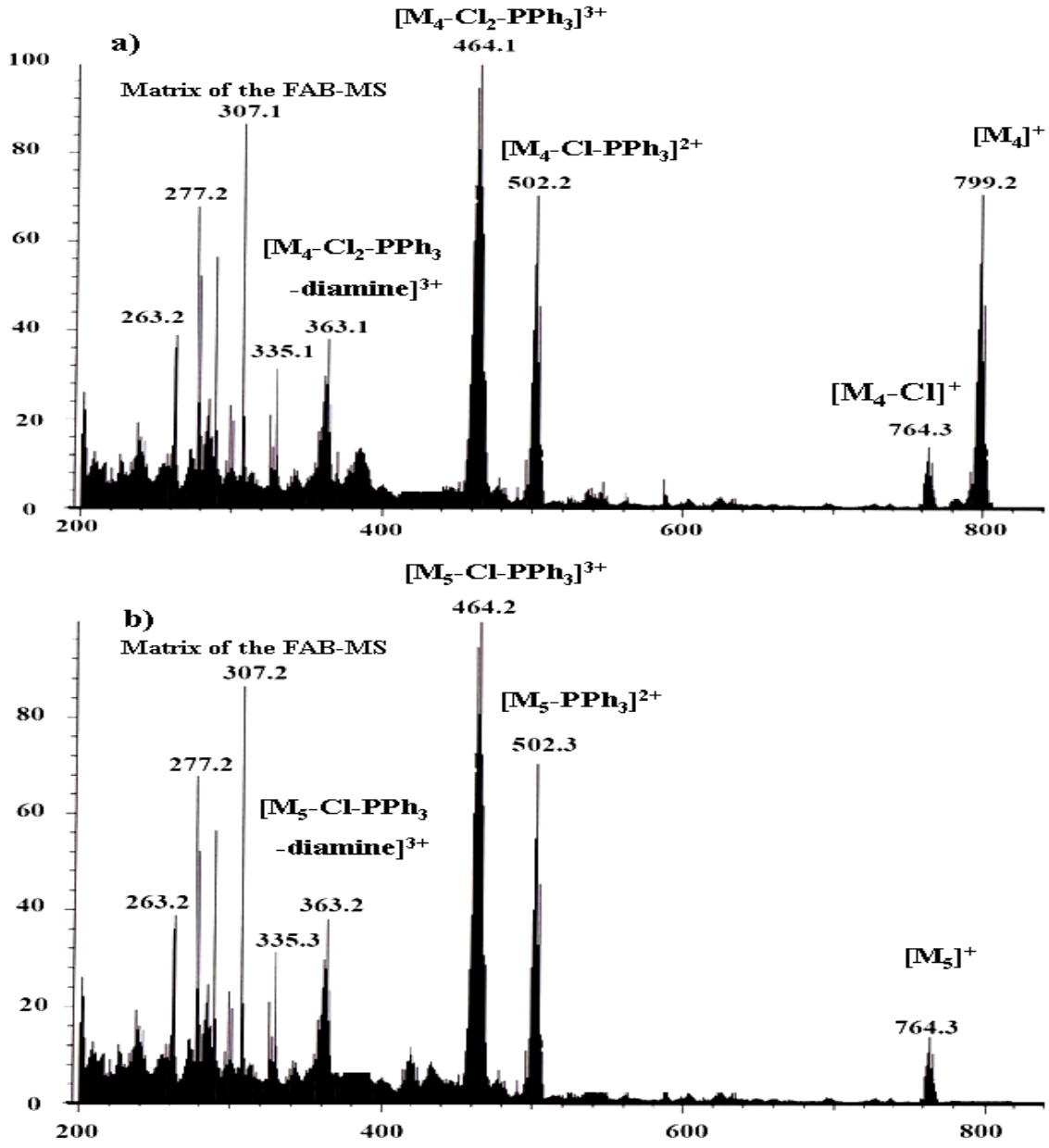

Figure 4. FAB-MS of *trans*-$RuCl_2$ complexes: a) complex 4 and b) complex 5.

Moreover, the chloride-abstraction reaction was followed by $^{31}P\{^{1}H\}$ NMR in CD_2Cl_2 as in Figure 5, the P-P coupling constant and the splitting as well as the chemical shift of phosphine ligand in $^{31}P\{^{1}H\}$ NMR confirmed the monocationic complex **5** formation. Unfortunately the full characterization of this complex was not possible due to instability and poor solubility in deuterated solvents.

IR Investigations

The IR spectra of complexes **3** and **4** in particular showed three main sets of characteristic absorptions in the ranges 3385-3310 cm^{-1}, 3267-3210 cm^{-1} and 3018-2709 cm^{-1}, which can be attributed to stretching vibrations of the main function group, NH_2, Ph-H and CH_2 function groups respectively. The IR spectrum which contained the chemical shifts of the main fragments represented the well-known function groups of complex **3** as an example was illustrated in Figure 5.

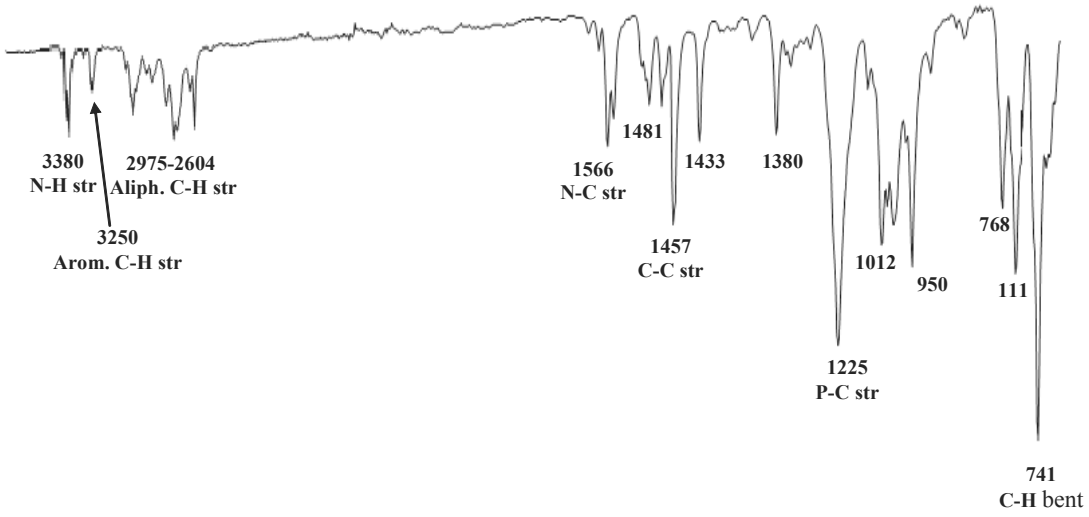

Figure 5. Infra-red spectrum cm^{-1} per well-known function group of complex 3.

FAB Mass Spectroscopy and Elemental Analysis Investigations

The molecular composition of complex **3** and **4** were corroborated by FAB mass spectra as well as elemental analysis. All these analyses have ascertained the structure and properties of the desire complexes. The FAB-Ms data which confirmed the expected complex **4** structures of formations with exact mass and expected fragments were collected in Figure 4 and other analysis data was already summarized in Table 1 somewhere in this test.

Catalytic Activity of the Ruthenium(II) Complexes 3 and 4 in the Selective Hydrogenation of Cyanamid Aldehyde

To study the catalytic activity of the ruthenium(II) complexes, *trans*-4-phenyl-3-propene-2-al was selected, because three different rego-selective hydrogenation are expected (Scheme 2).

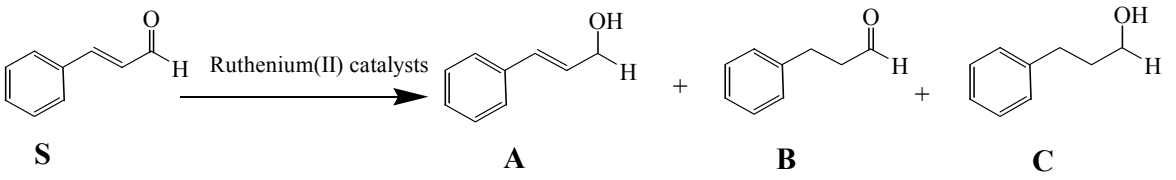

Scheme 2. Different hydrogenation possibilities of substrate S: Selective carbonyl function group hydrogenation to produce A, selective C=C function group hydrogenation to produce B, full hydrogenation path with no selectivity to produce C.

The selective hydrogenation of the carbonyl group affords the corresponding unsaturated alcohol (**A**). Unwanted and hence of minor interest both the hydrogenation of the C=C double bond, leading to the saturated aldehyde (**B**) and the full hydrogenation of C=O and C=C bonds resulting the saturated alcohol (**C**) formation. The hydrogenation reactions using complexes **3** and **4** as catalysts were carried out at 25 ^{o}C with a molar substrate: catalyst (TON, S/C) ratio of 500: 1, under 1 bar of hydrogen pressure, in 40 ml of 2-propanol [Ru: Co-catalysts (KOH, tBuOK and Na_2CO_3): cyanamid aldehyde] [1:10:500], the result were listed in Table 1.

Table 1: Hydrogenation of *trans*-4-phenyl-3-propene-2-al (S) by Ru(II) complexes at room temperature [a].

Run	Catalyst	Co-catalyst	Conversion (%)	Selectivity [b]	TOF[c]
1	**3**	*t*BuOK	96	100% **A**	480
2	**4**	*t*BuOK	100	100% **A**	620
3	**3**	KOH	98	100% **A**	510
4	**4**	KOH	100	100% **A**	650
5	**3**	Na_2CO_3	0	-	-
6	**4**	Na_2CO_3	0	-	-

[a]Reaction was conducted at 25 C^{o} using substrate (S/C = 500) in 40 ml of 2-propanol, PH_2 = 1 bar, [Ru : co-catalysts : Substrate][1:10:500]. [b]yield and selectivity were determined by GC. [c]Turnover frequency: mole of product per mole of catalyst per hour, h^{-1}.

During the hydrogenation process samples were frequently taken and directly inserted into a gas chromatography, in order to confirm the degree of conversion and control selectivity as presented in the GC graph (Figure 6). At 100 ^{o}C isotherm, R_f of the substrate (*trans*-4-phenyl-3-propene-2-al, **S**) equal 7.3 min and R_f of the corresponding unsaturated alcohol product (*trans*-4-phenyl-3-propene-2-ol, **A**) equal 8.2 min. Very good base line separation was observed, parallel to the GC-result, the product was isolated and characterized additionally by NMR.

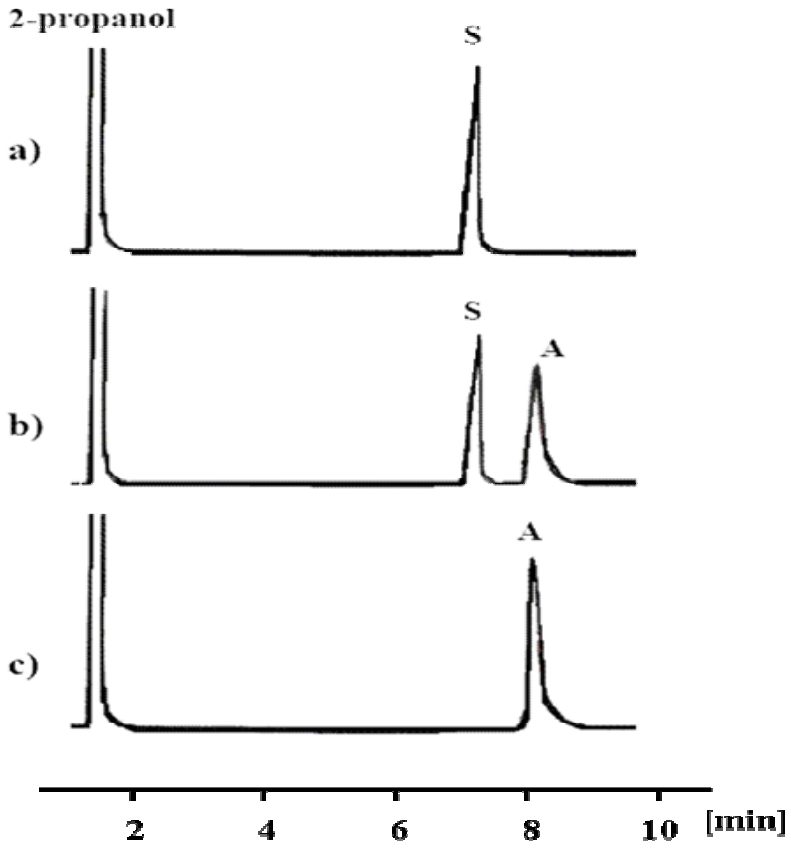

Figure 6. Gas-chromatographic separation of *trans*-4-phenyl-3-propene-2-al, (S) and (*trans*-4-phenyl-3-propene-2-ol, (A) product from 2-propanol solvent, resulting from catalyst 4. a) before pressurized with H_2 molecule, b) 35 min and c) 60 min from the hydrogenation starting. Oven temperature was 100 C^{o} isothermal for 10 min.

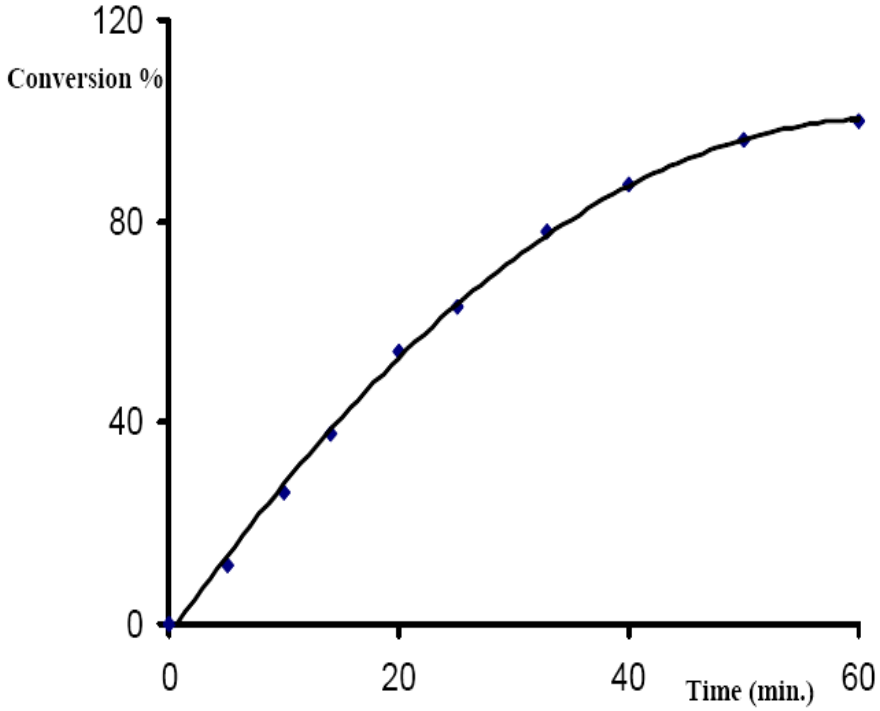

Figure 7. Hydrogenation reaction of *trans*-4-phenyl-3-butene-2-al (S) using complex 4 as catalyst under above mild condition.

The reaction under the above condition using complex 4 was finished within one hour with no side products (B and C), the conversion of the hydrogenation process as a function of time (min.) as illustrated in Figure 7.

The catalysts were only effective in the presence of excess hydrogen and a strong basic co-catalyst like KOH, and *t*BuOK, where Na_2CO_3 as co-catalyst was totally inactive. 2-propanol served as a solvent. All these complexes are highly active under mild conditions and gave rise to a 100% selective hydrogenation toward the C=O group in the presence of a C=C function (Table 1). While complex **3** was less active under exactly identical condition as compared to complex **4** which reflects its less stability of it during the hydrogenation process, due to the presence of seven-membered heterocyclic ring (ruthenium-diamine) as its backbone.

4. Conclusion

The diamine-*bis*(triphenyl-phosphine)ruthenium(II) complexes using 1,4-butane-diamine and η^2-N^1-(2-aminoethyl)-1,2-ethanediamine as co-ligand were made accessible. These complexes were characterized by NMR, IR, and FAB-mass spectroscopy in addition to the elemental analysis. The chemical behavior of the phosphine ligand in these complexes during the reactions path way was studied by $^{31}P\{^1H\}$ NMR spectroscopy at room temperature. Because of the hemilabile character of the triamine ligand in complex **4**, the chloride ligand was abstracted to the outer sphere coordination site by self assemble to form the monocationic complex **5**. The hybrid effect of N^1-(2-aminoethyl)-1,2-ethanediamine ligand on the chemical environments of the phosphine ligands maintained the following of the reaction by $^{31}P\{^1H\}$ NMR in addition FAB-MS.

The intention was to compare their catalytic performance in the selective hydrogenation of *trans*-4-phenyl-3-butene-2-al. Strong bases were the corner stone to activate these complexes, no reaction was observed in the absence of the hydrogen gas or weak base. A high catalytic activity and selectivity in the direct hydrogenation of the cyanamid aldehyde under mild condition was observed when **3** and **4** complexes were served as catalysts.

Acknowledgments

The Dr. S. Resayes and I. Warad would like to thank the research center in King Saud University for financial support and use of some measurement facilities.

References

[1] Noyori, R. (1994). **"**Asymmetric Catalysis in Organic Synthesis**"**, 1st , J. Wiley and Sons, New York, (1994), p 1-10.

[2] Takaya, H.; Ohno, T. and Noyori, R. **"**In Catalytic Asymmetric Synthesis**"**, 1s, Ojima, I., Ed.; VCH: New York, (1993), Chapter 1.

[3] Gao, J.-X.; Ikariya, T. and Noyori, R. "A ruthenium(II) Complex with a C2-Symmetric Diphosphine/Diamine Tetradentate Ligand for Asymmetric Transfer Hydrogenation of Aromatic Ketones". *Organometallics*, **15**, (1996), 1087-1089.

[4] Warad, I.; Lindner, E.; Eichele, K. and Mayer, A. H. "Supported Organometallic Complexes Part 39: Cationic Diamine(ether–phosphine)ruthenium(II) Complexes as Precursors for the Hydrogenation of Trans-4-phenyl-3-butene-2-one", *Inorg. Chim. Acta*, **357**, (2004), 1847-1853.

[5] Abdur-Rashid, K.; Faatz, M.; Lough, A. J. and Morris, H. R., "Catalytic Cycle for the Asymmetric Hydrogenation of Prochiral Ketones to Chiral Alcohols: Direct Hydride and Proton Transfer from Chiral Catalysts trans-$Ru(H)_2$(diphosphine)(diamine) to Ketones and Direct Addition of Dihydrogen to the Resulting Hydridoamido Complexes", *J. Am. Chem. Soc*., **123**, (2001), 7473-7474.

[6] Mathey, F. and Sevin, A. **"**Molecular Chemistry of the Transition Elements**"**, 1st, John Wiley & Sons: Chichester, U.K, (1996), p 144-145.

[7] Haack, K.-J.; Hashiguchi, S.; Fujii A.; Ikariya, T. and Noyori, R., "The Catalyst Precursor, Catalyst, and Intermediate in the Ru-II-Promoted Asymmetric Hydrogen Transfer Between Alcohols and Ketones", *Angew. Chem, Int. Ed. Engl.*, **36**, (1997), 285-288.

[8] Ohkuma, T.; Ikehira, H.; Ikariya, T. and Noyori, R., "Asymmetric Hydrogenation of Cyclic Alpha, Beta-unsaturated Ketones to Chiral Allylic Alcohols", *Synlett*. (1997), 467-469.

[9] Gamez, P.; Fache, F. and Lemaire, M., "Asymmetric Catalytic Reduction of Carbonyl Compounds Using C2 Symmetric Diamines as Chiral Ligands", *Tetrahedron Asymmetry*, **6**, (1995), 705-718.

[10] Ohkuma, T.; Noyori, R.; Nishiyama, H. and Itsuno, S., **"**In Comprehensive Asymmetric Catalysis**"**, Vol.1., E. N. Jacobsen, Springer, Berlin, (1999), Chapter 6.

[11] Gilheany, D. C. and Mitchell, C. M., **"**In the Chemistry of Organophosphorus Compounds**"**, Vol.1, J. Wiley and Sons: New York, (1990), p 151-190.

[12] Jiang, Y.; Jiang, Q. and Zhang, X., "A new Chiral *Bis*(oxazolinylmethyl)amine Ligand for Ru-Catalyzed Asymmetric Transfer Hydrogenation of Ketones", *J. Am. Chem. Soc.***, 120**, (1998), 3817-3818.

[13] Wang, G-Z. and Bäckvall, J.-E. "Ruthenium-Catalyzed Transfer Hydrogenation of Imines by Propan-2-ol". *J. Chem. Soc., Chem. Commun*., (1992), 980-982.

[14] Lindner, E.; Warad, I.; Eichele, K. and Mayer, H. A., "Supported Organometallic Complexes Part 34: Synthesis and Structures of An array of Diamine(ether-phosphine)ruthenium(II) Complexes and their Application in the Catalytic Hydrogenation of Trans-4-phenyl-3-butene-2-one", *Inorg. Chim. Acta*, **350**, (2003, a), 49-56.

[15] Lu, Z-L.; Eichele, K.; Warad, I.; Mayer, H. A.; Lindner, E.; Jiang, Z. and Schurig, V., "Supported Organometallic Complexes: *Bis*(methoxyethyldimethylphosphine)-ruthenium(II) Complexes as Transfer Hydrogenation Catalysts". *Z. Anorg. Allg. Chem.*, **629**, (2003), 1308-1315.

[16] Cornils, B. and Herrmann, A. W., "Aqueous-Phase Organometallic Catalysis", Wiley-VCH: Weinheim, (2003), Chapter 3.2.

[17] Nachtigal, C.; Al-Gharabli S.; Eichele, K.; Lindner, E. and Mayer, A. H.**,** "Structural Studies of an Array of Mixed Diamine Phosphine Ruthenium(II) Complexes", *Organometallics*, **21**, (2002), 105-112.

[18] Tolman, C. A. "Steric Effects of Phosphorus Ligand in Organometallic Chemistry and Homogeneous Catalysis", *Chem. Rev,*. **77**, (1977), 313-348.

[19] Lindner, E.; Warad, I.; Eichele, K. and Mayer, H. A.**,** "Supported Organometallic Complexes Part 35. Synthesis, Characterization, and Catalytic Application of a New Family of Diamine(diphosphine)ruthenium(II) Complexes". *J. Organomet. Chem.*, **665**, (2003, b), 176-185.

[20] Warad, I.; Al-Gharabli, S.; Al-labadi, A. and Abu-Rayyan, A., "Synthesis, Characterization and NMR Studies of Novel Hemilabile Neutral and Dicationic Palladium(II) complexes: $Pd(\eta^2\text{-}PH_2PCH_2CH_2OCH_3)_2$ and $Pd(\eta^1\text{-}PH_2PCH_2CH_2OCH_3)_2$diamine by Using Ether-phosphine Ligand", *J. Saudi Chem. Soc.*, **9**, (2005), 507-512.

[21] Lindner, E.; Al-Gharabli, S.; Warad, I.; Mayer, H. A., Steinbrecher, S.; Plies, E.; Seiler, M. and Bertagnolli, H., "Supported Organometallic Complexes: Diamine-diphosphine-ruthenium(II) Interphase Catalysts for the Hydrogenation of α,ß-Unsaturated Ketones", *Z. Anorg. Allg. Chem.*, **629**, (2003, c), 161-171.

[22] Warad, I.; Al-Reasyes, S.; Eichele, K., "Crystal structure of *trans*-dichloro-1,3-propanedi-amine-*bis*[(2-methoxyethyl)diphenylphosphine]ruthenium(II), $RuCl_2(C_3H_{10}N_2)(C_{15}H_{17}OP)_2$", *Z. Kristallogr.* NCS, **221**, (2006), 275-277.

[23] Wu, D-Y.; Lindner, E.; Mayer, A. H.; Jian, Z-J.; Krishnan, V. and Bertagnolli, H., "Sol-Gel Processed Diamine(Diphosphine)ruthenium(II) Complexes for the Catalytic Hydrogenation of α, β-Unsaturated Ketones", *Chem. Mater.*, (2005), 8-18.

[24] Ohkuma, T.; Takeno, H.; Honda, Y. and Noyori, R. "Asymmetric Hydrogenation of Ketones with Polymer-Bound BINAP/Diamine Ruthenium Catalysts", *Adv. Synth. Catal.,* **343**, (2001), 369-375.

[25] Warad, I.; "Crystal Structure of Neutral η^2-N^1-(2-aminoethyl)-1,2-ethane-diamine-*cis*-*bis*(triphenylphosphine)-Ruthenium(II) Complex, unpublished result.

[26] Warad, I.; "Diamine-(phosphine)ruthenium(II) Complexes and Their Application in the Catalytic Hydrogenation of α,ß-Unsaturated Ketones in Homogeneous and Heterogeneous Phase", (2003), University of Teubingen, Germany.

[27] Grasa, A. G.; Zanotti-Gerosa, A.; Medlock A. J. and Hems, P. W., "Asymmetric Hydrogenation of Isobutyrophenone using [(Diphosphine)-$RuCl_2$(1,4-Diamine)] Catalyst". *Org. Lett.*, **7**, (2005), 1449-1451.

[28] Warad, I.; **"**Synthesis and Characterization of 1,3-Diamine-(Phosphine)Ruthenium(II) Complexes using Monodentate and Bidentate Phosphine Ligands**",** *J. Saudi. Chem. Soc*. 10, (2007) 15-25.

[29] Lindner, E.; Warad, I.; Lu, Z-L.; Mayer, H. A.; Speiser, B.; Tittel, C., **"**Combinatorial Micro electrochemistry. Part 4: Cyclic Voltammetric Redox Screening of Homogeneous Ruthenium(II) Hydrogenation Catalysts**"**, *Electro-chemistry Communications,* 7, (2005) 1013-1020.

[30] Warad, I.; Al-Nuri, M.; Al-Sousi, G.; Al-Gobari, S.; Mabkhot, Y.; Al-Reasyes, S.; Issa, Z., **"**Synthesis, Support and Spectral Analysis of Novel Amine and Diamine-Ruthenium(II) Complexes Starting from

Triphenylphosphine-Ruthenium(II) Precursor", *J. Saudi. Chem.* In press (2008).

gÀTÀGاl ĞÆƏÀŎQ͈ɍl ĞDZøÆŦŁÒ ãÀÀHʉÕ ÀŦùÀÎφ§ (II)ÿƺÆÆϕ§ÀÒl ƙÀèƺƺ ŌÆÆƺ ʉϕϒϕ - Èǽ - ƙŋÛ ʉƏÀÀϕ ğlÆŐĤŋ ȐĤǽ خلصÎ ķ§ ƘȒʊ ÆÆŁÆÒl ÆÆŁÀÊÒ

ᴰÆŁIJ ĻÆŁlÀǽÛ Û ᶜ ğƺخGŋ łʒ ᶜûƺÀŢ ĶĤƺø ÛᶜخلصÒÀÒl åƺĤè Ûᶜ āÀÀǽ ÿÀŢφ Ûᶜålø§ ŌƐʒÀƨÛ

.GÀåƺĤÊÒl ĞÆÆÀĤÒl ĞȮŁاl ČČďĐČ ôÀÀÀÒl čďĐĐ ā î - åƺĤè ŌŁاl ĞĤŋÀDZ - ÿƺŁĤÒl ĞÆŁÕ ŏÀÆÆÆȮÒl ĻÊęᶜ

.ƙÛÊŁƺ - ƙÀÆDZ čďċ ā î - ĞÆȮÀÀŋɉl ĞÆÆÀĤÒl ĞĤŋÀƨl - ÿƺŁĤÒl ĞÆŁÕ ŏÀÆÆÆȮÒl ĻÊęᶜ

.GÀåƺĤÊÒl ĞÆÆÀĤÒl ĞȮŁاl čČĐēĚ gÆDZ ēċčċĎ ā î - ÀÀÂĤÒl ÆGʒ ŌŁاl ĞĤŋÀDZ - ÿƺŁĤÒl ĞÆŁÕ ŏÀÆÆÆȮÒl ĻÊęᴰ

Ź ʊضير كل من معقدات ثلاثي فنيل فوسفين الروثينيوÿ(II) باستخداÿ متصلاɣ ثنائي أمين مثل Č، č - و٤،Č - ثنائي أمين كمتصلات ثانوية للمرة الأولى والاɣ قد تأكد من تركيبها بواسطة الرنين النووي المغناŭيسي لكل مـن نŢـير الفـسفور(ĎČ) والكربـون(ČĎ) والهيدروجين(Č) باɁǭʠɓ افة إلى كل من ŭيف الأŤعة ʊت اΣمراء و الطيف كتلي الفاŸ وغيرƚا.

لوحȘ انتقال متصلة الكلوريد من دائرة التناسĘ المباŤر لايون الروثينيوÿ(II) إلى الدائرة التناسقية الثانية عند اسـتخداÿ ثلاثـي أمـين كمتصلة ثنائية المنĠ مكونة عدد تناسقي نيتروجيƗ ثلاثي، ƚذȼ الŢـاƚـرة باɁǭʠɓ ـافة إلى الـسلوȭ الهيملابلـي (hemilabile) للمتصلات Ź رصدƚا باستخداÿ الرنين النووي المغناŭيسي في اΣالة السائل لنŢير الفسفور(ĎČ) و ŭيف الكتلة الفاŸ معا. أɁ ـف إلى ǽلك إن متصلة ٤،Č - ثنائي أمين الثانوية فقط Ź خلعها من معقدƚا **Ď** واستبدالها بمتصلاɣ CH_3CN عند أǽابت كل من معقد **Ď** و **ď** كل على حدا في مذيب CH_3CN ƚذا يؤكد إن معقدات اΣلقة السباعية اقل ثابتيه مقارنة بالمعقدات الأخرى.

لقد أȘهرت ƚذȻ الدراسة أن ƚذȻ المعقدات عالية النشاɁ والانتقائية عند استخدامها كحفازات لهدرجة مركب سنميد ألدƚيـد ʊـت Șروȣ ƚدرجة معتدلة للغاية، باɁǭʠɓ افة إلى ǽلك Ź بشكل ʋتصر دراسة دور العديد من اΣفازات المساندة في ƚذȻ العملية.

المجلة العربية للكيمياء

المجلة العربية للكيمياء :

مجلة بحوث علمية محكمة أسسها اتحاد الكيميائيين العرب

المملكة العربية السعودية - جامعة الملك سعود بالرياض - كلية العلوم- قسم الكيمياء – بالتعاون مع الجمعية الكيميائية السعودية .